Raquel de Souza Vieira

A sinalização de STING induz imunidade inata e adaptativa protetoras contra a infecção pelo *Trypanosoma cruzi*

Dissertação apresentada à Faculdade de Medicina da Universidade de São Paulo para obtenção do título de Mestre em Ciências

Programa de Alergia e Imunopatologia

Orientador: Prof. Dr. Edécio Cunha Neto

(Versão corrigida. Resolução CoPGr 6018/11, de 11 de novembro de 2011. A versão original está disponível na Biblioteca da FMUSP)

São Paulo

2021

Raquel de Souza Vieira

A sinalização de STING induz imunidade inata e adaptativa protetoras contra a infecção pelo *Trypanosoma cruzi*

Dissertação apresentada à Faculdade de Medicina da Universidade de São Paulo para obtenção do título de Mestre em Ciências

Programa de Alergia e Imunopatologia

Orientador: Prof. Dr. Edécio Cunha Neto

(Versão corrigida. Resolução CoPGr 6018/11, de 11 de novembro de 2011. A versão original está disponível na Biblioteca da FMUSP)

São Paulo

2021

Dados Internacionais de Catalogação na Publicação (CIP)

Preparada pela Biblioteca da
Faculdade de Medicina da Universidade de São Paulo

Vieira, Raquel de Souza
A sinalização de STING induz imunidade inata e adaptativa protetoras contra a infecção pelo Trypanosoma cruzi / Raquel de Souza Vieira. -- São Paulo, 2021.
Dissertação(mestrado)--Faculdade de Medicina da Universidade de São Paulo.
Programa de Alergia e Imunopatologia.
Orientador: Edécio Cunha Neto.

Descritores: 1.Doença de Chagas 2.Trypanosoma cruzi 3.Sting 4.Infecções 5.Imunidade inata

USP/FM/DBD-311/21

Responsável: Erinalva da Conceição Batista, CRB-8 6755

À minha querida avó, que sempre acreditou em mim

AGRADECIMENTOS

Aos meus pais, Karla e Rógerio, por sempre priorizarem a minha educação. Ao meu irmão, João Pedro, pelo apoio incondicional às minhas escolhas. Ao meu parceiro, Bruno David, pela empatia e suporte durante todo esse período. Aos meus amigos, pelos momentos leves de descontração.

Ao meu orientador, professor Dr. Edécio Cunha-Neto, por me receber em seu grupo em seu grupo de pesquisa e permitir o desenvolvimento deste trabalho.

Ao meu co-orientador, Dr. Rafael Almeida, pela idealização deste projeto e pelos constantes ensinamentos.

Aos professores colaboradores, Dr. Niels Olsen e Dr. Ronnie Carvalho.

À Andréia Kuramoto, por toda ajuda e disponibilidade.

Aos colegas do Laboratório de Investigações Médicas 19 e do Biotério de Experimentação, pelos momentos de companheirismo e por toda e qualquer contribuição para o desenvolvimento deste trabalho.

À banca examinadora pelo tempo e ensinamentos disponibilizados.

À CAPES, pelo auxílio financeiro.

Esta dissertação está de acordo com as seguintes normas, em vigor no momento desta publicação:

Referências:

Adaptado de International Committee of Medical Journals Editors (Vancouver).

Universidade de São Paulo. Faculdade de Medicina. Divisão de Biblioteca e Documentação. Guia de apresentação de dissertações, teses e monografias. Elaborado por Anneliese Carneiro da Cunha, Maria Julia de A. L. Freddi, Maria F. Crestana, Marinalva de Souza Aragão, Suely Campos Cardoso, Valéria Vilhena. 3a ed. São Paulo: Divisão de Biblioteca e Documentação; 2011.

Abreviaturas dos títulos dos periódicos:

de acordo com *List of Journals Indexed in Index Medicus.*

SUMÁRIO

LISTA DE ABREVIATURAS, SÍMBOLOS E SIGLAS

%	**Porcentagem**
µl	**Microlitro**
Ca2+	**Cálcio**
CAPES	**Coordenação de Aperfeiçoamento de Pessoal de Nível Superior**
CCC	**Cardiomiopatia chagásica crônica**
c-di-AMP	**di-AMP cíclico**
c-di-GMP	**di-GMP cíclico**
CEUA	**Comissão de Ética no Uso de Animais**
cGAMP	**GMP-AMP cíclico**
cGAS	**GMP-AMP cíclico sintase**
CXCL9	**Ligante 9 da quimiocina C-X-C**
DCh	**Doença de Chagas**
DDX41	***DEAD-Box Helicase* 41**
DMEM 10	***Dulbecco's Modified Eagle Medium High glucose* acrescido de 10% de soro fetal bovino**
DMEM 2	***Dulbecco's Modified Eagle Medium High glucose* acrescido de 2% de soro fetal bovino**
DNA	**Ácido desoxirribonucleico**
EDTA	**Ácido etilenodiamino tetra-acético**
HCl	**Ácido clorídrico**
HIV	**Vírus da imuno deficiência humana**
HSV-1	**Vírus de herpes simples do tipo 1**
IFI16	**Proteína induzível por interferon gama**
IFN I	**Interferons do tipo I**
IFNAR	**Receptor de interferons alfa e beta**
IFN-β	**Interferon beta**
IFN-γ	**Interferon gama**
IL-12	**Interleucina 12**
IL-1R	**Receptor de interleucina 1**
IL-6	**Interleucina 6**

iNos	**Enzima óxido nítrico sintase induzida**
IP3	**Trifosfato Inositol**
IRF3	**Fator regulador de interferon 3**
ISG	**Genes induzidos por interferon**
ISRE	**Elemento responsivo ao interferon**
Lag-3	**Gene 3 de ativação de linfócitos**
LLCMK2	**Células epiteliais de rim de macaco Rhesus**
LPS	**Lipopolissacarídeo**
MDA5	**Diferenciação de melanoma associado à proteína 5**
ml	**Mililitro**
MyD88	**Proteína de diferenciação mielóide 88**
NaCl	**Cloreto de Sódio**
NADH	**Dinucleótido de nicotinamida e adenina**
NF-kB	**Factor nuclear kappa B**
NK	**Células Natural Killer**
NLR	**Repecetor do tipo NOD**
NLRP3	**Domínio pirina da família NLR contendo 3**
nm	**Nanómetro**
NO	**Óxido nítrico**
OAS1	**2’,5’-oligoadenilato sintase 1**
OMS	**Organização Mundial da Saúde**
PD-1	**Proteína de morte celular programada 1**
Poly I:C	**Sal de sódio do ácido Polyinosinic**
PRF1	**Perforina**
RIG-I	**Gene induzido por ácido retinóico**
ROS	**Espécies reativas de oxigênio**
SFB	**Soro fetal bovino**
STING	**Estimulador de genes de Interferon**
T. cruzi	**Trypanosoma cruzi**
TBK-1	***TANK-binding kinase1***
TGF-β	**Fator de crescimento transformador beta**
TH1	**T helper (auxiliar) 1**
TH17	**T helper (auxiliar) 17**

Tim-3	**Domínios de mucina e imunoglobulina de célula T**
TLR 2	**Receptor do tipo Toll 2**
TLR 4	**Receptor do tipo Toll 4**
TLR 9	**Receptor do tipo Toll 9**
TNF-α	**Fator de necrose tumoral alfa**
TRIF	**Domínio TIR que contém indutor de IFN-β**
ULK1	**Proteína quinase UNC-51**
WT	***Wildtype***

LISTA DE FIGURAS

RESUMO

Vieira RS. *A sinalização de STING induz imunidade inata e adaptativa protetoras contra a infecção pelo Trypanosoma cruzi* [dissertação]. São Paulo: Faculdade de Medicina, Universidade de São Paulo; 2021.

A doença de Chagas é causada pelo protozoário flagelado *Trypanosoma cruzi*. Dados da Organização Mundial da Saúde indicam que cerca de 1,2 milhão de pessoas estão infectadas por esse parasita no Brasil. A infecção pelo *T. cruzi* é marcada pela indução de IFN do tipo I e citocinas pró-inflamatórias. Dados da literatura apontam que uma via de reconhecimento do parasita dependente de TBK-1 e IRF3 é fundamental para a indução de IFN-β em células infectadas. Entretanto, os mecanismos ainda não são totalmente esclarecidos. Dessa forma, neste trabalho investigamos a participação da proteína STING na resposta inata e adaptativa ao *T. cruzi*, dada sua íntima interação com TBK-1 e IRF3. Nós demonstramos que a sinalização de STING é necessária para a produção de IFN-β, IL-6 e IL-12 em resposta à infecção pela cepa Y do *Trypanosoma cruzi* em macrófagos. Demonstramos também que a infecção celular é necessária para ativar a sinalização de STING e que STING é essencial para a ativação imune mediada pelo DNA do parasita. Além disso, nossos resultados revelaram que a sinalização de STING promove uma ativação mais intensa da resposta imune inata e que a deficiência de STING resulta em um menor número de linfócitos T CD8+ produtores de IFN-γ ou da combinação IFN-γ /perforina contra o parasita no baço dos animais infectados.

Observamos também que embora o infiltrado inflamatório no coração dos animais infectados tenha sido semelhante, a expressão de genes relacionados à proteção imune contra a infecção aguda pelo parasita foi menor na ausência de STING. Por fim, demonstramos que animais deficientes para STING apresentam maior parasitemia durante todo o curso da infecção aguda, além de apresentarem maior parasitismo no coração. Portanto, acreditamos que nosso trabalho traz uma contribuição importante para o entendimento da imunopatologia da infecção pelo *Trypanosoma cruzi* ao desvendar um novo mecanismo molecular envolvido na indução de respostas imunes inata e adaptativa contra o parasita.

Descritores: Doença de Chagas; Trypanosoma cruzi; Sting; Infecções; Imunidade inata.

ABSTRACT

Vieira RS. *STING signaling drives protective innate and adaptive immunity against Trypasonoma cruzi infection* [dissertation]. São Paulo: “Faculdade de Medicina, Universidade de São Paulo”; 2021.

Chagas disease is caused by the flagellate protozoan *Trypanosoma cruzi*. Data from the World Health Organization indicate that about 1.2 million people are infected by this parasite in Brazil. *T. cruzi* infection is marked by the induction of type I IFN and pro-inflammatory cytokines. Previous data indicate that a TBK-1 and IRF3-dependent pathway is essential for parasite recognition and induction of IFN-β in infected cells. However, the mechanisms are still not fully understood. Thus, in this work we investigated the participation of the STING protein in the innate and adaptive response to *T. cruzi*, given its close interaction with TBK-1 and IRF3. We demonstrated that STING signaling is necessary for the production of IFN-β , IL-6 and IL-12 in response to infection by the *Trypanosoma cruzi* Y strain in macrophages. We also demonstrated that cellular infection is necessary to activate STING signaling and that STING is essential for *T. cruzi* DNA-mediated immune activation. Our results revealed that STING signaling promotes a more intense innate immune activation and that STING deficiency resulted in a lower number of CD8+ T lymphocytes producing IFN-γ or the IFN-γ /perforin combination against the parasite in the spleen of infected animals. We also observed that although the inflammatory infiltrate in the hearts of infected animals was similar, the expression of genes

related to immune protection against acute infection by the parasite was lower in the absence of STING. Finally, we demonstrated that animals deficient for STING have greater parasitemia throughout the course of the acute infection, in addition to having greater parasitism in the heart. Therefore, we believe that our work makes an important contribution to the understanding of the immunopathology of *Trypanosoma cruzi* infection by unveiling a new molecular mechanism involved in the induction of innate and adaptive immune responses against the parasite.

Descriptors: Chagas Disease; Trypanosoma cruzi; Sting; Infections; Innate immunity.

1. INTRODUÇÃO

1.1. DOENÇA DE CHAGAS

A doença de Chagas (DCh) é causada pelo protozoário flagelado *Trypanosoma cruzi* (*T. cruzi*) e dados da Organização Mundial da Saúde (OMS) indicam que cerca de 1,2 milhões de pessoas estão infectadas por esse parasita no Brasil (1). Embora seja uma infecção endêmica na América Latina, observa-se um aumento significativo no número de pessoas infectadas na Europa e Estados Unidos (2) (Fig. 1). Estima-se que a DCh tenha um custo anual global de 7 bilhões de dólares (3).

Insetos hematófagos da subfamília *Triatominidae* são os principais transmissores do *T. cruzi*, tanto para seres humanos quanto para outras 150 espécies de mamíferos selvagens e animais domésticos. *Triatoma infestans*, *Rhodnius prolixus* e *Triatoma dimidiata* são as três espécies de vetores mais importantes na transmissão do *T. cruzi* para o homem. Na America latina, *Triatoma infestans* representa o principal vetor. A transmissão acontece quando as fezes e/ou urina do inseto vetor contaminado entram em contato com a pele ferida ou regiões de mucosa do hospedeiro mamífero, permitindo que o parasita acesse a corrente sanguínea. Além dos mecanismos vetoriais, o parasita pode ainda ser transmitido por transfusão sanguínea, via placenta ou mesmo pela ingestão de alimentos contaminados (2, 4, 5) (Fig. 2).

A maioria dos indivíduos infectados pelo *Trypanosoma cruzi* são assintomáticos e caracterizam a forma indeterminada da doença. Dentre os pacientes infectados cronicamente, cerca de 10% desenvolvem a forma

digestiva (2, 6) e 30% a cardiopatia chagásica crônica (CCC). Esta última é considerada a forma de manifestação mais grave da DCh, tendo atingido aproximadamente 230.000 pessoas no Brasil em 2010 (2, 7). A miocardite de baixa intensidade, mas crescente e incessante, leva à dilatação das quatro câmaras cardíacas, destruição tissular progressiva e fibrose extensa no coração, com consequente enfraquecimento da função contrátil (8). Um terço dos cardiopatas desenvolve a forma grave da CCC, que é particularmente fatal em consequência da insuficiência cardíaca, disfunção ventricular e arritmias (9).

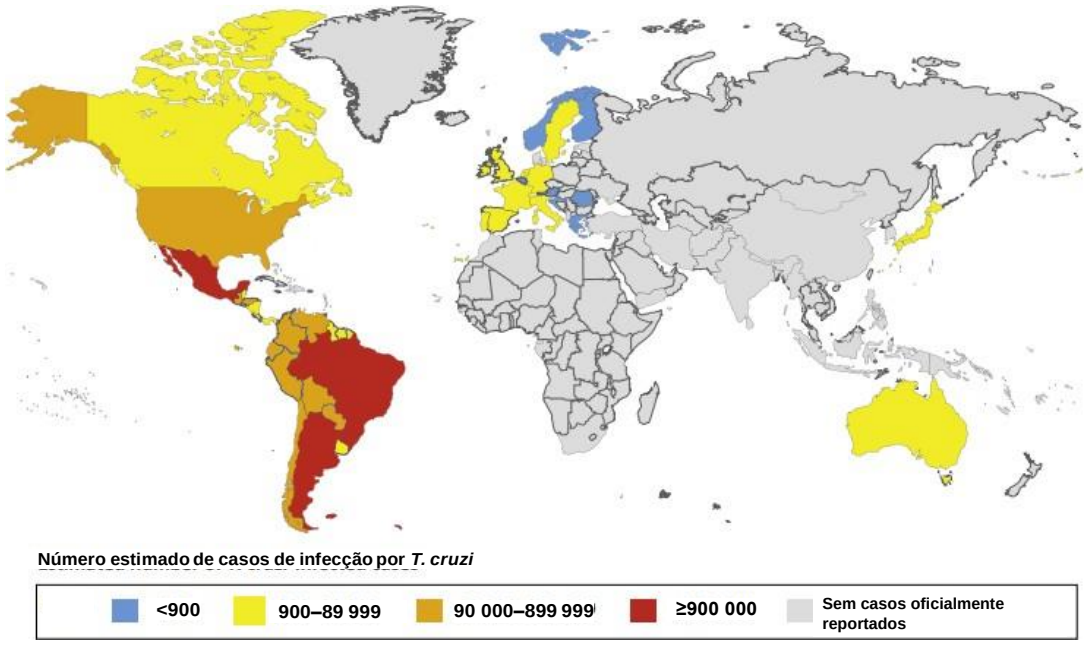

Figura 1. Distribuição global de Doença de Chagas. O mapa demonstra a distribuição estimada de casos de infecção pelo *T. cruzi* tanto em países naturalmente endêmicos quanto em países para onde houve migração de indivíduos infectados. Adaptado de Perez Catherine *et al (*10*)*.

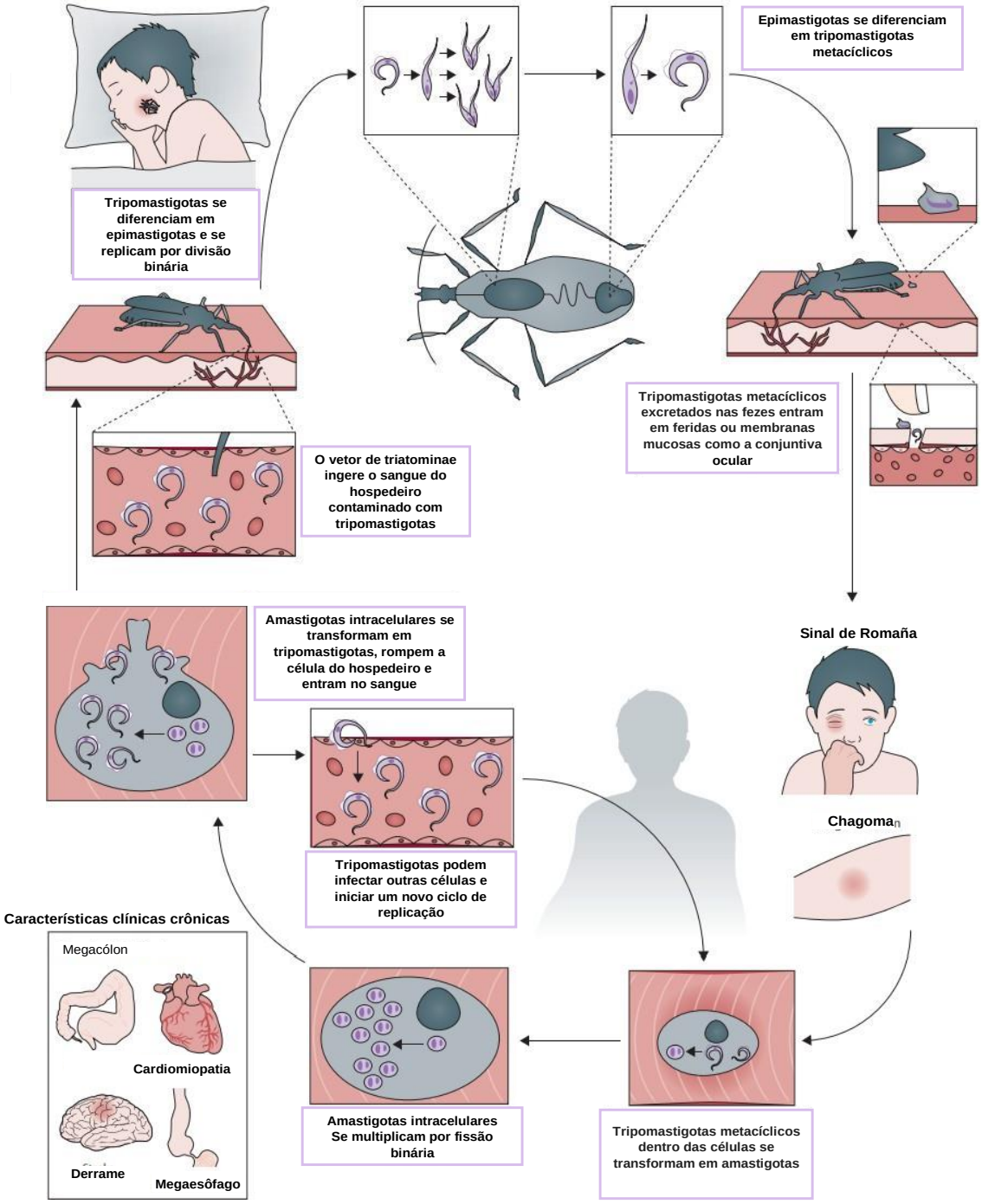

Figura 2. Transmissão vetorial e ciclo de vida do *Trypanosoma cruzi*. A penetração da membrana mucosa intacta do olho por tripomastigotas infecciosos leva a uma reação indolor da conjuntiva, com edema unilateral de ambas as pálpebras e linfadenite do gânglios pré-auriculares (sinal de Romaña). Uma picada em qualquer outra parte da pele pode levar a uma reação no tecido subcutâneo com edema local e rigidez, congestionamento vascular e infiltração celular (chagoma). O *T. cruzi* em sua forma tripomastigota adentra a célula do hospedeiro e passa pelo processo de transformação em diversos amastigotas. Quando a célula local está inchada com amastigotas, eles se transformam de volta em tripomastigotas flagelados.

Com o movimento excessivo dos flagelos dentro das células ocorre lise da membrana celular. Após isso, os parasitas se espalham através dos linfáticos e da corrente sanguínea para locais distantes, principalmente células musculares (cardíacas, lisas e esqueléticas) e células gânglios, onde passam por mais ciclos de células intracelulares de multiplicação. Adaptado de Pérez Molina et al. (2, 11).

1.2. INFECÇÃO E RESPOSTA IMUNE INATA AO *TRYPANOSOMA CRUZI*

O *Trypanosoma cruzi* pode invadir ativamente uma gama de células fagocíticas e não fagocíticas por dois mecanismos diferentes: uma rota responsável por 20-30% das invasões, que induz a sinalização de Ca2+ pela geração de trifosfato de inositol (IP3), seguida pelo recrutamento e fusão dos lisossomos da célula hospedeira no local de entrada do parasita e uma segunda rota (70-80% das invasões) que dependente da invaginação da membrana plasmática, seguida de fusão intracelular com lisossomos (12-17). A acidificação lisossômica do vacúolo contendo os parasitas (vacúolo parasitóforo) contribui para a diferenciação tripomastigota-amastigota que ocorre no citoplasma. Após várias rodadas de replicação, os amastigotas se diferenciam em tripomastigotas altamente móveis que causam a ruptura da membrana da célula hospedeira, podendo infectar células vizinhas ou até mesmo atingir a corrente sanguínea, disseminando a infecção a tecidos distantes (18, 19).

Macrófagos residentes no local da infecção estão entre os primeiros fagócitos profissionais a serem invadidos pelo parasita (20). Para estabelecer uma infecção produtiva nessas células, o *T. cruzi* tem que suportar um ambiente extremamente oxidativo dentro dos fagolisossomos (21), que só é possível graças a uma complexa rede de enzimas antioxidantes, como

peroxidases e superóxido dismutases, que protegem o parasita contra espécies reativas de oxigênio e nitrogênio liberadas pelos macrófagos via atividade da enzima óxido nítrico sintase induzida (iNOS), contribuindo assim para a morte do parasita (22-24). Embora o NO possa afetar a sobrevivência do parasita nos macrófagos, o estresse oxidativo causado pela produção de espécies reativas de oxigênio (ROS) e NO acaba sendo prejudicial ao hospedeiro, devido ao seu alto potencial de dano tecidual (23, 25-27).

Durante os estágios iniciais da infecção, o *T. cruzi* induz uma resposta inflamatória intensa, que desempenha um papel crucial na patogênese da doença. Um mecanismo imunológico inato proposto para a fase aguda da infecção envolve o desencadeamento da síntese de IL-12 por macrófagos, o que provoca a síntese de IFN-γ por células NK (28-30). De fato, a depleção de células NK1.1 em camundongos infectados com *T. cruzi* modula negativamente a produção inicial de IFN-γ por esplenócitos isolados (31) e a ausência de NK aumenta a susceptibilidade dos animais ao parasita, por mecanismos independentes de perforina (32), indicando que essas células possuem uma função efetora inicial contra a infecção. Macrófagos peritoneais deficientes para componentes da via de IL-12 apresentam polarização para o perfil M2 quando infectados com *T. cruzi*, secretando espontaneamente grandes quantidades de TGF-β e fraca produção de NO. A adição de IFN-γ à cultura celular não é suficiente para reverter a produção de TGF-β, sugerindo que a IL-12 possa ter um papel mais importante do que o IFN-γ nesse processo (33). Camundongos tratados com anticorpo monoclonal anti-IL12 apresentam aumento significativo na parasitemia e mortalidade (34), reforçando a ideia de que IL-12 é fundamental na resposta inicial ao parasita.

Receptores do tipo Toll (TLR) têm um papel crítico na resistência do hospedeiro ao *T. cruzi*. Camundongos deficientes para as moléculas MyD88, TLR2, TLR4 e TLR9 são mais susceptíveis à infecção, apresentando maior parasitemia e mortalidade. Essa susceptibilidade foi associada a menor produção das citocinas inflamatórias IL-12, TNF-α e IFN-γ. Animais deficientes para TLR4 apresentam menor produção de NO, o que pode contribuir para o menor controle dos parasitas (35-37). Há ainda um papel dos receptores citosólicos do tipo NOD (NLR) no controle da infecção. Animais deficientes para NOD1 se mostram altamente susceptíveis ao parasita, sucumbindo à infecção e exibindo grande quantidade de parasitas no sangue, tecido cardíaco e baço (38) . Foi verificada também a participação do inflamassoma NLRP3 no controle da parasitemia, via indução de NO por um mecanismo dependente de caspas-1 e independente de IL-1R (39). Em humanos, observa-se um aumento na quantidade das citocinas inflamatórias IL-6 e TNF-α no sangue de indivíduos infectados tanto na fase aguda quanto crônica, evidenciando uma ativação persistente da resposta imune inata ao longo da infecção (40, 41). Experimentalmente, animais deficientes para IL-6 apresentaram três vezes mais parasitemia, além do aumento na taxa de mortalidade, quando comparados aos animais controles infectados, atribuindo então um papel protetor à produção de IL-6 contra o parasita (42).

Outro ponto característico da infecção pelo *T. cruzi* é a produção de interferons do tipo I (IFN I). Dados anteriores descreveram uma indução robusta de genes estimulados pelos IFN I na pele de camundongos 24 horas após a infecção intradérmica. O trabalho aponta para a possibilidade do início da resposta do hospedeiro poder ser determinante para o parasita estabelecer

uma infecção bem sucedida, embora não tenha ficado claro se a resposta imediata de IFN I promove proteção ou suscetibilidade (43). A indução de IFN-β e genes relacionados, como 2',5'-oligoadenilato sintase 1 (OAS1) e os genes estimulados por IFN 15 (ISG15) e 44 (ISG44) também foi observada na infecção *in vitro* de fibroblastos humanos (44), indicando que o parasita estimula esses genes de uma maneira generalizada em seus hospedeiros mamíferos.

Evidências experimentais sugerem que a indução de IFN I de forma dependente de TLRs seja fundamental para o controle do parasita em células dendríticas e macrófagos, uma vez que essas células são mais susceptíveis à infecção quando duplo deficientes para MyD88 e TRIF ou MyD88 e receptor de IFN I (IFNAR) (45). Entretanto, dados contrastantes indicam que uma via dependente das proteínas TBK-1 (do inglês, TANK-binding kinase1) e fator regulador de interferon 3 (IRF3) seja a responsável pela indução de IFN I pelo parasita em macrófagos e fibroblastos, enquanto TLRs e os receptores de RNA da família dos RLRs (RIG-I e MDA5) não seriam necessários (46).

Embora os IFN I sejam induzidos de forma proeminente durante a infecção pelo *T. cruzi*, seu papel no controle ou susceptibilidade ao parasita ainda é controverso. Dados da literatura sugerem que os IFN I participam na indução de NO pelo *T. cruzi* e que isso possa ter um impacto positivo no controle do parasita. Demonstrou-se ainda que o tratamento de camundongos C57BL/6 selvagens (do inglês, *wildtype*: WT) com IFN I reduzia a parasitemia, enquanto camundongos IFNAR KO desenvolviam uma parasitemia 3 vezes maior na fase aguda da infecção (47). Animais duplo deficientes para MyD88 e IFNAR se mostraram mais susceptíveis ao parasita em comparação a animais

deficientes apenas para MyD88, salientando a importância da sinalização de IFN I na proteção contra infecção (45). Por outro lado, camundongos WT sucumbiram à infecção sob condição de desafio letal com o *T. cruzi*, enquanto camundongos IFNAR KO foram capazes de controlar o crescimento do parasita e sobreviver (48). Sugere-se que essas discrepâncias possam ter ocorrido devido a variações tanto na rota de infecção quanto na quantidade de parasitas utilizados. Portanto, é importante que novos estudos sejam desenvolvidos para um melhor entendimento do papel dos IFN I na interação entre o parasita e as células hospedeiras, bem como suas consequências na patogênese da infecção.

1.3. RESPOSTA IMUNE ADAPTATIVA AO *TRYPANOSOMA CRUZI*

O *Trypanosoma cruzi* é capaz de induzir a formação de respostas imunológicas complexas e diversas células já foram apontadas como importantes no controle da infecção. No contexto da imunidade adaptativa, a ausência de células B em camundongos infectados se mostrou letal, mesmo com a administrações de pequenas doses do parasita (49). Além disso, as células T CD4+ também se mostram importantes no contexto da infecção com *T. cruzi*, sendo sua depleção correlacionada com aumento de parasitismo e miocardite em camundongos (50). Pacientes HIV positivos, com deficiência na geração de resposta imune dependente de células T CD4+, apresentam pior prognóstico e maior mortalidade quando infectados com *T. cruzi* (51), indicando uma função protetora para essas células.

O subtipo mais característico de célula T CD4+ no contexto da infecção é a T-helper 1 (Th1) e seu papel protetor se dá principalmente pela produção de IFN-γ. A participação dessas células na infecção acaba sendo ampla, pois podem contribuir para a indução de anticorpos, ativação de células fagocíticas e no auxílio de diferenciação de outros subtipos de células T, incluindo as células T CD8+ (52-54). Além disso, temos as células Th17 como um outro subtipo de linfócitos T CD4+ observados na infecção, podendo também apresentar um papel protetor contra o parasita (55).

As células T CD8+ desempenham um papel crucial no controle da disseminação do *T. cruzi* (56), porém os mecanismos de indução dessas células ainda não são totalmente claros (57). De fato, as células T CD8+ específicas para o *T. cruzi* se diferenciam de maneira dependente do fator de transcrição T-bet e a resposta inicial de T CD8+ pode ser aumentada em resposta a adjuvantes de diferentes tipos de TLR (58). Entretanto, a formação de células T CD8+ específicas contra o parasita desencadeada pela infecção natural por *T. cruzi*, permanece preservada mesmo na ausência de TRL2, 4, 9 e MyD88, apesar do aumento na susceptibilidade à infecção, sugerindo então que uma via alternativa esteja relacionada à formação da resposta adaptativa dependente de T CD8+ (37).

Células T CD8+ isoladas de camundongo no estágio crônico da infecção, apresentam baixos níveis de expressão de marcadores de exaustão, como PD-1, Lag-3 e Tim-3, demonstrando que essas células permanecem funcionais e competentes em contribuir com o controle do crescimento do parasita, mesmo em estágios mais avançados da infecção (59). O papel protetor das células T CD8+ se dá pincipalmente pela produção de IFN-γ, TNF-α, granzimas

citotóxicas e perforina (60). Pacientes com cardiomiopatia chagásica crônica que apresentam melhor prognóstico possuem maior quantidade de células T CD8+ específicas para o parasita, produzindo IFN-γ (61). Em camundongos, o acumulo de células T CD8+ produtoras de IFN-γ está relacionado à menor lesão de cardiomiócitos, enquanto que as células T CD8+ produtoras de perforina desempenharam um papel prejudicial, agravando a lesão (62).

Embora os linfócitos T e suas citocinas tenham um papel protetor na infecção aguda experimental, dados em animais e pacientes cronicamente infectados indicam que uma resposta desregulada dos linfócitos T ao longo da infecção possa contribuir para o desenvolvimento da CCC (63). Portanto, um melhor entendimento dos mecanismos imunológicos relacionados a geração e manutenção dessas células é necessário para que possamos intervir de forma mais eficiente no combate à progressão para doença grave e melhorar as estratégias de tratamento.

1.4. STING E RESPOSTA IMUNE

A proteína STING (estimulador de genes de interferon), também conhecida como TMEM173, MPYS, MITA e ERIS, está localizada na membrana do retículo endoplasmático e é conhecida por ser um mediador crítico da resposta inata a ácidos nucleicos citoplasmáticos. Ela pode ser ativada por dinucelotídeos cíclicos bacterianos (c-di-GMP e c-di-AMP), assim como pelo GMP-AMP cíclico (cGAMP), produzido pela enzima cGAS (do inglês, *Cyclic GMP-AMP synthase*). Outros receptores de DNA como DDX41 e

IFI16 também podem participar na ativação de STING, embora cGAS ainda figure como o principal (64, 65).

A interação dos dinucleotídeos cíclicos com STING induz modificações conformacionais nessa proteína e sua translocação para o complexo de Golgi. Durante este processo, o terminal carboxila de STING recruta e ativa a quinase TBK-1, que por sua vez fosforila o fator de transcrição IRF3 (66). O IRF3 fosforilado se dimeriza e entra no núcleo, induzindo a expressão de IFN I. A proteína STING também ativa a quinase IKK, que fosforila a família de inibidores IkB do fator de transcrição NF-kB. As proteínas IkB fosforiladas são degradadas pela via ubiquitina-proteassoma, liberando NF-kB, que entra no núcleo juntamente a IRF3 e outros fatores de transcrição para induzir a expressão de IFN I e citocinas inflamatórias, como TNF-α, IL-1β e IL-6 (67-69) (Fig. 3). Em células humanas, STING se mostrou importante para a indução de IL-6 em resposta ao reconhecimento de DNA (70). Além disso, outro trabalho demonstrou que IL-6 e RIG-I promovem a degradação de STING, ativando a proteína quinase UNC-51 (ULK1), corroborando com a hipótese de haver um *feedback* negativo entre STING e IL-6 (71).

A via cGAS-STING tem sido estudada em diversos contextos, sendo observado um papel central da mesma na indução de resposta imune inata contra bactérias, vírus, protozoários, tumores e até mesmo ao DNA mitocondrial liberado frente a algum estresse celular (72-77). Parasitas da malária são capazes de liberar vesículas extracelulares, contendo RNA do parasita e DNA genômico que induzem a fosforilação de IRF3 de forma dependente de STING (30). No contexto da infecção com *Mycobacterium tuberculosis*, STING se mostrou importante para a produção das citocinas IFN-

β e IL-12 por células dendríticas (78). Mais recentemente, outro trabalho demonstrou que vesículas purificadas de *T. cruzi* eram suficientes em induzir as citocinas TNF-α, IL-6, and IL-1β em macrófagos, de forma dependente da sinalização PARP1 (enzima de reparo de DNA), cGas e NFkB (79), porém a participação direta de STING nesse contexto não foi abordada.

Além da interação da via de sinalização dependente STING com a indução de uma resposta imune inata, STING se mostrou importante para geração de células T CD8+ específicas contra HSV-1 e no controle da disseminação do vírus para diferentes órgãos (80). No mais, diversos trabalhos relacionam a via de sinalização de STING com a elaboração da resposta de linfócitos T em modelos tumorais (81, 82). Embora um estudo anterior tenha demonstrado que as proteínas TBK-1 e IRF3, intimamente relacionadas a STING, sejam fundamentais para a indução de IFN I em resposta ao *T. cruzi* em macrófagos e fibroblastos (46), o papel de STING no reconhecimento do parasita por células infectadas ainda não foi demonstrado. Portanto, nesse estudo visamos investigar os mecanismos moleculares resultantes da interação de STING com o *Trypanosoma cruzi* e seus impactos no desenvolvimento de imunidade contra o parasita e proteção contra a infecção aguda.

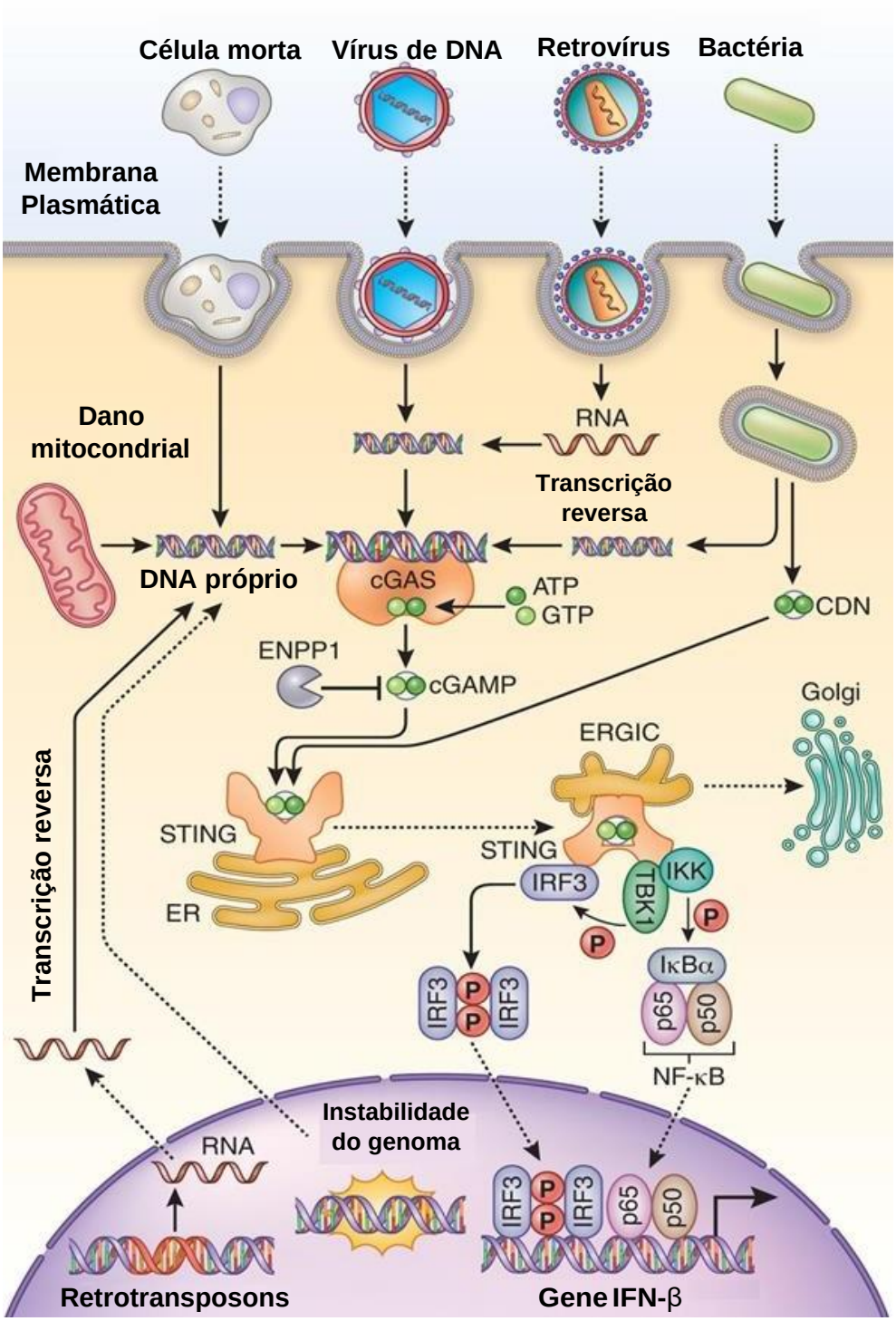

Figura 3. Via de sinalização cGas-STING. O DNA citosólico, podendo ser proveniente de diferentes fontes, se liga e ativa a molécula cGas, que catalisa a conversão de ATP e GTP em cGAMP. O cGAMP se liga à proteína STING no retículo endoplasmático. STING trafega para o compartimento intermediário entre o retículo endoplasmático e o complexo de golgi (ERGIC) e então ativa

IKK e TBK1. Uma vez fosforilado, TBK1 recruta IRF3 para a fosforilação. IRF3 fosforilado se dimeriza e entra no núcleo e induz a expressão de interferons do tipo I e outras moléculas imunomodulatórias. Adaptado de Chen Qi *et al* (83).

2. HIPÓTESE

A hipótese do nosso trabalho é que a proteína STING desempenha um papel importante na formação de uma resposta imunológica protetora contra o *Trypanosoma cruzi*.

3. OBJETIVO GERAL

Avaliar o papel da proteína STING na resposta imunológica à infecção pelo *Trypanosoma cruzi*.

4. OBJETIVOS ESPECÍFICOS

4.1. Avaliar o papel de STING na ativação imunológica de macrófagos infectados com T*. cruzi*.

4.2. Avaliar o papel de STING na ativação imunológica frente ao DNA do *T. cruzi*.

4.2. Avaliar o papel de STING na resposta imunológica de camundongos infectados com *T. cruzi*.

4.3. Avaliar o papel de STING no controle da infecção aguda com o *T. cruzi*.

5. MÉTODOS

5.1. CULTURA DE MACRÓFAGOS, INFECÇÃO PELO *TRYPANOSOMA CRUZI* E TRANSFECÇÕES

O parasita (cepa Y) foi mantido em células epiteliais de rim de macaco (LLCMK2). As células foram regularmente cultivadas em garrafas T75 (Thermo Fisher) em meio DMEM 10 (*Dulbecco's Modified Eagle Medium High glucose*, acrescido de 10% de soro fetal bovino (SFB) (Thermo Fisher)). Durante a infecção, as células LLCMK2 foram mantidas em meio DMEM 2 (2% de SFB). Os parasitas liberados no sobrenadante de cultura foram centrifugados a 1350 x g por 10 min, ressuspensos em meio DMEM 2 e as formas tripomastigotas foram contadas em câmara de Neubauer.

Macrófagos das linhagens RAW-Lucia™ ISG (InvivoGen) e RAW-Lucia™ ISG-KO-STING (InvivoGen) foram plaqueados em placas de 24 poços (Corning) na quantidade de 100.000 células por poço em meio DMEM 2, em volume final de 500 µl, 24 horas antes da infecção, da exposição ao parasita morto ou da transfecção. Para a infecção, o sobrenadante foi removido e os macrófagos foram incubados com $3x10^6$ parasitas por poço da placa, em volume final de 300 µl de DMEM 2. Dezesseis horas depois, os poços foram lavados com PBS vezes suficientes para retirar os parasitas e as células foram incubadas em 300 µl de DMEM 2 por mais 24h para obtenção do sobrenadante e do RNA total. Alternativamente, para os experimentos com o *T. cruzi* morto, os parasitas foram incubados a 56 °C por 10 minutos e a morte foi confirmada por visualização na câmara de Neubauer. Assim como a infecção convencional, os parasitas mortos foram deixados em contato com as células por 16h, em volume final de 300 µl de DMEM2 e depois as células foram

incubadas por mais 24h em 300 µl de DMEM 2 para obtenção do sobrenadante e do RNA total.

Os macrófagos foram também transfectados com DNA do *T. cruzi* (80ng/poço) complexado com 0,2 µl de Lipofectamina 2000 em volume final de 300 µl de OPTIMEM (Thermo Fisher), como sugerido pelo fabricante. Para isso, os poços foram previamente lavados com PBS e então transfectados. O sobrenadante e o RNA total foram obtidos 40h após a transfecção. Para obtenção do DNA do *T. cruzi*, os parasitas foram mortos por calor, 56ºC por 10 minutos, e centrifugados a 1350 x g por 10 minutos. O pellet foi incubado em 0,5 ml de tampão de lise (100 µl Tris.HCl 1M, pH 8,5; 10 µl EDTA 0,5M, pH 8,0; 200 µl NaCl 1M, 10 µl SDS 20%, 5,0 µl Proteinase K 20 µg/µl, 675 µl água Milli-Q autoclavada) a 37°C utilizando um Thermomixer (Eppendorf) a 600 rpm por18h. Após isso, foi acrescentado 0,5 ml de isopropanol e a solução foi homogeneizada até se formar a nuvem de DNA. A solução foi centrifugada a 8600 x g por 5 min e o sobrenadante descartado. Foi adicionado 0,5 ml de etanol 70% e a solução foi centrifugada a 8600 x g por 5 minutos. O sobrenadante foi descartado e o pellet de DNA foi seco ao ar. O DNA foi então ressuspenso em água e a pureza foi analisada com o auxílio do Nanodrop (Thermo Fisher).

Como controles positivos de estimulação dependente e independente de STING, alguns poços da placa foram lavados 1x com PBS e transfectados com 1,0 µg/ml de c-di-GMP (InvivoGen) ou 0,5 µg/ml de Poly I:C (InvivoGen) complexados com 0,8 µl de Lipofectamina 2000 (Thermo Fisher) em volume final de 300 µl de OptiMEM (Thermo Fisher), de acordo com as instruções do fabricante.

5.2. ATIVIDADE DE LUCIFERASE

Macrófagos das linhagens RAW-Lucia™ ISG (InvivoGen) e RAW-Lucia™ ISG-KO-STING (InvivoGen) secretam a proteína luciferase ao meio de cultura sob estímulos que iniciem vias de ativação dependentes de IRF, uma vez que o gene repórter está sob o domínio do promotor I-ISG54, que é composto pelo promotor ISG54 induzido por IFN e reforçado por um ISRE (do inglês I*FN-st*imula*ted response element*). Essas células foram cultivadas, infectadas, expostas ao parasita morto ou transfectadas como descrito acima. O sobrenadante das culturas infectadas ou expostas ao parasita morto foi coletado e diluído 10x em DMEM *High glucose*, enquanto o sobrenadante das células transfectadas foi diluído 10x em OPTMEM. Os sobrenadantes diluídos foram utilizados para a detecção da atividade de luciferase. Resumidamente, 20 µl de sobrenadante diluído 10x foram misturados a 50 µl de QUANTI-Luc™ (InvivoGen) e lidos imediatamente em um luminômetro Smart Line TL (Titertek Berthold), com tempo de aquisição de 1s.

5.3. LUMINEX

A detecção de IFN-β, IL-6 e IL-12 no sobrenadante de cultura de macrófagos foi feita com o *Kit Mouse Custom ProcartaPlex* (Invitrogen) de acordo com as instruções dos fabricantes. Resumidamente, as beads magnéticas ligadas a anticorpos foram adicionadas à placa e em seguida incubadas com 12,5 µl de amostra por 60 – 120 minutos, protegido da luz. Após as lavagens, foram adicionados 6,25 µl do Mix detector de anticorpo e

incubado por mais 30 minutos. A placa foi lavada e as amostras ressuspensas em 50 µl de *Reading Buffer*. A placa foi agitada em temperatura ambiente por 5 minutos antes de ser lida no aparelho *MagPix* (Merck) e analisada pelo software *Milliplex Analyst* (Millipore).

5.4. CAMUNDONGOS

Camundongos BALB/c, C57BL/6 e C57BL/6 deficientes para STING (STING-KO) machos (6-8 semanas de idade), foram mantidos no biotério do Instituto de Medicina Tropical II, Universidade de São Paulo. Os animais foram alojados em grupos de até 5 por gaiola em uma sala com luz e temperatura controlada (ciclos claro/escuro de 12 horas, 21 ± 2 ◦C) com livre acesso a alimentos e água. O estudo foi aprovado sob o número 1567/2020 e realizado de acordo com as recomendações da Comissão de Ética no Uso de Animais (CEUA) da Faculdade de Medicina da USP.

5.5. MANUTENÇÃO DO PARASITA *IN VIVO*

A cepa Y do *Trypanosoma cruzi* foi mantida em animais BALB/c machos (6-8 semanas de idade). Para o repique dos parasitas, os animais foram eutanasiados com injeção intraperitoneal de xilazina (30 mg/kg) e cetamina (300 mg/kg), o sangue foi coletado por punção cardíaca e armazenado em tubo contendo solução de citrato de sódio 3,2%, para evitar coagulação. Em seguida, foi feita a contagem de parasitas utilizando o método de Brenner (84). Resumidamente, 5 µl de sangue proveniente da punção cardíaca foi avaliado entre lâmina e lamínula de 22 x 22 mm, com a contagem de 50 campos no

aumento de 40x em microscópio óptico. O repique foi feito a cada 5 dias pós infecção (pico da parasitemia), passando-se 100 mil parasitas para cada novo animal por inoculação intraperitoneal.

5.6. INFECÇÃO *IN VIVO* E PARASITEMIA

O parasita foi coletado a partir da punção cardíaca de animais Balb/c, como descrito anteriormente. O sangue foi centrifugado por 10 minutos a 200 x g e o sobrenadante coletado. Feito isso, o sobrenadante foi centrifugado por 10 minutos a 3800 x g. O pellet foi ressuspenso em meio RPMI (Gibco) sem soro e a contagem dos parasitas foi feita na câmara de Neubauer. Os animais C57BL/6 WT e C57BL/6 SINTG-KO foram infectados de forma intraperitoneal com 50 mil tripomastigotas da cepa Y diluídos em 200 µl de meio RPMI. A parasitemia foi acompanhada utilizando-se 5 µl de sangue da cauda dos animais do dia 4 ao dia 12 pós infecção, pelo método de Brenner, como descrito anteriormente. Os animais foram eutanasiados nos dias 4, 7 e 13 pós infecção com injeção intraperitoneal de xilazina (30 mg/kg) e cetamina (300 mg/kg) seguido de deslocamento cervical. Coletamos coração e baço dos animais para as análises subsequentes.

5.7. DETECÇÃO DE ÓXIDO NÍTRICO (NO)

Para análise de NO, as células RAW foram plaqueadas e infectadas, como descrito anteriormente. Após a infecção, as células foram lavadas com PBS e cultivadas em 300 µl de meio DMEM *high glucose* sem fenol (Nova biotecnologia) por mais 48 horas. Alternativamente, esplenócitos de animais

C57BL6 e STING-KO infectados foram plaqueados em placas de 96 poços fundo U (Corning), sendo 0,5 x10^6 células por poço em meio 200 µl de DMEM *high glucose* sem fenol por 48 horas. Posteriormente, o sobrenadante de cultura foi coletado e armazenado a -80°C. Para o experimento, utilizamos *o kit Nitric Oxide Assay* (Thermo Fisher). Resumidamente, as amostras foram centrifugadas a 15.000 x g por 5 minutos, para a retirada de resquícios celulares e o sobrenadante foi coletado. Todas as amostras foram diluídas 2x, seguindo a recomendação do fabricante. O ensaio foi feito em placa de 96 poços e 50 µl de amostra foi incubado com 25 µl de NADH e 25 µl de nitrato redutase por 30 minutos a 37°C. Após isso, o reagente de Griess foi adicionado aos poços e a placa foi incubada por 10 minutos em temperatura ambiente. A leitura foi feita no espectrofotômetro E*poch* (Biotek) em um comprimento de onda de 540nm.

5.8. PCR EM TEMPO REAL

A extração de RNA total dos macrófagos foi feita utilizando *Trizol reagent* (Thermo Fisher). Resumidamente, 500 µl de Trizol foram adicionados a cada poço da placa para rompimento celular. As amostras foram homogeneizadas e transferidas para tubos de 1,5 ml livres de DNAse e RNAse (Axigen). Foram adicionados 100 µl de clorofórmio (Merck) em cada tubo e os mesmos foram vortexados e centrifugados por 15 min a 12.000 x g e 4°C. A fase aquosa contendo o RNA foi transferida para novos tubos de 1,5 ml (Axigen), nos quais 250 µl de isopropanol (Merck) foram adicionados. As amostras foram homogeneizadas por inversão. Os tubos foram centrifugados por 10 min a 12.000 x g e 4°C. O sobrenadante foi descartado e o pellet ressuspenso em

500 µl de etanol 75% (Merck). Os tubos foram centrifugados por 5 min a 12.000 x g e 4°C. O sobrenadante foi descartado e o excesso de etanol dos pellets secou ao ar. Os pellets foram então ressuspensos em 20 µl de água livre de RNAse e DNAse (Thermo Fisher). Para extração de RNA total do tecido cardíaco, utilizamos o *kit RNeasy Fibrous Tissue* (Qiagen) seguindo as recomendações do fabricante. Além disso, para a extração de RNA total do baço utilizamos o *kit RNeasy* (Qiagen) seguindo as recomendações do fabricante. Em todos os casos, a concentração de RNA foi determinada com o auxílio de um nanodrop (Thermo Fisher). A integridade do RNA foi confirmada em gel de agarose. O cDNA foi obtido a partir da transcrição reversa do RNA extraído, utilizando-se *Superscript II Reverse Transcriptase* (Thermo Fisher). Resumidamente, 1 µg de RNA total foi incubado com Oligo DT_{12-18} e dNTP (Thermo Fisher) a 65 ºC por 5 min, nas concentrações recomendadas pelo fabricante. Uma solução contendo DTT, a enzima Superscript II, o tampão 5x First-Strand buffer e RNAse OUT foi adicionada a cada tubo e os mesmos foram incubados a 42ºC por 50 min e 70º C por 15 min em um termociclador Veriti (Applied Biosystems). O PCR em tempo real foi feito utilizando *Power Sybr green Master mix* (Applied Biosystems) e o termociclador Quanti Studio 12k (Applied Biosystems). A amplificação foi feita com os parâmetros a seguir: 95ºC por 15 min; 40 ciclos de 95ºC por 15s e 60ºC por 1 min. Os primers utilizados foram sintetizados (Thermo Fisher) a partir das sequências: HPRT1 *forward* 5'-*GTTGGGCTTACCTCACTGCT-3';* HPRT1 *reverse* 5'-GCAAAAAGCGGTCTGAGGAG-3'; IFNβ *forward* 5'-TGGGAGATGTCCTCAACTGC-3'; IFNβ *reverse* 5'-CCAGGCGTAGCTGTTGTACT-3'; IL-6 *forward* 5'-

CCCCAATTTCCAATGCTCTCC-3’; IL-6 *reverse* 5’-GGATGGTCTTGGTCCTTAGCC-3’; IL-12 *forward* 5’-GAAGTCCAATGCAAAGGCGG-3’; IL-12 *reverse* 5’-GAACACATGCCCACTTGCTG-3’; TNFα *forward* 5’-ATGGCCTCCCTCTCATCAGT-3’; TNFα *reverse* 5’-TTTGCTACGACGTGGGCTAC-3’; CXCL9 *forward* 5’-CCAAGCCCCAATTGCAACAA-3’; CXCL9 *reverse* 5’-AGTCCGGATCTAGGCAGGTT-3’; IFNγ *forward* 5’-AGCAAGGCGAAAAAGGATGC-3’; IFNγ *reverse* 5’-TCATTGAATGCTTGGCGCTG-3’; PRF1 *forward* 5’-TGGTGGGACTTCAGCTTTCC-3’; PRF1 *reverse* 5’-GAAAAGGCCCAGGAGGAACA-3’.

Para detecção de DNA do parasita no coração de animais infectados, extraímos DNA do tecido cardíaco usando o *Kit FlexiGene* (Qiagen), seguindo as instruções do fabricante. Utilizamos as sequências de *primers* previamente descritas (85). O PCR quantitativo em tempo real foi feito utilizando *Power Sybr green Master mix* (Applyed Biosystems) e o termociclador Quanti Studio 3 (Applied Biosystems). O gene da beta-actina foi utilizado como controle endógeno nesse teste. O cálculo de parasitismo no coração foi feito a partir de uma curva de diluição de DNA de *T. cruzi*.

5.9. CITOMETRIA DE FLUXO

Os baços de animais C57BL6 ou STING KO, infectados ou não, foram coletados no dia 13 após infecção e macerados em 2 ml de RPMI1640

(Thermo Fisher) com auxílio de *Cell strainer* de 70 µm (Corning). Os macerados foram tratados por 2 minutos com ACK lysis buffer (Gibco), para a lise de hemácias. Após isso, as células totais foram plaqueadas em placas de 96 poços fundo U (Corning), sendo 0,5 x 10^6 células por poço em volume final de 200 µl de R10 (RPMI1640 suplementado com L-glutamina 2 mM (Sigma), solução de aminoácidos não essenciais (1% vol/vol) (Thermo Fisher), piruvato de sódio 1 mM (Thermo Fisher), 2β-Mercaptoetanol 5x10^{-5}M (Sigma), 10% vol/vol de soro fetal bovino (Thermo Fisher) e Gentamicina (40 µg/mL). As células foram estimuladas - ou não - com peptídeo do *Trypanosoma cruzi* específico para células T CD8+, restrito ao MHC H2-K^b (TSKB20), na concentração de 10 µg/mL, por 16 horas a 37 ºC e 5% de CO_2. Para o controle positivo, as células foram estimuladas pelo mesmo período com PMA (50 ng/mL) e Ionomicina (500 ng/mL). Simultaneamente aos estímulos, foram adicionados 5 µg/ml de Brefeldina A (Biolegend) em todos os poços. Após estímulo, as células foram transferidas para uma placa de 96 poços em fundo V (Corning), centrifugada a 300x g por 5 minutos. O sobrenadante foi descartado e as células foram marcadas em volume final de 25 µL de PBS, contendo os anticorpos monoclonais anti-CD3 APC-Cy7 (BD Biosciences), anti-CD4 PerCP (BD Biosciences) e anti-CD8 PE-Cy7 (BD Biosciences), ao abrigo da luz por 30 minutos a 4°C. As células foram lavadas duas vezes com 150 µL de PBS e foram incubadas em 50 µL de BD Cytofix/Cytoperm™ por poço, durante 15 minutos a temperatura ambiente. Posteriormente, as células foram lavadas duas vezes com 150 µL de BD Perm/Wash™ buffer e foram marcadas, ao abrigo da luz, em volume final de 25 µL de BD Perm/Wash™ buffer, contendo os anticorpos anti-IFNγ APC (BD Biosciences) e anti-Perforina PE (Biolegend)

por 30 minutos a 4°C. As células foram lavadas duas vezes com 150µL de BD Perm/Wash™ buffer e ressuspensas em volume final de 150 µL de PBS. As amostras foram adquiridas no citômetro FACS Canto II (BD) e analisadas com o auxílio *do software FlowJo 10 (BD)*.

5.10. ANÁLISE HISTOLÓGICA

As amostras de coração foram fixadas em solução de formalina tamponada a 10%, desidratadas em uma concentração crescente de soluções de etanol e embebidas em parafina. Os blocos foram seccionados com espessura de 5 µm e corados com hematoxilina-eosina (H&E). O patologista realizou a análise histológica desconhecendo os genótipos dos camundongos. O escore inflamatório foi determinado como: 0- ausência de miocardite: ausência ou mínimo infiltrado inflamatório focal; 1- miocardite leve: infiltrado inflamatório discreto, focal ou multifocal, com escassa agressão aos cardiomiócitos; 2- miocardite moderada: infiltrado inflamatório nítido, predominantemente multifocal com eventuais áreas difusas (coalescência), com múltiplos focos de agressão aos cardiomiócitos; 3- miocardite intensa: infiltrado inflamatório exuberante, predominantemente difuso, com múltiplos focos de agressão dos cardiomiócitos.

5.11. ANÁLISE ESTATÍSTICA

Os resultados foram analisados utilizando-se *o software Graph Pad Prism* 8. Para comparações entre 2 parâmetros utilizamos o teste Mann-Whitney e

para comparações de vários parâmetros utilizamos os testes Two-way ANOVA, Tukey's e Bonferroni para múltiplas comparações.

6. RESULTADOS

6.1. SINALIZAÇÃO DE STING É NECESSÁRIA PARA A PRODUÇÃO DE CITOCINAS EM RESPOSTA À INFECÇÃO PELO *TRYPANOSOMA CRUZI*

A infecção com *Trypanosoma cruzi* induz a produção de uma variedade de citocinas que são importantes para controlar a replicação dos parasitas e o estabelecimento da doença. Embora o aumento da expressão dos IFNs do tipo I, IL-6 e IL-12 tenha sido observado na infecção por *T. cruzi,* os mecanismos subjacentes ainda não são totalmente compreendidos. Dados anteriores sugerem que uma via de sinalização dependente de TBK-1 e IRF3 é essencial para a indução IFN-β em resposta a *T. cruzi* (46). Dado que o STING é uma das principais moléculas que interage com as proteínas TBK-1 e IRF3, buscamos avaliar seu papel na produção IFN-β em resposta ao parasita. Como o STING também está envolvido na indução de citocinas pró-inflamatórias dependentes de NF-kB (86), procuramos determinar seu papel na produção de IL-6 e IL-12 durante a infecção. Para responder nossa pergunta, usamos macrófagos RAW-Lucia™ ISG e RAW-Lucia™ ISG-STING-KO, que são suficientes ou deficientes para a expressão STING, respectivamente. Essa linhagem de macrófagos é capaz de produzir e liberar luciferase no meio da cultura em resposta à ativação de vias de sinalização dependentes de IRF. Incubamos essas células com a cepa Y do *T. cruzi* por 16 horas para permitir a infecção, removemos parasitas residuais e incubamos por mais 24 horas para

coletar RNA total e sobrenadante para análises subsequentes, como a avaliação da atividade de luciferase, expressão gênica e produção de citocina (Fig. 4A). Nós observamos que os macrófagos STING-KO apresentaram ativação significativamente menor das vias dependentes de IRF do que o controle em resposta à infecção por *T. cruzi* (Fig. 4B). Além disso, também observamos que as células STING-KO infectadas apresentaram expressão gênica significativamente menor de IFN-β, IL-6 e IL-12 (Fig. 4C, D e E, respectivamente). Corroborando nossos resultados, encontramos uma produção significativamente menor dessas citocinas por células STING-KO infectadas, quando comparadas às células ISG também infectadas (Fig. 4F, G e H respectivamente).

Para melhor caracterizar o papel da sinalização STING na infecção por *T. cruzi,* avaliamos a expressão gênica de TNF-α e a produção de óxido nítrico em resposta ao parasita e não observamos diferença significativa entre as células STING-KO e ISG (Figuras suplementares 1A e 2A, respectivamente). No geral, nossos resultados indicam que STING é necessário para a produção de citocinas-chave envolvidas na imunidade contra o *T.cruzi.*

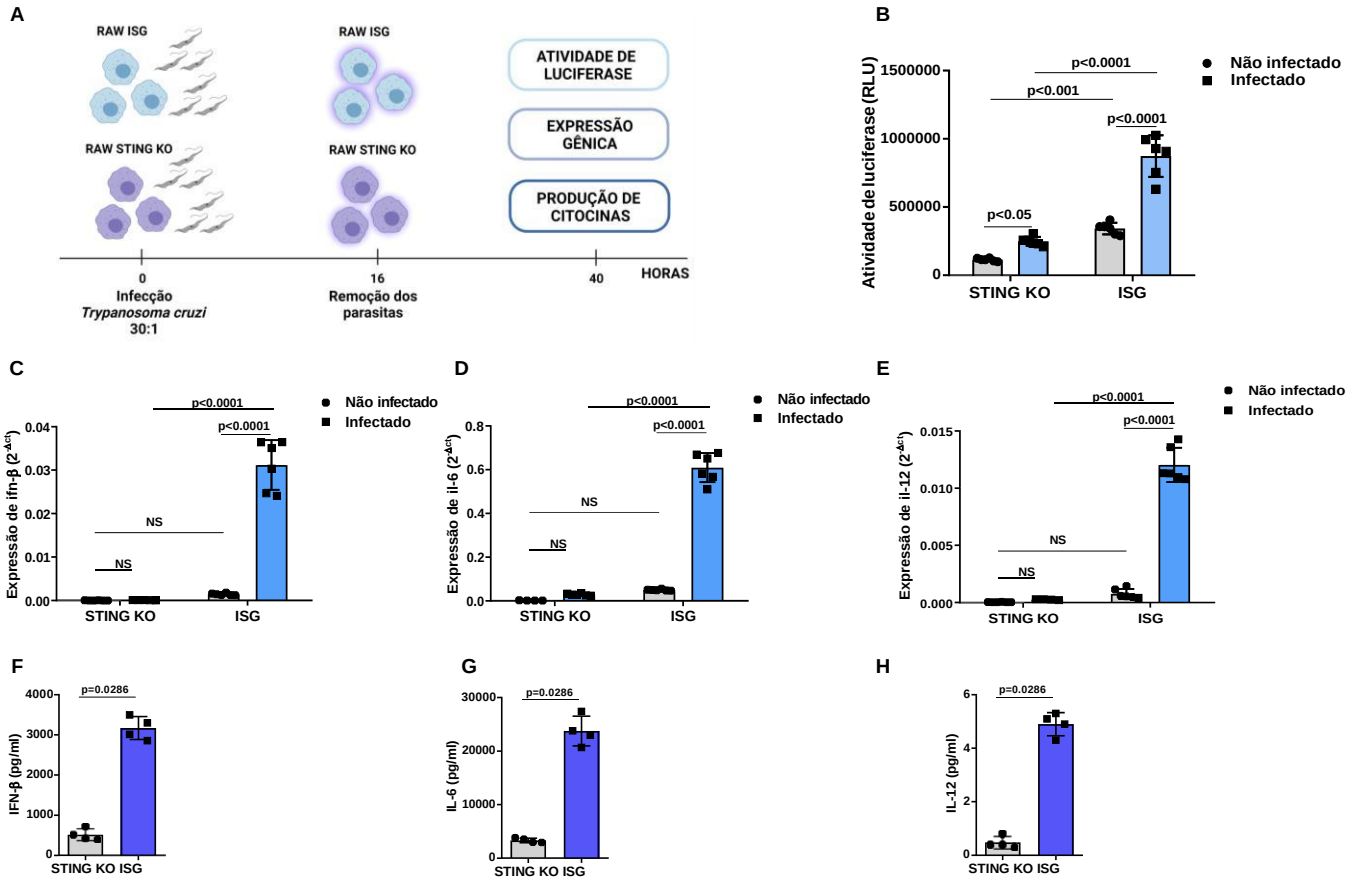

Figura 4. Sinalização de STING é necessária para a produção de citocinas em reposta à infecção pelo *T. cruzi*. Macrófagos RAW-ISG ou RAW-STING KO foram infectados por 16 horas com 30 tripomastigotas por célula. **(A)** Desenho experimental criado em *Biorender*. **(B)** Atividade de luciferase dependente da ativação de IRF em macrófagos RAW-ISG e RAW-STING KO infectados ou não. **(C-E)** Análise por PCR em tempo real da expressão gênica de IFN-β, IL-6 e IL-12 em células RAW-ISG e RAW-STING KO infectadas ou não. O gene HPRT1 foi usado como controle endógeno. **(F-H)** Análise por Luminex da produção das citocinas IFN-β, IL-6 e IL-12 no sobrenadante de cultura de células RAW-ISG ou RAW-STING KO infectadas. Os valores de IFN-β, IL-6 e IL-12 no sobrenadante de células não infectadas foram subtraídos. NS = não estatisticamente significante. *Two-way ANOVA* e *Tukey's multiple comparison test* **(B-E)**. *Mann-Whitney test* **(F-H)**. Os dados são apresentados como média ± S.D. **(B-H)**.

6.2. INFECÇÃO PELO PARASITA É NECESSÁRIA PARA ATIVAR SINALIZAÇÃO DEPENDENTE DE STING

Sabendo que o STING participa de sinalizações intracelulares, procuramos avaliar se a infecção seria necessária para ativar as vias

dependentes de STING. Para abordar essa questão, submetemos o parasita a uma temperatura de 56°C para que ele fosse morto, e então incubamos com macrófagos RAW-Lucia ISG e RAW-STING KO por 16 horas. Lavamos as células e incubamos por mais 24 horas para coletar RNA total e sobrenadante para avaliação da atividade luciferase e expressão gênica (Fig. 5A). Não observamos diferença significativa na atividade da luciferase ao comparar as células STING-KO e ISG expostas ao parasita morto com seus respectivos controles não expostos (Fig. 5B). Também não encontramos diferenças significativas na expressão gênica de IFN-β, IL-6 e IL-12 em resposta à exposição ao parasita morto pelo calor (Fig. 5C, D e E, respectivamente). Nenhuma indução significativa de expressão gênica de TNF-α foi encontrada em células STING-KO e ISG expostas ao parasita morto (figura suplementar 1B). Portanto, nossos resultados sugerem que a infecção pelo parasita é necessária para ativar a sinalização dependente de STING.

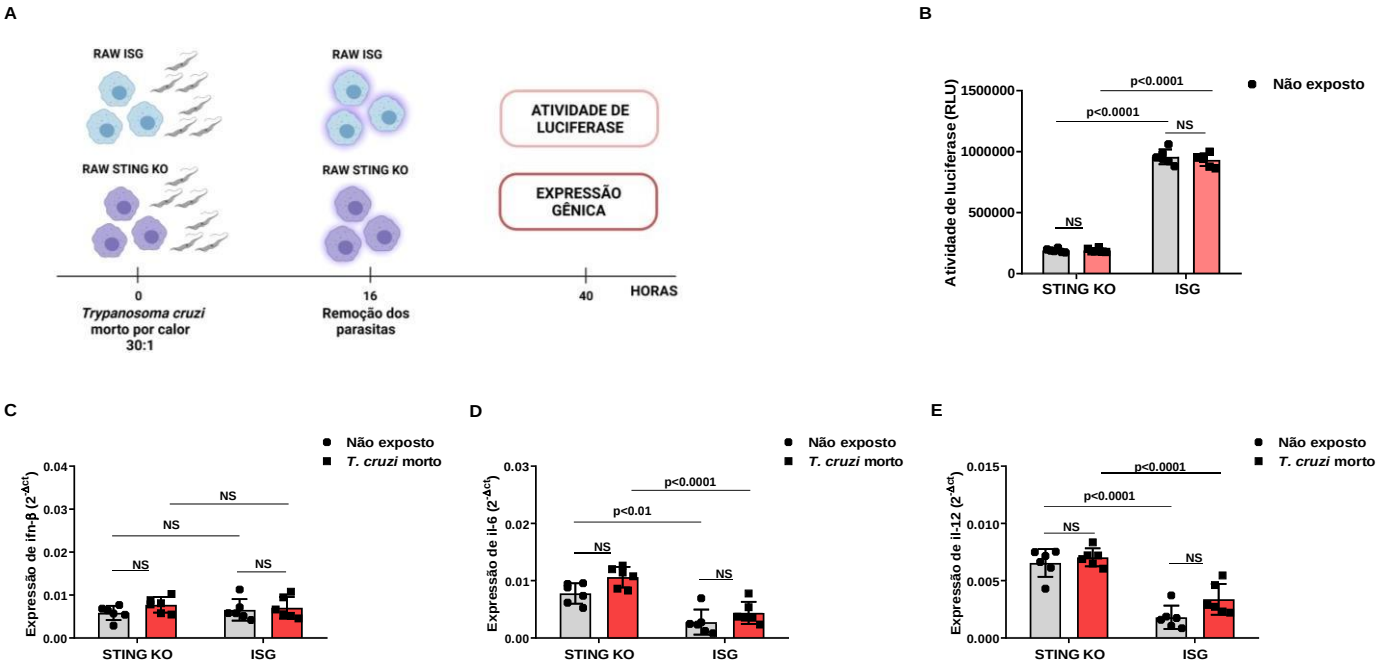

Figura 5. Infecção pelo parasita é necessária para ativar sinalização dependente de STING. Macrófagos RAW-ISG e RAW-STING KO foram expostos ao *T. cruzi* morto pelo calor, na proporção de 30 parasitas por célula, por 16 horas. **(A)** Desenho experimental criado em *Biorender*. **(B)** Atividade de luciferase dependente de IRF em macrófagos RAW-ISG e RAW-STING KO expostos ou não ao *T. cruzi* morto. **(C-E)** Análise por PCR em tempo real da expressão gênica de IFN-β, IL-6 e IL-12 em células RAW-ISG e RAW-STING KO expostas ou não ao parasita morto. O gene HPRT1 foi usado como controle endógeno. NS = não estatisticamente significante. *Two-way ANOVA* e *Tukey's multiple comparison test* **(B-E)**. Os dados são apresentados como média ± S.D. **(B-H)**.

6.3. DNA DO *TRYPANOSOMA CRUZI* INDUZ EXPRESSÃO DE CITOCINAS DE FORMA DEPENDENTE DE STING

A detecção de DNA intracelular por diferentes receptores resulta na ativação da sinalização dependente de STING (65, 77, 87-90). Por isso, acreditamos que STING desempenharia um papel no reconhecimento do DNA do parasita, levando à indução de citocinas. Para testar nossa hipótese, transfectamos células RAW-ISG e RAW-STING KO com DNA do *T. cruzi* e 40 horas após a transfecção, coletamos RNA total e sobrenadante para avaliação da atividade de luciferase e expressão gênica (Fig. 6A). Observamos que o STING foi essencial para a ativação de vias dependentes de IRF, uma vez que as células STING KO apresentaram atividade de luciferase significativamente menor após a transfecção quando comparadas às células ISG transfectadas (Fig. 6B). Como observado para a infecção, as células STING-KO apresentaram expressão gênica de IFN-β, IL-6 e IL-12 significativamente menor em resposta ao DNA do *T. cruzi* (Fig. 6C, D e E respectivamente). Embora as células STING-KO e ISG tivessem expressão gênica de TNF-α semelhante após a infecção, vimos que a transfecção do DNA do parasita

resultou no aumento da expressão gênica de TNF-α em células ISG quando comparada ao controle não infectado, o que não foi observado nas células STING-KO (Figura suplementar 1C).

Para garantir que nosso sistema estava funcionando corretamente, transfectamos células RAW-Lucia ISG e STING-KO com poly IC (ligante TLR3) e c-di-GMP (ligante STING). Observamos que, enquanto as células STING-KO respondiam ao poly IC, c-di-GMP não provocou nenhuma atividade de luciferase ou expressão gênica. Além disso, observamos que a transfecção com c-di-GMP não foi capaz de induzir a expressão gênica de IL-6 e IL-12, enquanto o poly IC falhou em induzir a expressão gênica IL-12 em células RAW-ISG, o que não ocorreu após infecção por parasitas ou transfecção de DNA (Figura suplementar. 3A, B, C e D, respectivamente), sugerindo que possa haver algum mecanismo alternativo para ativação da via. Juntos, nossos resultados indicam que STING é necessário para reconhecimento intracelular de DNA do *T. cruzi* e ativação imunológica contra o parasita.

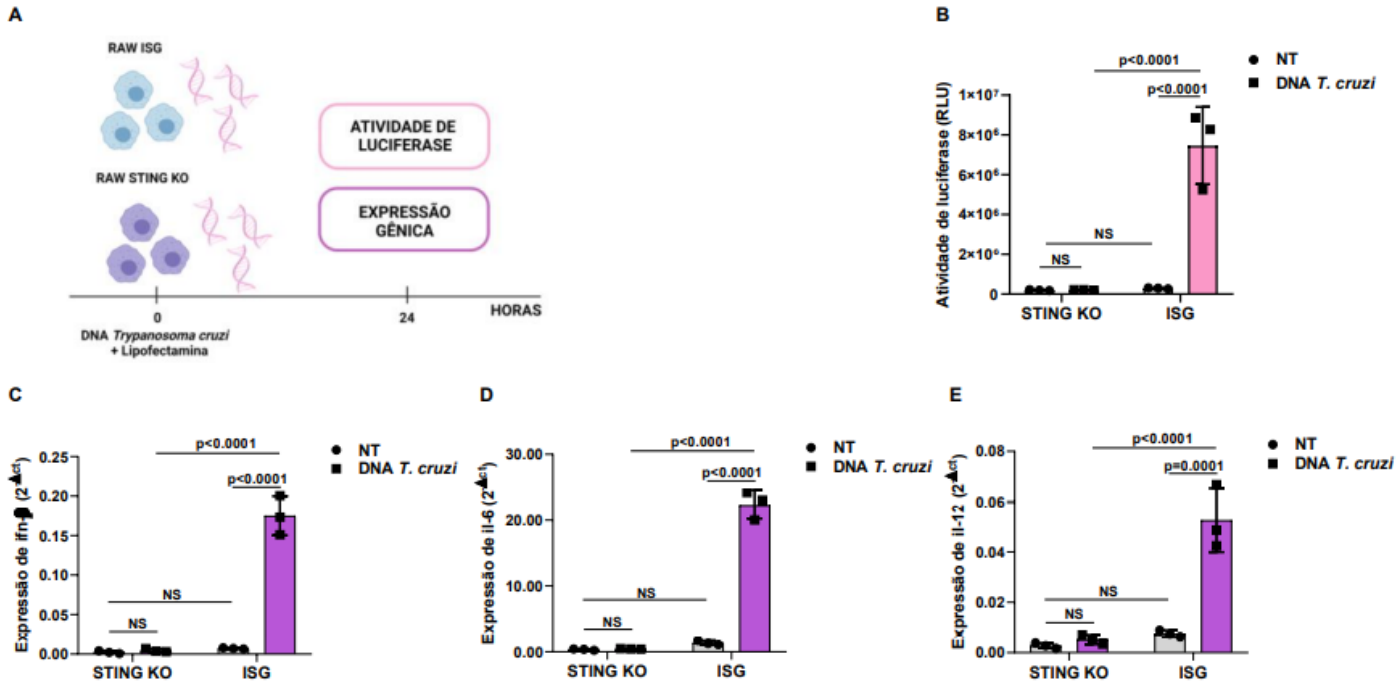

Figura 6. DNA do *Trypanosoma cruzi* induz expressão de citocinas de forma dependente de STING. Macrófagos RAW-ISG e RAW-STING KO foram transfectados com o DNA do parasita por 24 horas. **(A)** Desenho experimental criado em *Biorender*. **(B)** Atividade de luciferase dependente de IRF em macrófagos RAW-ISG e RAW-STING KO transfectados ou não (NT) com DNA do *T. cruzi*. **(C-E)** Análise por PCR em tempo real da expressão gênica de IFN-β, IL-6 e IL-12 em células RAW-ISG e RAW-STING KO transfectadas ou não. O gene HPRT1 foi usado como controle endógeno. NS = não estatisticamente significante. *Two-way ANOVA* e *Tukey's multiple comparison test* **(B-E)**. Os dados são apresentados como média ± S.D. **(B-H)**.

6.4. SINALIZAÇÃO DE STING AUMENTA RESISTÊNCIA À INFECÇÃO E PROMOVE RESPOSTAS IMUNE INATA E ADAPTATIVA CONTRA O *T. CRUZI*

Trabalhos anteriores demonstraram que IFN-β, IL-6 e IL-12 são necessários para o controle imunológico contra o *Trypanosoma cruzi (34, 42, 45)*. Dado nossos resultados *in vitro,* nós hipotetizamos que os camundongos STING-KO seriam mais suscetíveis à infecção, devido a uma resposta imune prejudicada ao parasita. Para testar nossa hipótese, infectamos camundongos

C57BL6 e STING-KO com a cepa Y do *T. cruzi* por via intraperitoneal (Fig. 7A) e observamos que os camundongos STING-KO eram menos eficazes em controlar a parasitamia (Fig. 7B). Além disso, análise de PCR mostrou maior quantidade de DNA do *T. cruzi* no coração de animais STING-KO infectados quando comparado aos camundongos C57BL6 (Fig. 7C), indicando que a sinalização de STING desempenha um papel no controle do parasita.

Para investigar o impacto da deficiência de STING na resposta imune ao *T. cruzi,* realizamos análise histológica cardíaca de animais infectados e não observamos diferença na magnitude do infiltrado inflamatório 13 dias após a infecção (Fig. 7D e E). Análise por PCR em tempo real do tecido cardíaco, nos dias 4, 7 e 13 pós infecção, revelou um aumento cinético na expressão de genes relacionados ao controle imunológico do parasita em ambos os grupos de animais. No entanto, encontramos uma menor expressão gênica de IFN-β, IL-12, CXCL9, IFN-γ e perforina no coração dos camundongos STING-KO quando comparados aos camundongos C57BL6 (Fig.8A, C, E e F, respectivamente). A expressão gênica de IL-6 foi menor no coração de camundongos STING-KO infectados, embora não tenha sido estatisticamente significante (Fig. 8B). Também encontramos menor expressão gênica de TNF-α no coração de camundongos STING-KO 13 dias após a infecção (Figura suplementar. 1D). Para avaliar mais a fundo nossos dados, realizamos análises de correlação e constatamos que, embora a expressão gênica de IFN-β, IL-6 e IL-12 não tenha apresentado correlação com o DNA de *T. cruzi* no coração (Fig. 8G, H e I, respectivamente), a expressão gênica de CXCL9, IFN-γ e perforina foi inversamente correlacionada com a quantidade de DNA de *T. cruzi* no coração de animais infectados 13 dias após a infecção (Fig. 8J, K e L,

respectivamente). Além disso, observamos uma correlação positiva entre a expressão gênica de CXCL9, IFN-γ e perforina no coração de animais infectados (Figura complementar 4A-C).

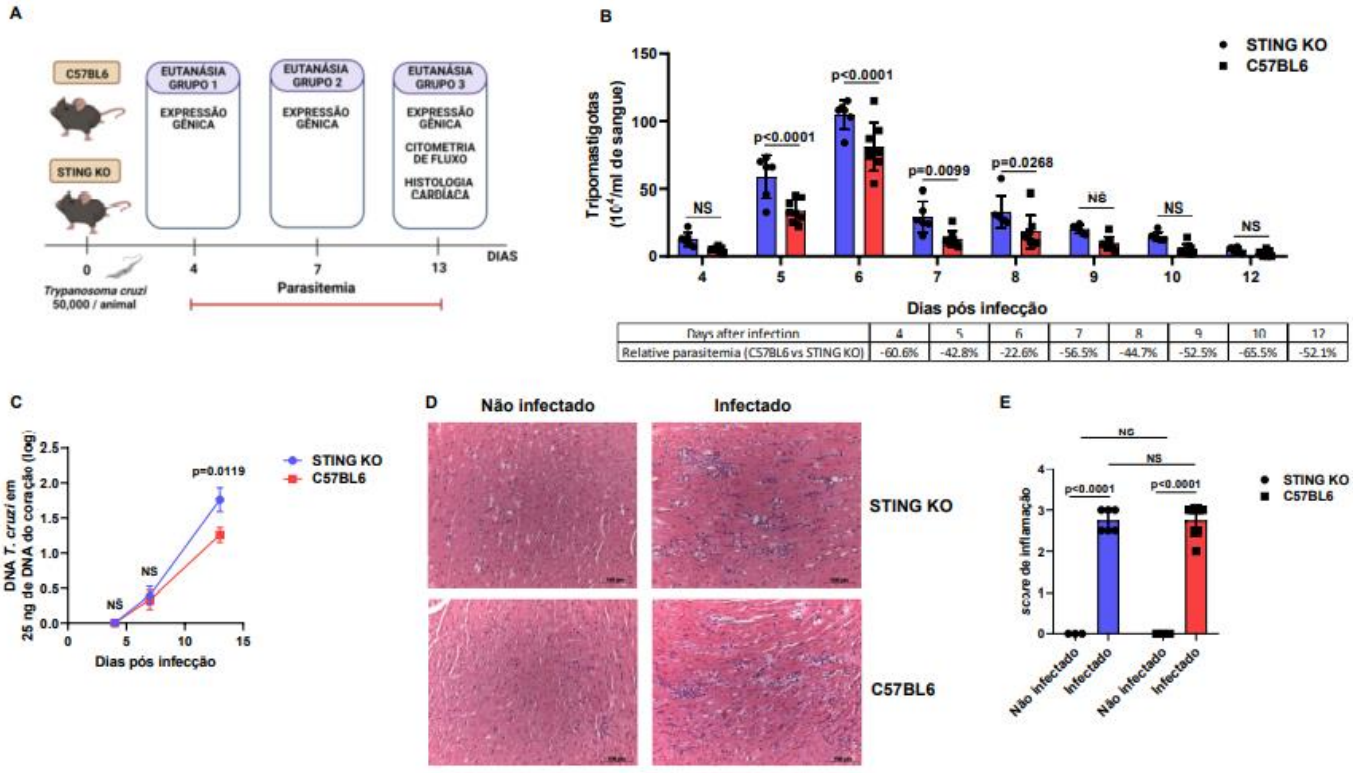

Figura 7. Sinalização de STING promove resistência contra a infecção com *T. cruzi*. Camundongos C57BL6 e STING KO foram infectados, de forma intraperitoneal, com 50 mil formas da cepa Y do *T. cruzi*. **(A)** Desenho experimental criado em *Biorender*. **(B)** Parasitemia de animais C57BL6 e STING KO. **(C)** PCR em tempo real para DNA do *T. cruzi* no coração dos animais nos dias 4, 7 e 13 pós infecção. **(D-E)** Análise histológica do coração de animais C57BL6 e STING KO 13 dias pós infecção. NS = não estatisticamente significante. *Two-way ANOVA* e *Bonferroni's multiple comparison test* **(B-C)**. *Two-way ANOVA* e *Tukey's multiple comparison test* **(E**

Os dados são apresentados como média ± S.D. **(B, D)**. Os dados são apresentados como média ± S.E.M. **(C)**.

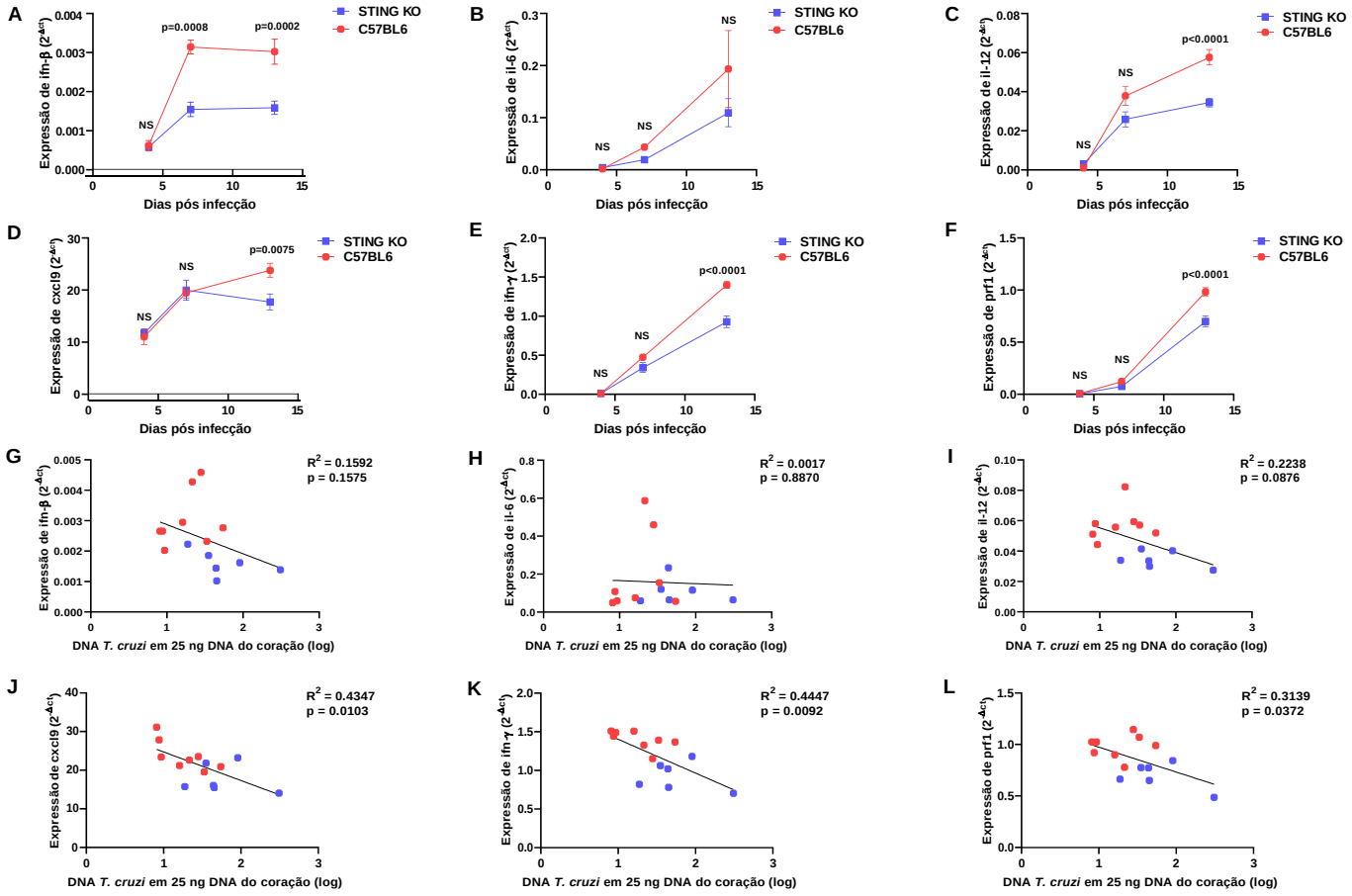

Figura 8. Deficiência de STING prejudica a resposta imune contra *T. cruzi* em camundongos infectados. (A-F) Análise por PCR em tempo real da expressão gênica de IFN-β, IL-6, IL-12, CXCL9, IFN-γ e perforina no coração de animais C57BL6 e STING KO nos dias 4, 7 e 13 pós infecção. **(G-L)** Análise de correlação da expressão de IFN-β, IL-6, IL-12, CXCL9 e perforina com DNA do parasita dos animais C57BL6 (círculos vermelhos) e STING KO (círculos azuis) 13 dias pós infecção. NS = não estatisticamente significante. *Two-way ANOVA* e *Bonferroni's multiple comparison test* **(A-F)**. *Pearson's correlation* **(G-L)**. Os dados são apresentados como média ± S.E.M.

Para ter uma visão mais sistêmica da resposta imune ao parasita no contexto da sinalização de STING, avaliamos o baço de camundongos STING-KO e C57BL6 infectados nos dias 4, 7 e 13 após a infecção. Observamos que a expressão gênica de IFN-β, IL-6 e IL-12 foi maior no dia 4 em ambos os grupos de animais, tendo uma diminuição nos dias 7 e 13 (Fig. 9A, B e C, respectivamente). No entanto, descobrimos que os camundongos C57BL6

apresentam expressão gênica de IFN-β e IL-6 significativamente maior no baço no dia 4 após a infecção quando comparados aos camundongos STING-KO (Fig. 9A e B), indicando que a sinalização de STING pode desempenhar um papel precoce na resposta imune inata, favorecendo a indução de citocinas-chave contra o *T. cruzi*. Como encontrado no nosso ensaio de *infecção in vitro*, a expressão gênica de TNF-α foi semelhante no baço dos camundongos STING-KO e C57BL6 infectados, sendo maior no dia 4 após a infecção e diminuindo ao longo do tempo (Figura suplementar 1E). Para complementar nossa análise, também foi avaliada a produção de óxido nítrico por esplenócitos de animais infectados 4, 7 e 13 dias após a infecção e não encontramos diferença significativa entre os grupos (Figura suplementar 2B).

Está bem estabelecido que as respostas imunes inatas e adaptativas contribuem para o controle do parasita e que as células T CD8+ são de extrema importância para imunidade contra o *T*. *cruzi* (56, 57). Por isso, perguntamos se a sinalização STING também seria importante para a diferenciação de células T CD8+. Para responder esta pergunta, realizamos um experimento de citometria de fluxo usando esplenócitos para investigar a produção de IFN-γ e de perforina por células T CD8+ específicas para o peptídeo TSKB20 (Fig. 9D). Como esperado, encontramos números muito baixos de células T CD8+ produzindo IFN-γ ou perforina e células duplo positivo para IFN-γ/perforina em animais não infectados (Fig. 9E-G). Por outro lado, quando infectados, observamos números significativamente maiores de células T CD8+ específicas para TSKB20 produzindo IFN-γ e IFN-γ/perforina em camundongos C57BL6 quando comparados aos camundongos STING-KO (Fig. 9H-J). Os números de células T CD8+ específicas que produzem apenas

perforina foram semelhantes em ambos os grupos (Fig. 9I). Coletivamente, nossos resultados indicam que a sinalização STING promove respostas imunológicas inata e adaptativa protetoras que ajudam a controlar a infecção por *T. cruzi.*

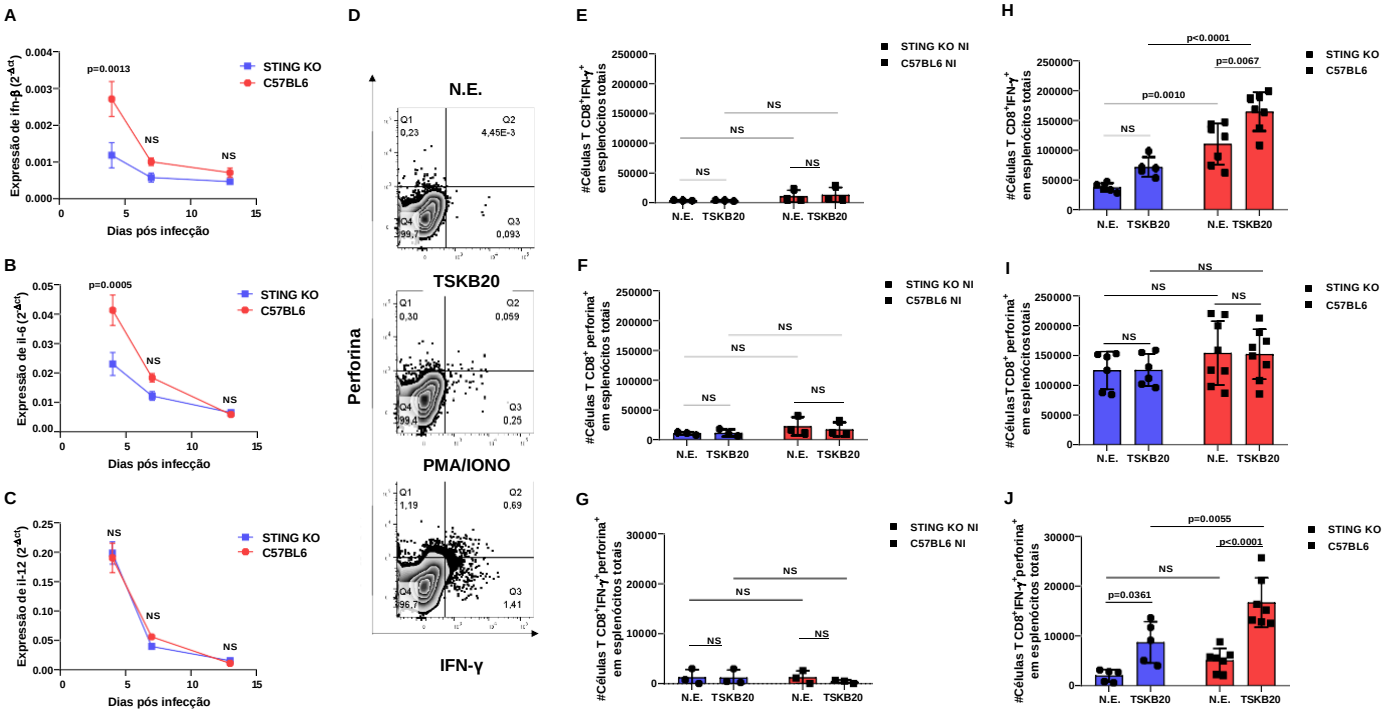

Figura 9. Deficiência de STING prejudica a imunidade contra *T. cruzi* em camundongos infectados. (A-C) Análise por PCR em tempo real da expressão gênica de IFN-β, IL-6 e IL-12 no baço de animais C57BL6 e STING KO nos dias 4, 7 e 13 pós infecção. **(D)** Análise intracelular por citometria de fluxo de células T CD8+ produzindo IFN-γ e perforina 13 dias pós infecção. **(E-F)** Número (#) de células T CD8+ produzindo IFN-γ e perforina em esplenócitos totais provenientes de camundongos não infectados, não estimulados (N.E.) ou estimulados com peptídeo TSKB20. **(H-J)** Número (#) de células T CD8+ produzindo IFN-γ e perforina em esplenócitos totais provenientes de camundongos infectados, não estimulados (N.E.) ou estimulados com peptídeo TSKB20. NS = não estatisticamente significante. *Two-way ANOVA* e *Bonferroni's multiple comparison test* **(A-C).** *Two-way ANOVA* e *Tukey's multiple comparison test* **(E-J)**. apresentados como média ± S.E.M. **(A-C)**. Os dados são apresentados como média ± S.D. **(E-J)**.

7. DISCUSSÃO

Neste estudo, mostramos que a sinalização STING é necessária para a produção de IFN-β, IL-6 e IL-12 por macrófagos em resposta à infecção pela cepa Y do *Trypanosoma cruzi*. Demonstramos também que a infecção celular é necessária para ativar a sinalização STING e que STING é essencial para a ativação imunológica mediada pelo DNA do *T. cruzi.* Além disso, nossos resultados revelaram que a sinalização STING promove respostas imunes inata e adaptativa contra o parasita em camundongos, contribuindo para um melhor controle da parasitemia e do parasitismo cardíaco.

Respostas imunes inata e adaptativa são necessárias para controlar a replicação do *T. cruzi* e o estabelecimento da doença (91). Previamente, a produção de IFN-β dependente de TLR foi associada ao controle de parasitas em células dendríticas e macrófagos, e ao aumento da resistência à infecção em camundongos (45). No entanto, dados contrastantes demonstraram que fibroblastos e macrófagos deficientes para MyD88, TRIF, TLR-2, 3 e 4 continuaram a produzir IFN-β em resposta ao *T. cruzi,* enquanto as células deficientes para TBK-1 e IRF3 foram significativamente prejudicadas (46). Aqui, mostramos que a sinalização STING, que está intimamente relacionada ao TBK-1 e IRF3 (86), não só é necessária para a ativação de vias dependentes de IRF e para a produção de IFN-β em macrófagos infectados, como também promove a produção de IL-6 e IL-12, citocinas que estão envolvidas na resistência do hospedeiro à infecção (34, 42, 45, 47, 92). Embora a sinalização de STING na imunidade a muitos patógenos tenha sido bem determinada (76,

93), nosso trabalho foi o primeiro a demonstrar sua implicância no contexto da infecção por *Trypanosoma cruzi*.

O fato de não termos observado ativação imunológica em macrófagos RAW-ISG após 16 horas de incubação com tripomastigotas mortos pelo calor indica que a infecção é necessária para impulsionar a sinalização dependente de STING, em contraste com dados anteriores em que observaram a produção de IFN-β por fibroblastos embrionários de camundongos contra parasitas mortos (46). Embora os macrófagos RAW possam internalizar o *T. cruzi* através da fagocitose (94), isso pareceu não ter impacto em nosso modelo. Como esperado, a transfecção com o DNA do parasita desencadeou uma ativação robusta das vias dependentes de IRF e expressão dos genes IFN-β, IL-6 e IL-12 de forma dependente de STING, reforçando o papel da sinalização STING na detecção de DNA intracelular e na defesa do hospedeiro, assim como contra infecção microbiana.

Dado nossos resultados *in vitro,* hipotetizamos que a sinalização de STING desempenharia um papel importante na proteção contra a infecção por *T. cruzi.* De fato, descobrimos que a ausência de STING prejudicou o controle do parasita, pois observamos maior parasitemia em camundongos STING-KO. Notamos também uma diferença precoce no controle da infecção sistêmica, com 60% menos parasitas sanguíneos em camundongos C57BL6 no dia 4 após a infecção, indicando que a imunidade inata possa ter um grande impacto no controle inicial da infecção. Maior expressão gênica de IFN-β e IL-6 nos baços de camundongos C57BL6 no mesmo período corrobora nossa hipótese. Outros estudos sobre imunidade inata têm mostrado intensidade e cinética distintas no controle de parasitas, com diferenças tardias na parasitemia sendo

observadas com maior frequência (37, 42, 45, 92). Além disso, deve-se considerar também variações na cepa do parasita e na quantidade do inóculo ao interpretar esses dados.

Em nosso modelo, a deficiência de STING resultou em maior parasitismo cardíaco, sugerindo comprometimento da imunidade local. Apesar de não encontramos diferença na intensidade do infiltrado inflamatório no coração, a baixa expressão de genes relacionados à proteção imunológica contra infecção aguda em camundongos STING-KO aponta para o papel da sinalização de STING na formação da resposta imunológica local. A cinética da resposta imune local pode ter contribuído para o controle precoce do parasita, uma vez que animais C57BL6 apresentaram aumento bem mais considerável nos níveis de expressão de IFN-β após 7 dias de infecção, simultaneamente ao início da detecção de DNA do parasita no coração desses animais, indicando que a sinalização STING leva à resposta local de IFN-β que pode impedir a infecção posterior. Nesse sentido, um trabalho anterior demonstrou indução precoce da resposta de IFN tipo I contra a cepa Y do *T. cruzi* na pele de camundongos infectados, embora nenhum papel na proteção tenha sido avaliado (43). O fato de termos observado expressão gênica de IL-12 significativamente maior nos corações dos camundongos C57BL6 no dia 13 após a infecção sugere que a sinalização STING pode ter um impacto distinto na cinética de diferentes respostas imunes inatas contra o parasita.

A quimiocina CXCL9, conhecida por promover infiltrado de células T efetoras em tecidos infectados e resposta imune protetora contra *T. cruzi* (95-97), estava significativamente mais expressa no coração de animais C57BL6 após 13 dias de infecção, assim como IFN-γ e perforina. Além disso, nossa

análise demonstrou uma correlação positiva entre esses 3 genes, indicando que a sinalização de STING promove um influxo de células produtoras de IFN-γ e perforina para o coração de animais infectados, de maneira dependente de CXCL9. Embora as células T CD4+ tenham sido demonstradas como uma fonte importante de IFN- γ durante a infecção (98, 99) e as células NK também possam migrar em resposta ao CXCL9 (100) e produzir IFN- γ e perforina (32, 101), as células T CD8+ ainda são a população mais abundante no coração de animais infectados (102, 103), corroborando a nossa hipótese de que essas células desempenham um papel importante nos nossos achados. No entanto, entendemos que uma investigação mais aprofundada será necessária para demonstrar se a via de sinalização dependente de STING é capaz de modular células T CD4+ e NK durante a infecção.

Nossa análise de citometria de fluxo revelou que a deficiência de STING tem um impacto negativo nos números de células T CD8+ IFN-γ+ específicas para o *T. cruzi* e células T CD8+ produtoras de IFN-γ/perforina no dia 13 após a infecção, o que pode explicar por que encontramos menor expressão gênica de IFN-γ e perforina nos corações de camundongos STING-KO infectados. Em contraste ao nosso trabalho, animais com deficiência para TLR4 mostraram ter a produção de IFN-γ, TNF-α e óxido nítrico no baço em resposta a *T. cruzi* prejudicada, mas ter imunidade celular mediada por células T CD8+ preservada (37). Embora trabalho anterior tenha demonstrado que a geração de células T CD8+ específicas para o *T. cruzi* não seja afetada pela ausência de sinalização de interferon tipo I (104), o prejuízo na produção de IFN-β, IL-6 e IL-12 contra o parasita em camundongos STING-KO visto no nosso estudo pode ter tido um impacto mais considerável na geração de linfócitos T CD8+.

De fato, essas três citocinas têm sido demonstradas como promotoras de ativação, proliferação e sobrevivência de células T CD8+, apoiando nossa hipótese (105-109).

As células T CD8+ produtoras de perforina têm um papel contraditório na infecção aguda e crônica pelo *T. cruzi* (62, 110). No entanto, as células T CD8+ produtoras de IFN-γ foram indicadas como protetoras tanto em modelos experimentais quanto em pacientes (62, 111-114). Aqui, mostramos um prejuízo mais proeminente em células T CD8+ produtoras de IFN-γ em camundongos STING-KO, sugerindo que a sinalização de STING possa ser responsável por promover uma resposta imune mediada por células T CD8+ mais eficaz contra *T. cruzi*. Portanto, acreditamos que nossos resultados trazem uma contribuição importante para o campo da imunoparasitologia, revelando novos mecanismos moleculares subjacentes à imunidade contra este notável patógeno.

8. CONCLUSÃO

Nossos dados sugerem que a via dependente de STING é importante para o reconhecimento do *Trypanosoma cruzi* e para a formação da resposta imunológica contra o parasita, contribuindo para a proteção contra a infecção aguda.

9. REFERÊNCIAS

1. Chagas disease in Latin America: an epidemiological update based on 2010 estimates. Wkly Epidemiol Rec. 2015;90(6):33-43.
2. Rassi A, Marin-Neto JA. Chagas disease. Lancet. 2010;375(9723):1388-402.
3. Lee BY, Bacon KM, Bottazzi ME, Hotez PJ. Global economic burden of Chagas disease: a computational simulation model. Lancet Infectious Diseases. 2013;13(4):342-8.

4. Stanaway JD, Roth G. The Burden of Chagas Disease Estimates and Challenges. Global Heart. 2015;10(3):139-44.
5. Schmunis GA, Yadon ZE. Chagas disease: A Latin American health problem becoming a world health problem. Acta Tropica. 2010;115(1-2):14-21.
6. Coura JR, Borges-Pereira J. Chagas disease: 100 years after its discovery. A systemic review. Acta Tropica. 2010;115(1-2):5-13.
7. World Health O. Chagas disease in Latin America: an epidemiological update based on 2010 estimates. Weekly Epidemiological Record= Relevé épidémiologique hebdomadaire. 2015;90(06):33-44.
8. Marin JA, Cunha E, Maciel BC, Simoes MV. Pathogenesis of chronic Chagas heart disease. Circulation. 2007;115(9):1109-23.
9. Cunha-Neto E, Chevillard C. Chagas Disease Cardiomyopathy: Immunopathology and Genetics. Mediators of Inflammation. 2014.
10. Perez CJ, Lymbery AJ, Thompson RCA. Reactivation of Chagas Disease: Implications for Global Health. Trends Parasitol. 2015;31(11):595-603.
11. Pérez-Molina JA, Molina I. Chagas disease. Lancet. 2018;391(10115):82-94.
12. Tardieux I, Nathanson MH, Andrews NW. ROLE IN HOST-CELL INVASION OF TRYPANOSOMA-CRUZI-INDUCED CYTOSOLIC-FREE CA2+ TRANSIENTS. Journal of Experimental Medicine. 1994;179(3):1017-22.
13. Rodriguez A, Rioult MG, Ora A, Andrews NW. A TRYPANOSOME-SOLUBLE FACTOR INDUCES IP3 FORMATION, INTRACELLULAR CA2+ MOBILIZATION AND MICROFILAMENT REARRANGEMENT IN HOST-CELLS. Journal of Cell Biology. 1995;129(5):1263-73.
14. Rodriguez A, Samoff E, Rioult MG, Chung A, Andrews NW. Host cell invasion by trypanosomes requires lysosomes and microtubule/kinesin-mediated transport. Journal of Cell Biology. 1996;134(2):349-62.
15. Woolsey AM, Sunwoo L, Petersen CA, Brachmann SM, Cantley LC, Burleigh BA. Novel PI 3-kinase-dependent mechanisms of trypanosome invasion and vacuole maturation. Journal of Cell Science. 2003;116(17):3611-22.
16. Andrade LO, Andrews NW. Lysosomal fusion is essential for the retention of Trypanosoma cruzi inside host cells. Journal of Experimental Medicine. 2004;200(9):1135-43.
17. Epting CL, Coates BM, Engman DM. Molecular mechanisms of host cell invasion by Trypanosoma cruzi. Exp Parasitol. 2010;126(3):283-91.
18. Andrews NW, Abrams CK, Slatin SL, Griffiths G. A TRYPANOSOMA-CRUZI SECRETED PROTEIN IMMUNOLOGICALLY RELATED TO THE COMPLEMENT COMPONENT-C9 - EVIDENCE FOR MEMBRANE PORE-FORMING ACTIVITY AT LOW PH. Cell. 1990;61(7):1277-87.
19. Manning-Cela R, Cortes A, Gonzalez-Rey E, Van Voorhis WC, Swindle J, Gonzalez A. LYT1 protein is required for efficient in vitro infection by Trypanosoma cruzi. Infection and Immunity. 2001;69(6):3916-23.
20. Burleigh BA, Andrews NW. THE MECHANISMS OF TRYPANOSOMA-CRUZI INVASION OF MAMMALIAN-CELLS. Annual Review of Microbiology. 1995;49:175-200.
21. Piacenza L, Peluffo G, Alvarez MN, Martinez A, Radi R. Trypanosoma cruzi Antioxidant Enzymes As Virulence Factors in Chagas Disease. Antioxidants & Redox Signaling. 2013;19(7):723-34.
22. Munozfernandez MA, Fernandez MA, Fresno M. ACTIVATION OF HUMAN MACROPHAGES FOR THE KILLING OF INTRACELLULAR TRYPANOSOMA-CRUZI BY TNF-ALPHA AND IFN-GAMMA THROUGH A NITRIC OXIDE-DEPENDENT MECHANISM. Immunology Letters. 1992;33(1):35-40.
23. Gutierrez FRS, Mineo TWP, Pavanelli WR, Guedes PMM, Silva JS. The effects of nitric oxide on the immune system during Trypanosoma cruzi infection. Memorias Do Instituto Oswaldo Cruz. 2009;104:236-45.
24. Basso B. Modulation of immune response in experimental Chagas disease. World J Exp Med. 2013;3(1):1-10.

25. Venturini G, Salvati L, Muolo M, Colasanti M, Gradoni L, Ascenzi P. Nitric oxide inhibits cruzipain, the major papain-like cysteine proteinase from Trypanosoma cruzi. Biochemical and Biophysical Research Communications. 2000;270(2):437-41.
26. Gupta S, Wen J-J, Garg NJ. Oxidative Stress in Chagas Disease. Interdisciplinary Perspectives on Infectious Diseases. 2009;2009:8.
27. Piacenza L, Zago MP, Peluffo G, Alvarez MN, Basombrio MA, Radi R. Enzymes of the antioxidant network as novel determiners of Trypanosoma cruzi virulence. International Journal for Parasitology. 2009;39(13):1455-64.
28. Abrahamsohn IA, Coffman RL. Trypanosoma cruzi: IL-10, TNF, IFN-gamma, and IL-12 regulate innate and acquired immunity to infection. Exp Parasitol. 1996;84(2):231-44.
29. Sathler-Avelar R, Vitelli-Avelar DM, Teixeira-Carvalho A, Martins-Filho OA. Innate immunity and regulatory T-cells in human Chagas disease: what must be understood? Mem Inst Oswaldo Cruz. 2009;104 Suppl 1:246-51.
30. Gazzinelli RT, Hieny S, Wynn TA, Wolf S, Sher A. Interleukin 12 is required for the T-lymphocyte-independent induction of interferon gamma by an intracellular parasite and induces resistance in T-cell-deficient hosts. Proc Natl Acad Sci U S A. 1993;90(13):6115-9.
31. Cardillo F, Nomizo A, Postól E, Mengel J. NK1.1 cells are required to control T cell hyperactivity during Trypanosoma cruzi infection. Med Sci Monit. 2004;10(8):BR259-67.
32. Lieke T, Graefe SEB, Klauenberg U, Fleischer B, Jacobs T. NK cells contribute to the control of Trypanosoma cruzi infection by killing free parasites by perforin-independent mechanisms. Infection and Immunity. 2004;72(12):6817-25.
33. Bastos KR, Alvarez JM, Marinho CR, Rizzo LV, Lima MR. Macrophages from IL-12p40-deficient mice have a bias toward the M2 activation profile. J Leukoc Biol. 2002;71(2):271-8.
34. Aliberti JCS, Cardoso MAG, Martins GA, Gazzinelli RT, Vieira LQ, Silva JS. Interleukin-12 mediates resistance to Trypanosoma cruzi in mice and is produced by murine macrophages in response to live trypomastigotes. Infection and Immunity. 1996;64(6):1961-7.
35. Campos MA, Closel M, Valente EP, Cardoso JE, Akira S, Alvarez-Leite JI, et al. Impaired production of proinflammatory cytokines and host resistance to acute infection with Trypanosoma cruzi in mice lacking functional myeloid differentiation factor 88. Journal of Immunology. 2004;172(3):1711-8.
36. Bafica A, Santiago HC, Goldszmid R, Ropert C, Gazzinelli RT, Sher A. Cutting edge: TLR9 and TLR2 signaling together account for MyD88-dependent control of parasitemia in Trypanosoma cruzi infection. Journal of Immunology. 2006;177(6):3515-9.
37. Oliveira AC, de Alencar BC, Tzelepis F, Klezewsky W, da Silva RN, Neves FS, et al. Impaired Innate Immunity in Tlr4(-/-) Mice but Preserved CD8(+) T Cell Responses against Trypanosoma cruzi in Tlr4-, Tlr2-, Tlr9- or Myd88-Deficient Mice. Plos Pathogens. 2010;6(4).
38. Silva GK, Gutierrez FRS, Guedes PMM, Horta CV, Cunha LD, Mineo TWP, et al. Cutting Edge: Nucleotide-Binding Oligomerization Domain 1-Dependent Responses Account for Murine Resistance against Trypanosoma cruzi Infection. Journal of Immunology. 2010;184(3):1148-52.
39.Goncalves VM, Matteucci KC, Buzzo CL, Miollo BH, Ferrante D, Torrecilhas AC, et al. NLRP3 Controls Trypanosoma cruzi Infection through a Caspase-1-Dependent IL-1R-Independent NO Production. Plos Neglected Tropical Diseases. 2013;7(10).
40. Moretti E, Basso B, Cervetta L, Brigada A, Barbieri G. Patterns of cytokines and soluble cellular receptors in the sera of children with acute Chagas' disease. Clinical and Diagnostic Laboratory Immunology. 2002;9(6):1324-7.
41. Samudio M, Montenegro-James S, de Cabral M, Martinez J, de Arias AR, Woroniecky O, et al. Differential expression of systemic cytokine profiles in Chagas' disease is associated with endemicity of Trypanosoma cruzi infections. Acta Tropica. 1998;69(2):89-97.
42. Gao WD, Pereira MA. Interleukin-6 is required for parasite specific response and host resistance to Trypanosoma cruzi. International Journal for Parasitology. 2002;32(2):167-70.

43. Chessler ADC, Unnikrishnan M, Bei AK, Daily JP, Burleigh BA. Trypanosoma cruzi Triggers an Early Type I IFN Response In Vivo at the Site of Intradermal Infection. Journal of Immunology. 2009;182(4):2288-96.
44. Li Y, Shah-Simpson S, Okrah K, Belew AT, Choi J, Caradonna KL, et al. Transcriptome Remodeling in Trypanosoma cruzi and Human Cells during Intracellular Infection. Plos Pathogens. 2016;12(4).
45. Koga R, Hamano S, Kuwata H, Atarashi K, Ogawa M, Hisaeda H, et al. TLR-dependent induction of IFN-beta mediates host defense against Trypanosoma cruzi. Journal of Immunology. 2006;177(10):7059-66.
46. Chessler ADC, Ferreira LRP, Chang TH, Fitzgerald KA, Burleiph BA. A Novel IFN Regulatory Factor 3-Dependent Pathway Activated by Trypanosomes Triggers IFN-beta in Macrophages and Fibroblasts. Journal of Immunology. 2008;181(11):7917-24.
47. Costa VMA, Torres KCL, Mendonca RZ, Gresser I, Gollob KJ, Abrahamsohn IA. Type I IFNs stimulate nitric oxide production and resistance to Trypanosoma cruzi infection. Journal of Immunology. 2006;177(5):3193-200.
48. Chessler ADC, Caradonna KL, Da'dara A, Burleigh BA. Type I Interferons Increase Host Susceptibility to Trypanosoma cruzi Infection. Infection and Immunity. 2011;79(5):2112-9.
49. Kumar S, Tarleton RL. The relative contribution of antibody production and CD8+ T cell function to immune control of Trypanosoma cruzi. Parasite Immunol. 1998;20(5):207-16.
50. Tarleton RL, Sun J, Zhang L, Postan M. Depletion of T-cell subpopulations results in exacerbation of myocarditis and parasitism in experimental Chagas' disease. Infect Immun. 1994;62(5):1820-9.
51. Pérez-Molina JA. Management of Trypanosoma cruzi coinfection in HIV-positive individuals outside endemic areas. Curr Opin Infect Dis. 2014;27(1):9-15.
52. Tarleton RL, Grusby MJ, Postan M, Glimcher LH. Trypanosoma cruzi infection in MHC-deficient mice: further evidence for the role of both class I- and class II-restricted T cells in immune resistance and disease. Int Immunol. 1996;8(1):13-22.
53. Padilla A, Xu D, Martin D, Tarleton R. Limited role for CD4+ T-cell help in the initial priming of Trypanosoma cruzi-specific CD8+ T cells. Infect Immun. 2007;75(1):231-5.
54. Kumar S, Tarleton RL. Antigen-specific Th1 but not Th2 cells provide protection from lethal Trypanosoma cruzi infection in mice. Journal of Immunology. 2001;166(7):4596-603.
55. Cai CW, Blase JR, Zhang XL, Eickhoff CS, Hoft DF. Th17 Cells Are More Protective Than Th1 Cells Against the Intracellular Parasite Trypanosoma cruzi. Plos Pathogens. 2016;12(10).
56. Tarleton RL. CD8(+) T cells in Trypanosoma cruzi infection. Seminars in Immunopathology. 2015;37(3):233-8.
57. Rodriguez EVA, Furlan CLA, Vernengo FF, Montes CL, Gruppi A. Understanding CD8(+) T Cell Immunity to Trypanosoma cruzi and How to Improve It. Trends in Parasitology. 2019;35(11):899-917.
58. Cobb D, Guo S, Lara AM, Manque P, Buck G, Smeltz RB. T-bet-dependent regulation of CD8+ T-cell expansion during experimental Trypanosoma cruzi infection. Immunology. 2009;128(4):589-99.
59. Pack AD, Collins MH, Rosenberg CS, Tarleton RL. Highly competent, non-exhausted CD8+T cells continue to tightly control pathogen load throughout chronic Trypanosoma cruzi infection. Plos Pathogens. 2018;14(11).
60. Pipkin ME, Lieberman J. Delivering the kiss of death: progress on understanding how perforin works. Curr Opin Immunol. 2007;19(3):301-8.
61. Laucella SA, Postan M, Martin D, Fralish BH, Albareda MC, Alvarez MG, et al. Frequency of interferon-gamma-producing T cells specific for Trypanosoma cruzi inversely correlates with disease severity in chronic human Chagas disease. Journal of Infectious Diseases. 2004;189(5):909-18.

62. Silverio JC, Pereira IR, Cipitelli MD, Vinagre NF, Rodrigues MM, Gazzinelli RT, et al. CD8(+) T-Cells Expressing Interferon Gamma or Perforin Play Antagonistic Roles in Heart Injury in Experimental Trypanosoma Cruzi-Elicited Cardiomyopathy. Plos Pathogens. 2012;8(4).
63. Chevillard C, Nunes JPS, Frade AF, Almeida RR, Pandey RP, Nascimento MS, et al. Disease Tolerance and Pathogen Resistance Genes May Underlie Trypanosoma cruzi Persistence and Differential Progression to Chagas Disease Cardiomyopathy. Frontiers in Immunology. 2018;9.
64.Dutta D, Dutta S, Veettil MV, Roy A, Ansari MA, Iqbal J, et al. BRCA1 Regulates IFI16 Mediated Nuclear Innate Sensing of Herpes Viral DNA and Subsequent Induction of the Innate Inflammasome and Interferon-beta Responses. Plos Pathogens. 2015;11(6).
65.Zhang ZQ, Yuan B, Bao MS, Lu N, Kim T, Liu YJ. The helicase DDX41 senses intracellular DNA mediated by the adaptor STING in dendritic cells. Nature Immunology. 2011;12(10):959-U62.
66.Tanaka Y, Chen ZJ. STING Specifies IRF3 Phosphorylation by TBK1 in the Cytosolic DNA Signaling Pathway. Science Signaling. 2012;5(214).
67. Fang R, Wang CG, Jiang QF, Lv MZ, Gao PF, Yu XY, et al. NEMO-IKK beta Are Essential for IRF3 and NF-kappa B Activation in the cGAS-STING Pathway. Journal of Immunology. 2017;199(9):3222-33.
68. Chen Q, Sun LJ, Chen ZJJ. Regulation and function of the cGAS-STING pathway of cytosolic DNA sensing. Nature Immunology. 2016;17(10):1142-9.
69. Abe T, Barber GN. Cytosolic-DNA-Mediated, STING-Dependent Proinflammatory Gene Induction Necessitates Canonical NF-kappa B Activation through TBK1. Journal of Virology. 2014;88(10):5328-41.
70. Dunphy G, Flannery SM, Almine JF, Connolly DJ, Paulus C, Jønsson KL, et al. Non-canonical Activation of the DNA Sensing Adaptor STING by ATM and IFI16 Mediates NF-κB Signaling after Nuclear DNA Damage. Mol Cell. 2018;71(5):745-60.e5.
71. Wu X, Yang J, Na T, Zhang K, Davidoff AM, Yuan BZ, et al. RIG-I and IL-6 are negative-feedback regulators of STING induced by double-stranded DNA. PLoS One. 2017;12(8):e0182961.
72. Marinho FV, Benmerzoug S, Oliveira SC, Ryffel B, Quesniaux VFJ. The Emerging Roles of STING in Bacterial Infections. Trends in Microbiology. 2017;25(11):906-18.
73. Ng KW, Marshall EA, Bell JC, Lam WL. cGAS-STING and Cancer: Dichotomous Roles in Tumor Immunity and Development. Trends in Immunology. 2018;39(1):44-54.
74. Ni GX, Ma Z, Damania B. cGAS and STING: At the intersection of DNA and RNA virus-sensing networks. Plos Pathogens. 2018;14(8).
75. Liu S, Feng M, Guan WX. Mitochondrial DNA sensing by STING signaling participates in inflammation, cancer and beyond. International Journal of Cancer. 2016;139(4):736-41.
76. Sun YF, Cheng Y. STING or Sting: cGAS-STING-Mediated Immune Response to Protozoan Parasites. Trends in Parasitology. 2020;36(9):773-84.
77. Ahn J, Barber GN. STING signaling and host defense against microbial infection. Experimental and Molecular Medicine. 2019;51.
78. Marinho FV, Benmerzoug S, Rose S, Campos PC, Marques JT, Bafica A, et al. The cGAS/STING Pathway Is Important for Dendritic Cell Activation but Is Not Essential to Induce Protective Immunity against Mycobacterium tuberculosis Infection. Journal of Innate Immunity. 2018;10(3):239-52.
79. Choudhuri S, Garg NJ. PARP1-cGAS-NF-κB pathway of proinflammatory macrophage activation by extracellular vesicles released during Trypanosoma cruzi infection and Chagas disease. PLoS Pathog. 2020;16(4):e1008474.
80. Royer DJ, Conrady CD, Carr DJ. Herpesvirus-Associated Lymphadenitis Distorts Fibroblastic Reticular Cell Microarchitecture and Attenuates CD8 T Cell Responses to Neurotropic Infection in Mice Lacking the STING-IFNα/β Defense Pathways. J Immunol. 2016;197(6):2338-52.
81. Vatner RE, Janssen EM. STING, DCs and the link between innate and adaptive tumor immunity. Mol Immunol. 2019;110:13-23.

82. Klarquist J, Hennies CM, Lehn MA, Reboulet RA, Feau S, Janssen EM. STING-mediated DNA sensing promotes antitumor and autoimmune responses to dying cells. J Immunol. 2014;193(12):6124-34.
83. Chen Q, Sun L, Chen ZJ. Regulation and function of the cGAS-STING pathway of cytosolic DNA sensing. Nat Immunol. 2016;17(10):1142-9.
84. BRENER Z. Therapeutic activity and criterion of cure on mice experimentally infected with Trypanosoma cruzi. Rev Inst Med Trop Sao Paulo. 1962;4:389-96.
85. Piron M, Fisa R, Casamitjana N, López-Chejade P, Puig L, Vergés M, et al. Development of a real-time PCR assay for Trypanosoma cruzi detection in blood samples. Acta Trop. 2007;103(3):195-200.
86. Hopfner KP, Hornung V. Molecular mechanisms and cellular functions of cGAS-STING signalling. Nature Reviews Molecular Cell Biology. 2020;21(9):501-21.
87. Takaoka A, Wang Z, Choi MK, Yanai H, Negishi H, Ban T, et al. DAI (DLM-1/ZBP1) is a cytosolic DNA sensor and an activator of innate immune response. Nature. 2007;448(7152).
88. Yang P, An H, Liu X, Wen M, Zheng Y, Rui Y, et al. The cytosolic nucleic acid sensor LRRFIP1 mediates the production of type I interferon via a beta-catenin-dependent pathway. Nature Immunology. 2010;11(6).
89. Unterholzner L, Keating SE, Baran M, Horan KA, Jensen SB, Sharma S, et al. IFI16 is an innate immune sensor for intracellular DNA. Nature Immunology. 2010;11(11).
90. Sun L, Wu J, Du F, Chen X, Chen ZJ. Cyclic GMP-AMP Synthase Is a Cytosolic DNA Sensor That Activates the Type I Interferon Pathway. Science. 2013;339(6121):786-91.
91. Acevedo GR, Girard MC, Gomez KA. The Unsolved Jigsaw Puzzle of the Immune Response in Chagas Disease. Frontiers in Immunology. 2018;9.
92. Graefe SEB, Jacobs T, Gaworski I, Klauenberg U, Steeg C, Fleischer B. Interleukin-12 but not interleukin-18 is required for immunity to Trypanosoma cruzi in mice. Microbes and Infection. 2003;5(10):833-9.
93. Ahn J, Barber GN. STING signaling and host defense against microbial infection. Exp Mol Med. 2019;51(12):1-10.
94. Maganto-Garcia E, Punzon C, Terhorst C, Fresno M. Rab5 activation by Toll-like receptor 2 is required for Trypanosoma cruzi internalization and replication in macrophages. Traffic. 2008;9(8):1299-315.
95. Hardison JL, Wrightsman RA, Carpenter PM, Lane TE, Manning JE. The chemokines CXCL9 and CXCL10 promote a protective immune response but do not contribute to cardiac inflammation following infection with Trypanosoma cruzi. Infection and Immunity. 2006;74(1):125-34.
96. Ferreira CP, Cariste LM, Moraschi BF, Zanetti BF, Han SW, Ribeiro DA, et al. CXCR3 chemokine receptor guides Trypanosoma cruzi-specific T-cells triggered by DNA/adenovirus ASP2 vaccine to heart tissue after challenge. Plos Neglected Tropical Diseases. 2019;13(7).
97. Teixeira MM, Gazzinelli RT, Silva JS. Chemokines, inflammation and Trypanosoma cruzi infection. Trends in Parasitology. 2002;18(6):262-5.
98. Sanoja C, Carbajosa S, Fresno M, Girones N. Analysis of the Dynamics of Infiltrating CD4(+) T Cell Subsets in the Heart during Experimental Trypanosoma cruzi Infection. Plos One. 2013;8(6).
99. Albareda MC, Olivera GC, Laucella SA, Alvarez MG, Fernandez ER, Lococo B, et al. Chronic Human Infection with Trypanosoma cruzi Drives CD4(+) T Cells to Immune Senescence. Journal of Immunology. 2009;183(6):4103-8.
100. Thapa M, Welner RS, Pelayo R, Carr DJJ. CXCL9 and CXCL10 expression are critical for control of genital herpes simplex virus type 2 infection through mobilization of HSV-specific CTL and NK cells to the nervous system. Journal of Immunology. 2008;180(2):1098-106.

101. Cardillo F, Voltarelli JC, Reed SG, Silva JS. Regulation of Trypanosoma cruzi infection in mice by gamma interferon and interleukin 10: Role of NK cells. Infection and Immunity. 1996;64(1):128-34.
102. dos Santos PVA, Roffe E, Santiago HC, Torres RA, Marino A, Paiva CN, et al. Prevalence of CD8(+)alpha beta T cells in Trypanosoma cruzi-elicited myocarditis is associated with acquisition of CD62L(Low)LFA-1(High)VLA-4(High) activation phenotype and expression of IFN-gamma-inducible adhesion and chemoattractant molecules. Microbes and Infection. 2001;3(12):971-84.
103. Reis DD, Jones EM, Tostes S, Lopes ER, Gazzinelli G, Colley DG, et al. CHARACTERIZATION OF INFLAMMATORY INFILTRATES IN CHRONIC CHAGASIC MYOCARDIAL LESIONS - PRESENCE OF TUMOR NECROSIS FACTOR-ALPHA+ CELLS AND DOMINANCE OF GRANZYME A+, CD8+ LYMPHOCYTES. American Journal of Tropical Medicine and Hygiene. 1993;48(5):637-44.
104.Martin DL, Murali-Krishna K, Tarleton RL. Generation of Trypanosoma cruzi-Specific CD8(+) T-Cell Immunity Is Unaffected by the Absence of Type I Interferon Signaling. Infection and Immunity. 2010;78(7):3154-9.
105. Wilson DC, Matthews S, Yap GS. IL-12 signaling drives CD8(+) T cell IFN-gamma production and differentiation of KLRG1(+) effector subpopulations during Toxoplasma gondii infection. Journal of Immunology. 2008;180(9):5935-45.
106. Henry CJ, Ornelles DA, Mitchell LM, Brzoza-Lewis KL, Hiltbold EM. IL-12 Produced by Dendritic Cells Augments CD8(+) T Cell Activation through the Production of the Chemokines CCL1 and CCL17. Journal of Immunology. 2008;181(12):8576-84.
107. Li BF, Jones LL, Geiger TL. IL-6 Promotes T Cell Proliferation and Expansion under Inflammatory Conditions in Association with Low-Level ROR gamma t Expression. Journal of Immunology. 2018;201(10):2934-46.
108. Sanmarco LM, Visconti LM, Eberhardt N, Ramello MC, Ponce NE, Spitale NB, et al. IL-6 Improves the Nitric Oxide-Induced Cytotoxic CD8+T Cell Dysfunction in Human Chagas Disease. Frontiers in Immunology. 2016;7.
109. Kolumam GA, Thomas S, Thompson LJ, Sprent J, Murali-Krishna K. Type I interferons act directly on CD8 T cells to allow clonal expansion and memory formation in response to viral infection. Journal of Experimental Medicine. 2005;202(5):637-50.
110. Nickell SP, Sharma D. Trypanosoma cruzi: roles for perforin-dependent and perforin-independent immune mechanisms in acute resistance. Experimental Parasitology. 2000;94(4):207-16.
111. Michailowsky V, Silva NM, Rocha CD, Vieira LQ, Lannes-Vieira J, Gazzinelli RT. Pivotal role of interleukin-12 and interferon-gamma axis in controlling tissue parasitism and inflammation in the heart and central nervous system during Trypanosoma cruzi infection. American Journal of Pathology. 2001;159(5):1723-33.
112. Laucella SA, Postan M, Martin D, Hubby Fralish B, Albareda MC, Alvarez MG, et al. Frequency of interferon- gamma -producing T cells specific for Trypanosoma cruzi inversely correlates with disease severity in chronic human Chagas disease. J Infect Dis. 2004;189(5):909-18.
113. Albareda MC, Laucella SA, Alvarez MG, Armenti AH, Bertochi G, Tarleton RL, et al. Trypanosoma cruzi modulates the profile of memory CD8(+) T cells in chronic Chagas' disease patients. International Immunology. 2006;18(3):465-71.
114. Reis MM, Higuchi MD, Benvenuti LA, Aiello VD, Gutierrez PS, Bellotti G, et al. An in situ quantitative immunohistochemical study of cytokines and IL-2R(+) in chronic human chagasic myocarditis: Correlation with the presence of myocardial Trypanosoma cruzi antigens. Clinical Immunology and Immunopathology. 1997;83(2):165-72.

10. ANEXOS

10.1 ANEXO A – FIGURAS SUPLEMENTARES

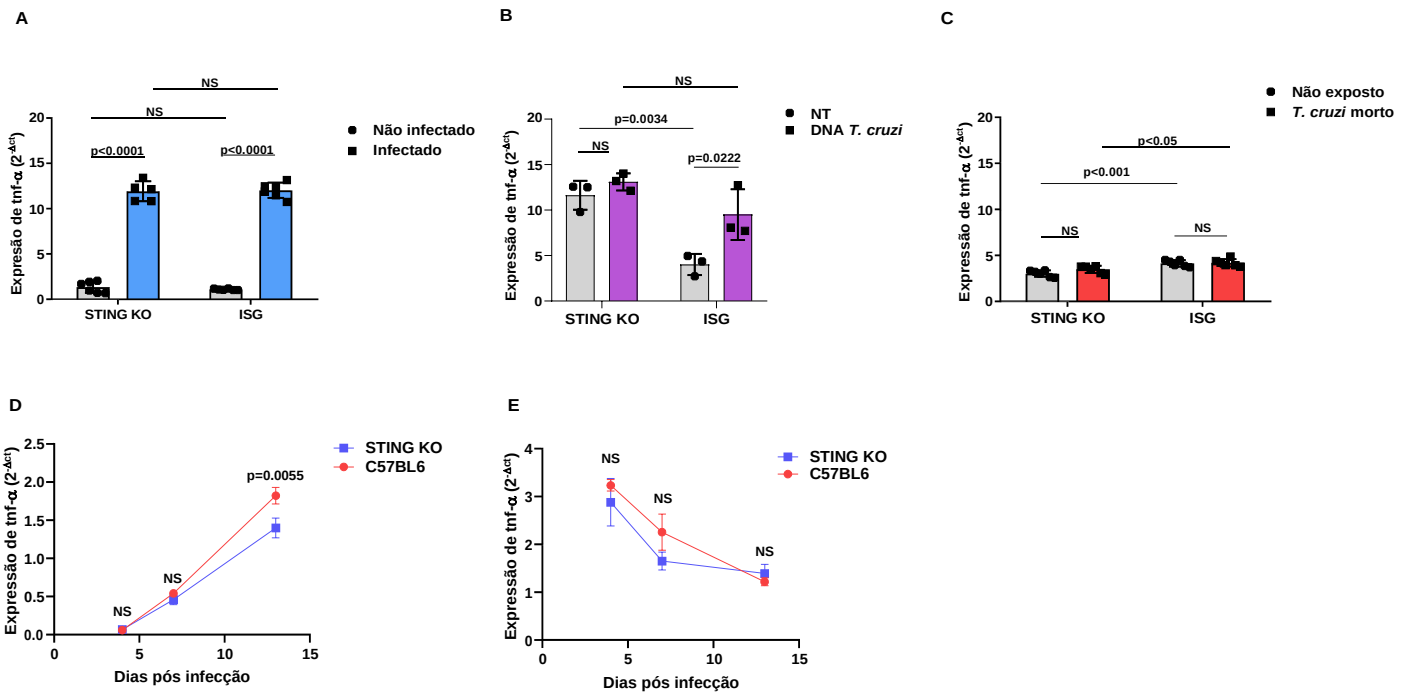

Figura suplementar 1. Deficiência de STING tem impacto variável na indução de TNF-α em resposta ao *T. cruzi*. (A) Análise por PCR em tempo real da expressão gênica de tnf-α em células RAW-ISG e RAW-STING KO infectadas ou não. **(B)** Análise por PCR em tempo real da expressão gênica de tnf-α em células RAW-ISG e RAW-STING KO expostas ou não ao *T. cruzi* morto. **(C)** Análise por PCR em tempo real da expressão gênica de TNF-α em células RAW-ISG e RAW-STING KO transfectadas ou não com DNA do *T. cruzi*. **(D, E)** Análise por PCR em tempo real da expressão gênica de TNF-α no coração de animais C57BL6 e STING KO nos dias 4, 7 e 13 pós infecção. O gene HPRT1 foi usado como controle endógeno em todas as situações. NS = não estatisticamente significante. *Two-way ANOVA* e *Tukey's multiple comparison test* **(A-C)**. Os dados são apresentados como média ± D.P. **(A-C)**. Os dados são apresentados como média ± S.E.M. **(D, E)**.

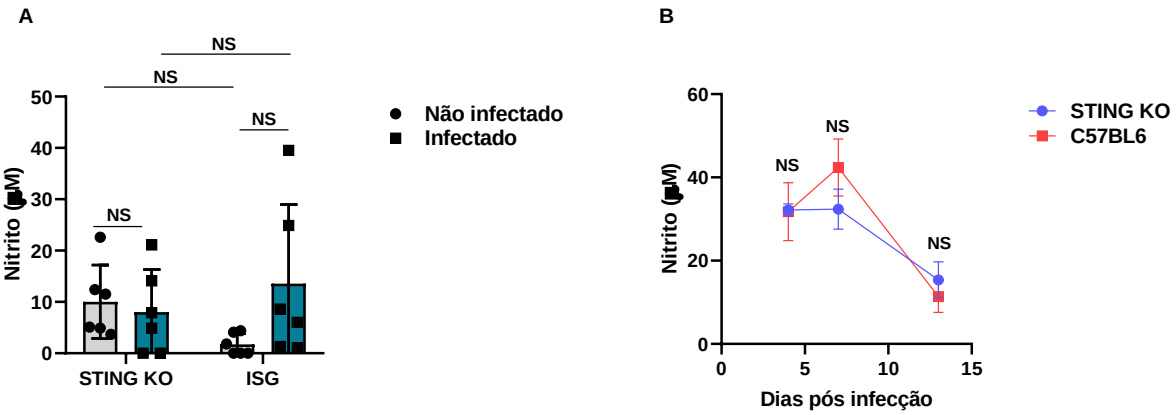

Figura suplementar 2. Deficiência de STING não tem impacto na produção de óxido nítrico contra o *T. cruzi*. (A) Detecção de nitrito no sobrenadante de células RAW-ISG e RAW-STING KO, 48 horas após a infecção. **(B)** Detecção de nitrito no sobrenadante de esplenócitos provenientes de camundongos C57BL6 e STING KO dos dias 4, 7 e 13 pós infecção, incubados por 48 horas. NS = não estatisticamente significante. *Two-way ANOVA* e *Tukey's multiple comparison test* **(A)**. *Two-way ANOVA* e *Bonferroni's multiple comparison test* **(B)**. Os dados são apresentados como média ± S.D. **(A)**. Os dados são apresentados como média ± S.E.M. **(B)**.

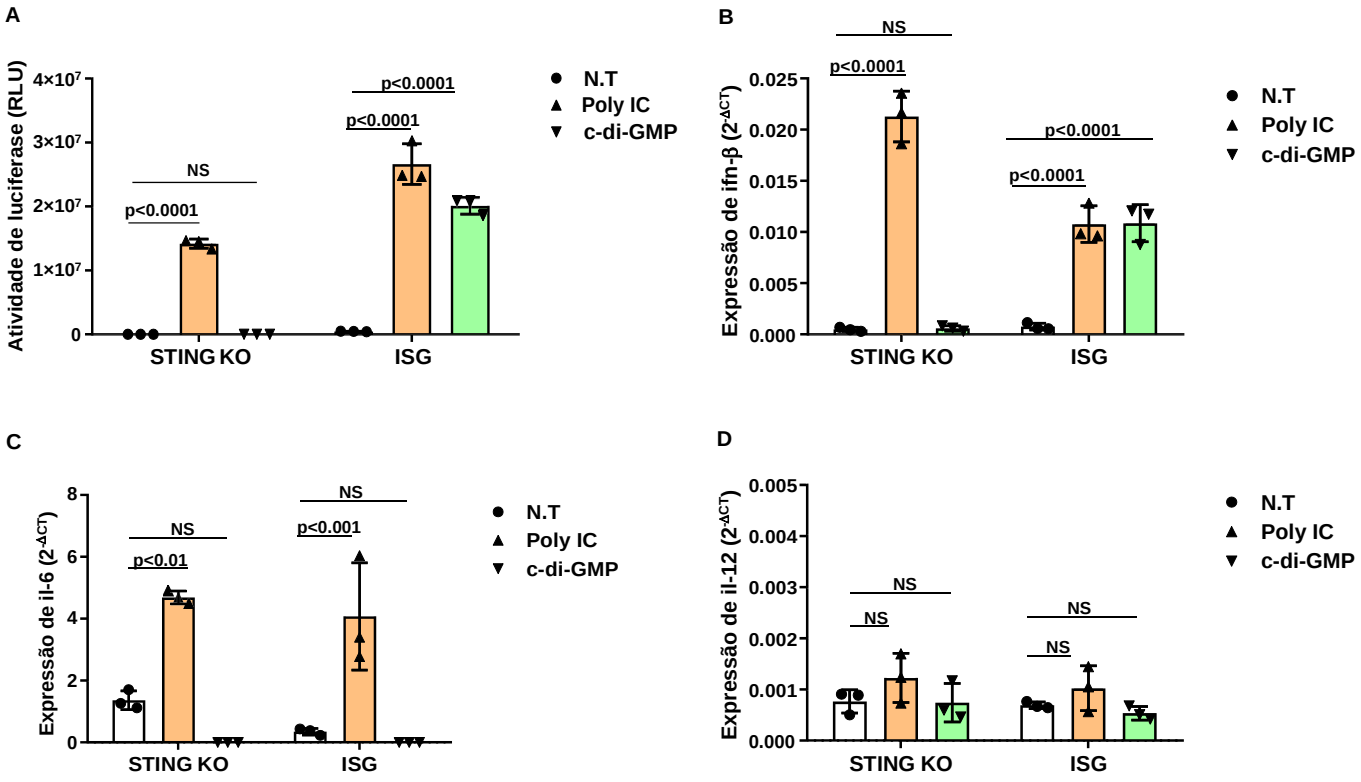

Figura suplementar 3. Células RAW STING-KO são responsivas à transfecção com poly IC, mas não ao c-di-GMP. (A) Atividade de luciferase dependente da ativação de IRF em células RAW-ISG e RAW-STING KO transfectadas ou não (NT). **(B-D)** Análise por PCR em tempo real da expressão gênica de IFN-β, IL-6 e IL-12 em células RAW-ISG e RAW-STING KO transfectadas ou não. O gene hprt foi usado como controle endógeno. NS = não estatisticamente significante. *Two-way ANOVA* e *Tukey's multiple comparison test* **(A-D)**. Os dados são apresentados como média ± S.D. **(A-D)**.

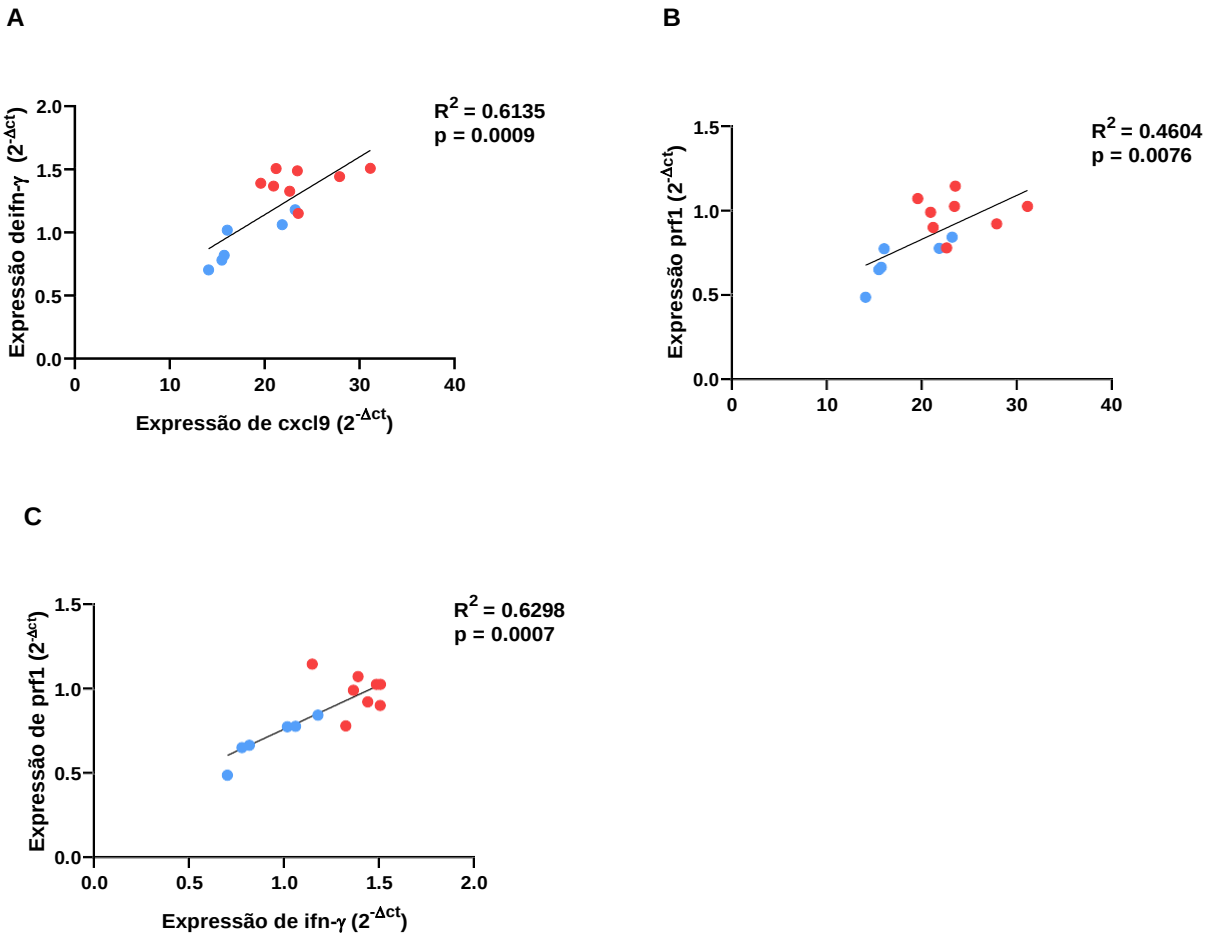

Figura suplementar 4. A expressão gênica de IFN-γ, perforina e CXCL9 apresentam correlação positiva no coração de animais infectados. (A) Análise de correlação da expressão gênica de IFN-γ, perforina e CXCL9 no coração de animais C57BL6 e STING KO 13 dias pós infecção. NS = não estatisticamente significante. *Pearson's correlation* **(A-C)**. Os dados são apresentados como média ± S.E.M.

10.2. ANEXO B – APROVAÇÃO DO COMITÊ DE ÉTICA

Faculdade de Medicina da Universidade de São Paulo
Avenida Dr. Arnaldo, 455
Pacaembu – São Paulo – SP

COMISSÃO DE ÉTICA NO USO DE ANIMAIS

Certificamos que a proposta intitulada **"O papel da proteína STING na patogenia da infecção pelo Trypanosoma cruzi"** registrada com o **nº 1567/2020**, sob a responsabilidade de **Rafael Ribeiro Almeida** e **Raquel de Souza Vieira**, apresentada pelo Departamento de Clínica Médica - que envolve a produção, manutenção e/ou utilização de animais pertencentes ao filo Chordata, subfilo Vertebrata (exceto humanos), para fins de pesquisa científica (ou ensino) - encontra-se de acordo com os preceitos da Lei nº 11.794, de 8 de outubro de 2008, do Decreto nº 6.899, de 15 de julho de 2009, e com as normas editadas pelo Conselho Nacional de Controle de Experimentação Animal (CONCEA), e foi aprovada pela COMISSÃO DE ÉTICA NO USO DE ANIMAIS (CEUA) da Faculdade de Medicina da USP em 15/09/2020

Finalidade	( ) Ensino (x) Pesquisa Científica
Vigência da autorização	Início: 08-09-2020 Término: 08-09-2022
Espécie/linhagem/raça	**72** Camundongo Balb/c **116** Camundongo C57BI/6 **80** Camundongo Knockout C57BL6 STING KO **36** Camundongo Knockout C57BL6 IFNAR KO
Peso/Idade	6 semanas
Sexo	machos
Origem	Biotério FMUSP/Biotério ICB

A CEUA FMUSP solicita que ao final da pesquisa seja enviado Relatório com todas as atividades.

CEUA-FMUSP, 15 de setembro de 2020

Dr. Eduardo Pompeu
Coordenador
Comissão de Ética no Uso de Animais

10.3. ANEXO C – TEXTO SUBMETIDO PARA PUBLICAÇÃO

PLOS Pathogens

STING signaling drives protective innate and adaptive immunity against Trypasonoma cruzi infection

--Manuscript Draft--

Manuscript Number:	
Full Title:	STING signaling drives protective innate and adaptive immunity against Trypasonoma cruzi infection
Short Title:	STING drives immunity against Trypanosoma cruzi
Article Type:	Research Article
Section/Category:	Parasitology
Keywords:	Trypanosoma cruzi; STING; IFN-beta; IL-6; IL-12; CD8+ T cells; innate immunity; adaptive immunity
Corresponding Author:	Rafael R Almeida, Ph.D Instituto do Coração, Faculdade de Medicina da Universidade de São Paulo São Paulo, BRAZIL
Corresponding Author's Institution:	Instituto do Coração, Faculdade de Medicina da Universidade de São Paulo
First Author:	Raquel de Souza Vieira
Order of Authors:	Raquel de Souza Vieira
	Marilda Savoia Nascimento
	Isaú Henrique Noronha
	José Ronnie Carvalho Vasconcelos
	Luiz Alberto Benvenuti
	Niels Olsen Saraiva Câmara
	Jorge Kalil
	Edecio Cunha-Neto
	Rafael R Almeida, Ph.D

Abstract:	Compelling evidence point towards type I interferons, innate cytokines and CD8+ T cells as major players in protection against acute Trypanosoma cruzi infection. However, the mechanisms underlying parasite-driven immunity are still not fully understood. Previous data indicate that a TBK-1/IRF3-dependent signaling pathway is responsible for IFN-β production in response to the parasite. Therefore, we hypothesized that STING would play a role in immunity to *T. cruzi* , given its intimate interaction with TBK-1 and IRF3. Here, we showed that STING signaling is required for production of IFN-β, IL-6 and IL-12 in response to infection in macrophages. We demonstrated that cellular infection is necessary to trigger STING signaling and that STING is essential for *T. cruzi* DNA-mediated induction of IFN-β, IL-6 and IL-12 gene expression. Our data revealed that STING signaling promotes splenic and heart IFN-β, IL-6 and IL-12 expression in mice and that STING deficiency results in a lower number of splenic parasite-specific IFN-γ and IFN-γ/perforin-producing CD8+ T cells. Although we observed similar heart inflammatory infiltrates in infected animals, the expression of IFN-β, IL-12, CXCL9, IFN-γ and perforin genes was lower in the absence of STING. Moreover, we found an inverse correlation between CXCL9, IFN-γ and perforin gene expression with parasite DNA in the hearts of infected animals and a positive correlation among these 3 genes. Finally, we demonstrated that STING-knockout mice had higher parasitemia throughout the course of infection, in addition to having higher parasitism in the heart. Therefore, our work demonstrates a pivotal role for STING signaling in immunity to Trypanosoma cruzi, contributing to a better understanding of the molecular mechanisms involved in acute infection.
Suggested Reviewers:	José Mosig Universidade de São Paulo

	jmamosig@icb.usp.br Professor Mosig works on the cellular and molecular elements of the immune system involved in parasite control and associated pathology in the acute and chronic phases of murine infection by Trypanosoma cruzi.
	Sergio Oliveira Universidade Federal de Minas Gerais scozeus1@gmail.com Professor Sergio Costa works on STING signaling in infection and have published many papers on the role of STING in Brucella abortus infection.
	Kenneth Gollob Hospital AC Camargo: ACCamargo Cancer Center kenneth.gollob@accamargo.org.br Dr. Kenneth works on host-pathogen interaction, aimed at the development of new therapies, diagnoses and biomarkers of Chagas disease progression.
	Nobuko Yoshida Universidade Federal de São Paulo: Universidade Federal de Sao Paulo nyoshida@unifesp.br Professor Yoshida works on cellular and molecular mechanisms of target cell invasion by Trypanosoma cruzi.
Opposed Reviewers:	
Additional Information:	
Question	**Response**
Financial Disclosure Enter a financial disclosure statement that describes the sources of funding for the work included in this submission. Review the submission guidelines for detailed requirements. View published research articles from *PLOS Pathogens* for specific examples. This statement is required for submission and **will appear in the published article** if the submission is accepted. Please make sure it is accurate.	This work was supported by grants from Conselho Nacional de Desenvolvimento Científico e Tecnológico to ECN (CNPq, www.cnpq.br, grant #465434/2014-2) and Fundação de Amapro à Pesquisa do Estado de São Paulo to ECN (Fapesp, www.fapesp.br, grants #2014/50890-5 and #2016/152090).

Unfunded studies Enter: *The author(s) received no specific funding for this work.* **Funded studies** Enter a statement with the following details: • Initials of the authors who received each award • Grant numbers awarded to each author • The full name of each funder • URL of each funder website • Did the sponsors or funders play any role in the study design, data collection and analysis, decision to publish, or preparation of the manuscript? • **NO** - Include this sentence at the end of your statement: *The funders had no role in study design, data collection and analysis, decision to publish, or preparation of the manuscript.* • **YES** - Specify the role(s) played. * typeset	
Competing Interests Use the instructions below to enter a competing interest statement for this submission. On behalf of all authors, disclose any competing interests that could be perceived to bias this work—acknowledging all financial support and any other relevant financial or non-financial competing interests. This statement **will appear in the published article** if the submission is accepted. Please make sure it is accurate. View published research articles from *PLOS Pathogens* for specific examples.	The authors have declared that no competing interests exist.

NO authors have competing interests Enter: *The authors have declared that no competing interests exist.* **Authors with competing interests** Enter competing interest details beginning with this statement: *I have read the journal's policy and the authors of this manuscript have the following competing interests: [insert competing interests here]* * typeset This statement is required for submission and **will appear in the published article** if the submission is accepted. Please make sure it is accurate and that any funding sources listed in your Funding Information later in the submission form are also declared in your Financial Disclosure statement.	
Data Availability Authors are required to make all data underlying the findings described fully available, without restriction, and from the time of publication. PLOS allows rare exceptions to address legal and ethical concerns. See the PLOS Data Policy and FAQ for detailed information. A Data Availability Statement describing where the data can be found is required at submission. Your answers to this question constitute the Data Availability Statement and **will be published in the article**, if accepted. **Important:** Stating 'data available on request from the author' is not sufficient. If your data are only available upon request, select 'No' for the first question and explain your exceptional situation in the text box.	Yes - all data are fully available without restriction

Do the authors confirm that all data underlying the findings described in their manuscript are fully available without restriction?	
Describe where the data may be found in full sentences. If you are copying our sample text, replace any instances of XXX with the appropriate details. • If the data are **held or will be held in a public repository**, include URLs, accession numbers or DOIs. If this information will only be available after acceptance, indicate this by ticking the box below. For example: *All XXX files are available from the XXX database (accession number(s) XXX, XXX.*). • If the data are all contained **within the manuscript and/or Supporting Information files**, enter the following: *All relevant data are within the manuscript and its Supporting Information files.* • If neither of these applies but you are able to provide **details of access elsewhere**, with or without limitations, please do so. For example: *Data cannot be shared publicly because of [XXX]. Data are available from the XXX Institutional Data Access / Ethics Committee (contact via XXX) for researchers who meet the criteria for access to confidential data.* *The data underlying the results presented in the study are available from (include the name of the third party and contact information or URL).* • This text is appropriate if the data are owned by a third party and authors do not have permission to share the data. * typeset	All relevant data are within the manuscript and its Supporting Information files.
Additional data availability information:	

Dear Editor,

We are submitting our manuscript entitled “STING signaling drives protective innate and adaptive immunity against *Trypasonoma cruzi* infection” by Raquel de Souza Vieira, Marilda Savoia Nascimento, Isaú Henrique Noronha, José Ronnie Carvalho Vasconcelos, Luiz Alberto Benvenuti, Niels Olsen Saraiva Câmara, Jorge Kalil, Edecio Cunha-Neto and Rafael Ribeiro Almeida for consideration for publication as a research article by Plos Pathogens. This manuscript has not been published nor is it currently under consideration for publication elsewhere. The authors declare that they have no competing interests.

Compelling evidence point towards type I interferons, innate cytokines and CD8+ T cells as major players in protection against acute *Trypanosoma cruzi* infection. Although Toll-like receptors have been extensively studied in parasite-driven immunity, previous data has demonstrated that a TBK-1/IRF3-dependent signaling pathway might be necessary for IFN-β production in response to infection. Despite the intimate interaction among TBK-1, IRF3 and the stimulator of interferon genes (STING), its role in *T. cruzi* infection still remained to be addressed. In this paper, we bring an important contribution to the field of immunoparasitology by showing that STING signaling is not only required for IFN-β production in response to *T. cruzi*, but also IL-6 and IL-12, which are key cytokines involved in host resistance to infection. We also demonstrated that cellular infection is necessary to trigger STING signaling and that STING is essential for *T. cruzi* DNA-mediated immune activation. In addition, our results revealed that STING signaling promotes innate and adaptive immune responses to the parasite in mice, contributing to control of parasitemia and heart parasitism. We believe that our work contributes to a better comprehension of the

mechanisms underlying host-parasite interactions and will stimulate the pursue for new molecular pathways involved in *T. cruzi* infection. Our data also provide valuable information that may impact the understanding of disease establishment. In this sense, Plos Pathogens seems the journal suitable for publication due its policy, scientific quality and relevant audience.

We hope that our data reach the high quality requirements of the journal and it could be reviewed by experts.

Sincerely,

Rafael Ribeiro Almeida, PhD

Full title: STING signaling drives protective innate and adaptive immunity against *Trypasonoma cruzi* infection

Short title: STING drives immunity against *Trypanosoma cruzi*

Raquel de Souza Vieira[1], Marilda Savoia Nascimento[1], Isaú Henrique Noronha[4], José Ronnie Carvalho Vasconcelos[4], Luiz Alberto Benvenuti[5], Niels Olsen Saraiva Câmara[6,7], Jorge Kalil[1,2,3], Edecio Cunha-Neto[1,2,3] and Rafael Ribeiro Almeida[1,*].

1. Laboratório de Imunologia, Instituto do Coração, Faculdade de Medicina da Universidade de São Paulo, São Paulo, Brasil.
2. Disciplina de Imunologia Clínica e Alergia, Faculdade de Medicina da Universidade de São Paulo, São Paulo, Brasil.
3. Instituto de Investigação em Imunologia (iii), INCT, São Paulo, Brasil.
4. Laboratório de Vacinas Recombinantes, Departamento de Biociências, Universidade Federal de São Paulo, Campus Baixada Santista, Santos, Brasil.
5. Divisão de Patologia, Instituto do Coração (INCOR), Faculdade de Medicina, Universidade de São Paulo, São Paulo, Brasil.
6. Laboratório de Imunologia Experimental e Clínica, Departamento de Clínica Médica, Faculdade de Medicina, Universidade Federal de São Paulo, São Paulo, Brasil.
7. Laboratório de Imunologia de Transplantes, Departamento de Imunologia, Instituto de Ciências Biomédicas, Universidade de São Paulo, São Paulo, Brasil.

*Corresponding author

rafaelbio13@alumni.usp.br

Abstract

Compelling evidence point towards type I interferons, innate cytokines and CD8+ T cells as major players in protection against acute *Trypanosoma cruzi* infection. However, the mechanisms underlying parasite-driven immunity are still not fully understood. Previous data indicate that a TBK-1/IRF3-dependent signaling pathway is responsible for IFN-β production in response to the parasite. Therefore, we hypothesized that STING would play a role in immunity to *T. cruzi*, given its intimate interaction with TBK-1 and IRF3. Here, we showed that STING signaling is required for production of IFN-β, IL-6 and IL-12 in response to infection in macrophages. We demonstrated that cellular infection is necessary to trigger STING signaling and that STING is essential for *T. cruzi* DNA-mediated induction of IFN-β, IL-6 and IL-12 gene expression. Our data revealed that STING signaling promotes splenic and heart IFN-β, IL-6 and IL-12 expression in mice and that STING deficiency results in a lower number of splenic parasite-specific IFN-γ and IFN-γ/perforin-producing CD8+ T cells. Although we observed similar heart inflammatory infiltrates in infected animals, the expression of IFN-β, IL-12, CXCL9, IFN-γ and perforin genes was lower in the absence of STING. Moreover, we found an inverse correlation between CXCL9, IFN-γ and perforin gene expression with parasite DNA in the hearts of infected animals and a positive correlation among these 3 genes. Finally, we demonstrated that STING-knockout mice had higher parasitemia throughout the course of infection, in addition to having higher parasitism in the heart. Therefore, our work demonstrates a pivotal role for STING signaling in immunity to *Trypanosoma* cruzi, contributing to a better understanding of the molecular mechanisms involved in acute infection.

Author summary

Chagas disease is caused by the flagellate protozoan *Trypanosoma cruzi* and affects over 8 million people worldwide. Although the inability of mounting a balanced, protective immune response has been suggested to contribute to the development of lifelong chronic illness with different clinical forms in 30-40% of the infected individuals, the molecular mechanisms underlying host-parasite interactions are still unclear. Here, we demonstrated that a well-known signaling molecule involved in intracellular DNA sensing (STING) is required for *T. cruzi*-driven induction of key innate cytokines related to immune protection against the parasite. We also showed that STING signaling is important for generation of parasite-specific CD8+ T cells, which are major players in adaptive immunity against *T. cruzi.* Our data revealed that impaired STING signaling results in increased number of blood parasites and higher amounts of *T. cruzi* DNA in the hearts of infected mice, indicating a protective role for this signaling pathway in infection. Therefore, our study brings a valuable contribution to the field of immunoparasitology by unveiling new molecular mechanisms underlying host-parasite interactions and immune responses to *T. cruzi*, which may impact the understanding of disease establishment and how to improve treatment.

Introduction

Chagas disease is caused by the flagellate protozoan *Trypanosoma cruzi* and affects over 8 million people worldwide. While most individuals present chronic asymptomatic infection with low parasitism, 30-40% either have or will develop cardiomyopathy, digestive megasyndromes, or both [1]. Imbalanced host immune response to persistent infection is suggested to favor heart inflammation and development of chronic Chagas cardiomyopathy (CCC) [2, 3]. Nevertheless, effective innate and adaptive immunity are still likely to be the most reasonable form of protection against disease establishment.

Host-parasite interactions during acute *T. cruzi* infection are complex and incompletely understood. Toll-like receptors (TLRs) 2, 4 and 9, and their adaptor molecule MyD88 have been implicated in the recognition of pathogen-associated molecular patterns (PAMPs), parasite-driven immune activation and resistance to infection [4-8]. In addition, NOD-like receptors (NLRs) were shown to promote infection control, since NOD1 and NLRP3-deficient mice present higher susceptibility to the parasite [9, 10]. Although TLR deficiency leads to impaired innate immunity against *T. cruzi*, preserved parasite-specific CD8+ T cells were observed [11]. NOD1 and NLRP3 deficiency were related to lower production of nitric oxide (NO) and inflammatory cytokines, while the impact on adaptive immunity was not evaluated [9, 10]. Whether other molecular pathways participate in *T. cruzi*-directed immunity remains to be addressed.

Interleukin-6 (IL-6) and IL-12 are crucial for immune-mediated resistance to *T. cruzi*, as shown either by infection of genetically deficient mice or *in vivo* cytokine neutralization [12-15]. Type I interferon (IFN I) responses are early triggered at the site of parasite inoculation [16] and may provide protection or susceptibility,

depending on the infection route [17, 18]. NK cells are early IFN-γ producers against *T. cruzi* and are responsible for killing extracellular parasites [19, 20]. In terms of adaptive immunity, Th1 cells figure as an important source of IFN-γ, promoting activation of macrophages in addition to providing help for other effector cells [21-23]. Th17 cells can also protect infected macrophages and were shown to provide IL-21-dependent activation of CD8+ T cells [24]. Unlike CD4+ T cells, parasite-specific CD8+ T cells are essential for infection control, either by promoting protection during early contact with the parasite or by limiting parasite burden during chronic infection [25, 26]. Perforin-producing CD8+ T cells have a contradictory role against *T. cruzi*, being related to myocarditis and heart damage in chronically infected mice [27, 28]. On the other hand, IFN-γ-producing CD8+ T cells have been indicated as protective in both experimental models and patients, although a dysregulated IFN-γ response may be suggested as detrimental in CCC [3, 28-32].

TLR-dependent IFN-β production has been previously implicated in parasite control in dendritic cells and macrophages, and shown to increase resistance to infection in mice [33]. However, contrasting data have demonstrated that TLR-deficient cells still produce IFN-β in response to *T. cruzi*, while TANK-binding kinase 1 (TBK-1) and interferon regulatory factor 3 (IRF3)-deficient cells are significantly impaired [34]. TBK-1 and IRF3 participate in multiple molecular processes [35, 36], including the stimulator of interferon genes (STING) signaling pathway [37]. STING-driven signaling is known to result in production of IFN I and inflammatory cytokines in response to intracellular DNA and cyclic dinucleotides, promoting host defense against pathogens, including many protozoans [38, 39]. Despite the intimate interaction among TBK-1, IRF3 and STING, its function in *T.*

cruzi infection still needed to be determined. Here, we demonstrated that STING signaling is required for IFN-β, IL-6 and IL-12 production in response to *T. cruzi* infection in macrophages. We also demonstrated that cellular infection is necessary to trigger STING signaling and that STING is essential for *T. cruzi* DNA-mediated immune activation. Our results revealed that STING signaling promotes innate and adaptive immune responses to the parasite in mice, contributing to better control of parasitemia and heart parasitism.

Results

STING is required for cytokine production in response to *Trypanosoma cruzi* infection

Trypanosoma cruzi elicits a variety of cytokines that are important for controlling parasite replication and disease establishment. Although increased expression of type I IFNs, IL-6 and IL-12 have been implicated in *T. cruzi* infection, the underlying mechanisms are still not fully understood. Previous data suggest that a signaling pathway dependent on TBK-1 and IRF3 is essential for IFN-β induction in response to *T. cruzi* [34]. Given that STING is a main interactor of TBK-1 and IRF3 proteins, we aimed to evaluate its role on IFN-β production in response to the parasite. As STING has also been involved in induction of NF-kB-dependent pro-inflammatory cytokines [37], we sought to determine its role in IL-6 and IL-12 production during infection. To answer our question, we used RAW-Lucia™ ISG and RAW-Lucia™ ISG-STING-KO macrophages, which are sufficient or deficient for STING expression, respectively, and are designed to secrete luciferase into the culture medium in response to activation of IRF-

dependent signaling pathways. We incubated these cells with *T. cruzi* Y strain for 16 hours to allow infection, removed residual parasites and incubated for additional 24 hours to collect supernatant and total RNA for evaluation of luciferase activity, gene expression and cytokine production (Fig 1A).

We observed that STING-KO macrophages had significantly lower activation of IRF-dependent pathways than control upon *T. cruzi* infection (Fig 1B). Our analysis also showed significantly lower IFN-β, IL-6 and IL-12 gene expression in STING-KO-infected cells (Fig 1C-1E). Corroborating our results, we found significantly lower cytokine production by STING-KO-infected cells when compared to RAW ISG-infected cells (Fig 1F-1H). To further characterize the role of STING signaling in *T. cruzi* infection, we also evaluated TNF-α gene expression and nitric oxide production in response to the parasite and observed no significant differences between STING-KO and RAW ISG cells (S1A and S2A Fig). Overall, our results indicate that STING is required for production of key cytokines involved in anti-*T. cruzi* immunity.

Parasite infection is necessary to activate STING-dependent signaling

STING is known to be involved in intracellular signaling. Therefore, we sought to evaluate whether cellular infection would be necessary to activate STING-dependent pathways. To address this question, we heat-killed the parasite, incubated with RAW-Lucia™ ISG and RAW-Lucia™ ISG-STING-KO macrophages for 16 hours, washed the cells and incubated for additional 24 hours to collect supernatant and total RNA for evaluation of luciferase activity and gene expression (Fig 2A).

We observed no significant difference in luciferase activity when comparing heat-killed *T. cruzi*-exposed STING-KO and RAW ISG cells with their respective unexposed controls (Fig. 2B). We also did not find significant differences in IFN-β, IL-6 and IL-12 gene expression in response to the heat-killed parasite (Fig 2C-2E). In addition, no significant induction of TNF-α gene expression was found in heat-killed *T. cruzi*-exposed STING-KO and RAW ISG cells (S1B Fig). Thus, our results suggest that parasite infection is necessary to activate STING-dependent signaling.

Trypanosoma cruzi DNA induces STING-dependent cytokine expression

Intracellular DNA sensing by different receptors has been shown to result in activation of STING-dependent signaling [40-45]. Therefore, we hypothesized that STING would play a role in parasite DNA recognition, leading to cytokine induction. To test our hypothesis, we transfected RAW-Lucia™ ISG and RAW-Lucia™ ISG-STING-KO cells with *T. cruzi* Y strain DNA, collected supernatant and total RNA 40 hours after transfection and evaluated luciferase activity and gene expression (Fig 3A).

We found that STING was essential for DNA-mediated activation of IRF-dependent pathways, as STING KO cells showed significantly lower luciferase activity upon transfection (Fig 3B). As observed for infection, STING-KO cells had significantly lower IFN-β, IL-6 and IL-12 gene expression in response to *T. cruzi* DNA (Fig 3C-3E). Although STING-KO and RAW ISG cells had similar TNF-α gene expression upon infection, we found that parasite DNA transfection resulted

in increased TNF-α gene expression in RAW ISG cells when compared to uninfected control, which was not observed in STING-KO cells (S1C Fig).

To ensure our system was working properly, we transfected RAW ISG and STING-KO cells with poly IC (TLR3 ligand) and c-di-GMP (STING ligand). We observed that while STING-KO cells were responsive to poly IC, c-di-GMP elicited no luciferase activity or gene expression. Transfection with c-di-GMP failed to induce IL-6 and IL-12 gene expression while poly IC failed to induce IL-12 gene expression in RAW ISG cells, which did not occur upon parasite infection or DNA transfection (S3A-S3D Fig). Taken together, these results indicate that STING is required for immune activation in response to intracellular recognition of *T. cruzi* DNA.

STING signaling increases resistance to infection and promotes anti-*T. cruzi* innate and adaptive immune responses

Previous works have demonstrated that IFN-β, IL-6 and IL-12 are required for immune control of *Trypanosoma cruzi* [12, 13, 33]. Given our *in vitro* results, we hypothesized that STING-KO mice would be more susceptible to infection, due to an impaired immune response to the parasite. To test our hypothesis, we intraperitoneally infected C57BL6 and STING-KO mice with *T. cruzi* Y strain (Fig 4A) and found that STING-KO mice were less effective in controlling parasitemia (Fig 4B). PCR analysis showed higher amounts of *T. cruzi* DNA in the hearts of STING-KO infected animals when compared to C57BL6 (Fig 4C), indicating that STING signaling plays a role in parasite control.

To investigate the impact of STING deficiency on immune response to *T. cruzi*, we performed heart histological analysis of infected animals and observed no difference in the magnitude of inflammatory infiltration 13 days after infection (Fig 4D and 4E). Real-time PCR analysis of the heart tissue at days 4, 7 and 13 after infection revealed a kinetic increase in the expression of genes related to immune control of the parasite in both groups of animals. However, we found significantly lower IFN-β, IL-12, CXCL9, IFN-γ and perforin gene expression in the hearts of STING-KO mice when compared to C57BL6 mice (Fig 5A and 5C-5F). IL-6 gene expression was lower in the hearts of STING-KO-infected mice, although it was not statistically significant (Fig 5B) and we also found lower TNF-α gene expression in the hearts of STING-KO mice 13 days after infection (S1D Fig). To further evaluate our data, we performed correlation analysis and found that although IFN-β, IL-6 and IL-12 gene expression had no correlation with *T. cruzi* DNA in the heart at day 13 after infection (Fig 5G-5I), CXCL9, IFN-γ and perforin gene expression were inversely correlated with *T. cruzi* DNA (Fig 5J-5L). We also observed a positive correlation between CXCL9, IFN-γ and perforin gene expression in the heart of infected animals (S4A-4C Fig).

To have a more systemic view of the immune response to the parasite in the context of STING signaling, we evaluated the spleens of STING-KO and C57BL6-infected mice at days 4, 7 and 13 after infection and observed that IFN-β, IL-6 and IL-12 gene expression was higher at day 4 in both groups of animals, decreasing at days 7 and 13 (Fig 6A-6C). However, we found that C57BL6 mice had significantly higher IFN-β and IL-6 gene expression in the spleen at day 4 after infection when compared to STING-KO mice (Fig 6A and 6B), indicating that STING signaling may play a role in early induction of key cytokines against *T.*

cruzi. TNF-α gene expression was similar in the spleens of STING-KO and C57BL6-infected mice, being higher at day 4 after infection and decreasing over time (S1E Fig). We also evaluated nitric oxide production by splenocytes of infected animals 4, 7 and 13 days after infection and found no significant difference between groups (S2B Fig).

It is well-established that innate and adaptive immune responses contribute to parasite control and that CD8+ T cells are major players in anti-*T. cruzi* immunity [46, 47]. Therefore, we asked whether STING signaling would also be important for effector CD8+ T cell differentiation. To answer this question, we performed flow cytometry using splenocytes to investigate IFN-γ and perforin production by CD8+ T cells against a *T. cruzi* H-2K^{b}-restricted peptide named TSKB20 (Fig 6D). As expected, we found very low numbers of splenic IFN-γ, perforin and IFN-γ/perforin-producing CD8+ T cells in uninfected animals (Fig 6E-6G). On the other hand, we observed significantly higher numbers of splenic TSKB20-specific IFN-γ and IFN-γ/perforin-producing CD8+ T cells in C57BL6 mice when compared to STING-KO mice (Fig 6H and 6J). The numbers of splenic TSKB20-specific CD8+ T cells producing only perforin were similar in both groups (Fig 6I). Collectively, our results indicate that STING signaling promotes innate and adaptive immune responses that help control *T. cruzi* infection.

Discussion

Innate and adaptive immune responses are required for controlling *T. cruzi* replication and disease establishment [48]. Although TLR-dependent IFN-β production increase resistance to infection in mice [33], contrasting data have

demonstrated that MyD88, TRIF, TLR-2, 3 and 4-deficient cells still produce IFN-β in response to *T. cruzi*, while TBK-1 and IRF3-deficient cells are significantly impaired [34]. Here, we showed that STING signaling, which is intimately related to TBK-1 and IRF3 [37], is not only required for activation of IRF-dependent pathways and for production of IFN-β in infected macrophages, but also promotes IL-6 and IL-12 production, which are involved in host resistance to infection [12-14, 17, 33]. Although STING signaling in immunity to many pathogens has been well-determined [38, 39], our work is the first to address its implication in *Trypanosoma cruzi* infection.

Our data showing no immune activation of RAW ISG macrophages upon 16 hours of incubation with heat-killed trypomastigotes indicates that infection is necessary to drive STING-dependent signaling, in contrast to previous data demonstrating IFN-β production by mouse embryonic fibroblasts against dead parasites [34]. Although RAW macrophages may internalize *T. cruzi* through phagocytosis [49], it seemed to have no impact on our model. As expected, parasite DNA transfection triggered robust STING-driven activation of IRF-dependent pathways and expression of IFN-β, IL-6 and IL-12 genes, reinforcing the role of STING signaling in intracellular DNA sensing and host defense against microbial infection [45].

Given our *in vitro* results, we conceived that STING signaling would play a role in protection against *T. cruzi* infection. In fact, we found that STING absence disrupted parasite control, as we observed higher parasitemia in STING-KO mice. We noticed an early difference in systemic infection control, with 60% less blood parasites in C57BL6 mice at day 4 after infection, indicating that innate immunity may have had a major impact on initial parasite infection. Higher IFN-β and IL-6

gene expression in the spleens of C57BL6 mice at the same period corroborates our hypothesis. Although other studies regarding innate immunity have shown distinct intensity and kinetics in parasite control, late differences in parasitemia were more frequently observed [11, 12, 14, 33]. Moreover, one should also consider variations in parasite strain and inoculum when interpreting these data.

STING deficiency resulted in higher heart parasitism, suggesting impairment of local immunity. Although we found no difference in the intensity of myocardial inflammatory infiltrate, the quality of the immune response may have been affected, as suggested by lower expression of genes related to immune protection against acute infection in the hearts of STING-KO mice. The kinetics of the local immune response may have also contributed to early parasite control, as C57BL6 mice presented a much more efficient IFN-β response at day 7 after infection, when parasite DNA started to be detected in the heart. Supporting our hypothesis, previous data have demonstrated early induction of type I IFN response against *T. cruzi* Y strain at the skin of infected mice [16].

CXCL9 chemokine gene expression, known to promote migration of effector T cells to infected tissues and protective immune response against *T. cruzi [50-53]*, was found to be significantly higher in the hearts of C57BL6 mice at day 13 after infection, as was IFN-γ and perforin gene expression. In addition, our analysis also demonstrated a positive correlation among these 3 genes, indicating that STING signaling drives CXCL9-dependent infiltration of IFN-γ and perforin-producing cells in the hearts of acutely infected animals. Although CD4+ T cells have been demonstrated as an important source of IFN-γ during infection [54, 55] and NK cells may also migrate in response to CXCL9 [56] and express IFN-γ and perforin [19, 20], CD8+ T cells are still the most predominant infiltrated population

316 in the heart [57, 58], leading to the hypothesis that these cells may play a major
317 role in ours findings. Nevertheless, further investigation will be necessary to
318 demonstrate whether STING signaling modulates NK and CD4+ T cells during
319 infection.

320 Our flow cytometry analysis revealed a negative impact of STING deficiency on
321 the numbers of splenic parasite-specific IFN-γ and IFN-γ/perforin-producing
322 CD8+ T cells at day 13 after infection, which may explain why we found lower
323 IFN-γ and perforin gene expression in the hearts of STING-KO-infected mice. In
324 contrast to our data, TLR4-deficient animals were shown to have preserved CD8+
325 T cells while having impaired innate immunity against *T. cruzi* [11], indicating a
326 broader function of STING signaling in immune responses to the parasite. While
327 generation of *T. cruzi*-specific CD8+ T cells has been shown to be unaffected by
328 the absence of type I interferon signaling [59], we believe that impairment in the
329 production of IFN-β, IL-6 and IL-12 against the parasite in STING-KO mice may
330 have had a major impact on the adaptive immunity. In fact, these three cytokines
331 have been shown to promote CD8+ T cell activation, proliferation, and survival
332 [60-64], supporting our hypothesis.

333 Perforin-producing CD8+ T cells have a contradictory role in acute and chronic
334 *T. cruzi* infection, being related to myocarditis and heart damage in chronically
335 infected mice [27, 28]. IFN-γ-producing CD8+ T cells have been indicated as
336 protective in both experimental models and patients, although a dysregulated
337 IFN-γ response may be suggested as detrimental in chronic Chagas disease
338 cardiomyopathy [3, 28-32]. Here, we showed an inverse correlation of CXCL9,
339 IFN-γ and perforin expression with parasite DNA in the hearts of infected animals,
340 reinforcing a protective role for these genes in acute infection. Moreover, we

found a more prominent impairment in parasite-specific IFN-γ-producing CD8+ T cells in STING-KO mice, suggesting that STING signaling may be responsible to promote a more effective CD8+ T cell-mediated immune response against *T. cruzi*. Therefore, we believe our results bring an important contribution to the field of imunoparasitology by unveiling new molecular mechanisms underlying immunity against this remarkable pathogen.

Materials and methods

Cell culture, *Trypanosoma cruzi* infection and cellular transfections

LLC-MK2 cells (ATCC) were routinely cultured in DMEM10 (high glucose Dulbecco's Modified Eagle Medium, supplemented with 10% fetal bovine serum (FBS) (Thermo Fisher)) at 37°C and 5% CO2. These cells were infected with the *Trypanosoma cruzi* Y stain in DMEM2 to maintain the parasite.

Heat-killed parasites were obtained by incubation of trypomastigotes in DMEM2 at 56°C for 10 minutes. Parasite DNA was obtained by incubating heat-killed trypomastigotes in lysis buffer (Tris.HCl 0.1M, pH 8.5; EDTA 5mM, pH 8.0; NaCl 0.2M, SDS 0.2%, and 100 µg of Proteinase K in water) at 37°C and 600 rpm for 18h, followed by precipitation with isopropanol at 8600 x g for 5 min, washing with ethanol 70%, centrifugation at 8600 x g for 5 min and resuspension in DNAse/RNAse-free water.

RAW-Lucia™ ISG and RAW-Lucia™ ISG-KO-STING macrophages (InvivoGen) were plated in 24-well plates (Corning) at density of 10^5 cells per well in 500 µl of DMEM2 24h before infection, exposure to heat-killed trypomastigotes or transfections. The cells were incubated for 16h with $3x10^6$ live or heat-killed

trypomastigotes per well in 300 µl of DMEM2, washed with PBS and incubated for additional 24h in 300 µl of DMEM2. Supernatant was harvested and total RNA extracted. Alternatively, the cells were transfected with 80 ng of parasite DNA complexed with lipofectamine 2000 (Thermo Fisher) in 300 µl of OPTIMEM (Thermo Fisher) per well, accordingly to manufacturer's instructions. As experimental controls, the cells were transfected either with 1.0 µg/ml of c-di-GMP (InvivoGen) or 0.5 µg/ml of Poly I:C (InvivoGen) complexed with lipofectamine 2000 in 300 µl of OPTIMEM. Supernatant was harvested and total RNA extracted 40h after transfection.

Luciferase activity and cytokine measurement

Twenty microliters of supernatant from infected, heat-killed parasite-exposed or transfected RAW-Lucia™ ISG and RAW-Lucia™ ISG-KO-STING macrophages were mixed with 50 µl of QUANTI-Luc™ (InvivoGen) and immediately read in a Smart Line TL luminometer (Titertek Berthold), with acquisition time of 1 second for determination of luciferase activity. The detection of IFN-β, IL-6 and IL-12 cytokines in the supernatant of infected RAW-Lucia™ ISG and RAW-Lucia™ ISG-KO-STING macrophages was performed using the Mouse Custom ProcartaPlex kit (Thermo Fisher), accordingly to manufacturer's instructions. The samples were read with a MagPix Luminex system (Merck Millipore) and analyzed using the Milliplex Analyst software (Merck Millipore).

Ethics statement

The study was approved by the Ethics Committee on the Use of Animals (CEUA) of the Faculty of Medicine, University of Sao Paulo (FMUSP), under protocol number 1567/2020, and carried out in accordance with Brazilian Federal Law number 11,794 on scientific use of animals and the National Institutes of Health guide for the care and use of Laboratory animals.

Mice and experimental infection

Six to eight weeks old male wild-type BALB/c, wild-type C57BL/6 and STING-knockout mice (STING-KO) were maintained at the Tropical Medicine Institute II, Faculty of Medicine, University of Sao Paulo. The animals were housed in groups of up to 5 per cage in a room with controlled light and temperature (12h light/dark cycles, 21 ± 2°C), and free access to food and water.

The *Trypanosoma cruzi* Y strain was maintained in BALB/c mice and used to infect wild-type C57BL6 and STING-KO mice. Blood was collected from euthanized BALB/c mice at the peak of infection and centrifuged at 200 x g for 10 min. The supernatant was harvested, centrifuged at 3800 x g and the pellet of parasites resuspended in RPMI1640 (Thermo Fisher). Fifty thousand trypomastigotes in 200 µl of RPMI1640 were intraperitoneally injected in each C57BL6 and STING-KO mouse. Parasitemia was monitored by counting the number of trypomastigotes in 5 µl of fresh blood collected from the tail vein as previously described [65].

Nitrite detection

RAW-Lucia™ ISG and RAW-Lucia™ ISG-KO-STING macrophages were plated and incubated with live trypomastigotes for 16h, as previously described. The cells were washed with PBS and incubated for additional 48h in 300 µl of high glucose DMEM without phenol red (Nova Biotecnologia). Alternatively, splenocytes from 4, 7 and 13 days-infected C57BL6 and STING-KO mice were incubated for 48h at a density of 5 $x10^5$ cells in 200 µl of high glucose DMEM without phenol red per well. The supernatant was harvested, centrifuged at 15000 x g for 5 min. The Nitric Oxide Assay kit (Thermo Fisher) was used accordingly to manufacturer's instructions for total nitrate and nitrite detection with an Epoch spectrophotometer (Biotek).

Real-time PCR

Total RNA extraction from RAW macrophages, hearts and spleens was performed using Trizol reagent (Thermo Fisher), RNeasy Fibrous Tissue kit (Qiagen) and RNeasy mini kit (Qiagen), respectively. Synthesis of cDNA was performed using the Superscript II Reverse Transcriptase (Thermo Fisher), accordingly to manufacturer's instructions. Real-time PCR was performed using Power SyBr green master mix (Thermo Fisher) and a QuantStudio 12k thermocycler (Thermo Fisher) with the following parameters: 95 °C for 15 min, 40 cycles of 95°C for 15s and 60°C for 1 min. The primer sequences were: HPRT1 forward 5'-GTTGGGCTTACCTCACTGCT-3'; HPRT1 reverse 5'-GCAAAAAGCGGTCTGAGGAG-3'; IFNβ forward 5'-TGGGAGATGTCCTCAACTGC-3'; IFNβ reverse 5'-CCAGGCGTAGCTGTTGTACT-3'; IL-6 forward 5'-CCCCAATTTCCAATGCTCTCC-3'; IL-6 reverse 5'-

GGATGGTCTTGGTCCTTAGCC-3’; IL-12 forward 5’-GAAGTCCAATGCAAAGGCGG-3’; IL-12 reverse 5’-GAACACATGCCCACTTGCTG-3’; TNFα forward 5’-ATGGCCTCCCTCTCATCAGT-3’; TNFα reverse 5’-TTTGCTACGACGTGGGCTAC-3’; CXCL9 forward 5’-CCAAGCCCCAATTGCAACAA-3’; CXCL9 reverse 5’-AGTCCGGATCTAGGCAGGTT-3’; IFN-γ forward 5’-AGCAAGGCGAAAAAGGATGC-3’; IFN-γ reverse 5’-TCATTGAATGCTTGGCGCTG-3’; PRF1 forward 5’-TGGTGGGACTTCAGCTTTCC-3’; PRF1 reverse 5’-GAAAAGGCCCAGGAGGAACA-3’.

For detection of parasite DNA in the hearts of infected animals, we extracted DNA using the FlexiGene Kit (Qiagen), accordingly to manufacturer's instructions and used previously described primer sequences [66]. Real-time quantitative PCR was performed using Power Sybr green Master mix and the Quanti Studio 3 thermocycler (Thermo Fisher). The β-actin gene was used as an endogenous control and the calculation of parasitism in the heart was based on a *T. cruzi* DNA dilution curve.

Flow cytometry

Spleens from uninfected and 13 days-infected C57BL6 and STING-KO mice were aseptically removed and disrupted using 70 µm Cell strainer (Corning). Red blood cells were lysed using ACK lysis buffer (Thermo Fisher), the samples were centrifuged at 300 x g for 5 min and splenocytes resuspended in R10 medium

(RPMI1640 supplemented with 10% FBS, 2 mM L-glutamine, 1 mM sodium pyruvate, 1% vol/vol non-essential amino acids solution, 1% vol/vol vitamin solution, 40 µg/mL of Gentamicin and 5×10^{-5} M 2β-mercaptoethanol, all from Thermo Fisher). Splenocytes were plated in 96-well round bottom plates (Corning) at a density of 0.5 x 10^6 cells in 200 µl of R10 medium and stimulated with 10 µg/mL of the *T. cruzi* H2-K^b-restricted peptide TSKB20 in the presence of 5 µg/ml of Brefeldin A (Biolegend) for 14h at 37ºC and 5% CO2. DMSO and PMA (50 ng/mL) plus Ionomycin (500 ng/mL) (Sigma) were used as negative and positive control stimuli, respectively.

After stimulation, the cells were transferred to 96-well V-bottom plates (Corning), centrifuged at 300x g for 5 minutes and stained with the monoclonal antibodies anti-CD3 APC-Cy7 (BD Biosciences), anti-CD4 PerCP (BD Biosciences) and anti-CD8 PE-Cy7 (BD Biosciences) diluted in PBS for 30 minutes at 4°C. The cells were washed twice with PBS and fixed with BD Cytofix/Cytoperm™, accordingly to manufacturer's instructions. Thereafter, the cells were washed twice with BD Perm/Wash™ buffer and stained with the monoclonal antibodies anti-IFN-γ APC (BD Biosciences) and anti-Perforin PE (Biolegend) diluted in BD Perm/Wash™ buffer for 30 minutes at 4°C. The cells were washed twice with BD Perm/Wash™ buffer and resuspended in PBS. The samples were acquired with a FACS Canto II (BD Biosciences) cytometer and analyzed with FlowJo 10 software (BD Biosciences).

Histological analysis

Heart samples were fixed in a 10% buffered formalin solution, dehydrated in an increasing concentration of ethanol, and embedded in paraffin. The blocks were sectioned with a thickness of 5 µm and stained with hematoxylin-eosin (H&E). The pathologist performed blinded histological analysis and provided a score for the intensity of myocarditis.

Statistical analysis

The results were analyzed using the Graph Pad Prism 8 software. We used Mann-Whitney test for comparisons between 2 parameters and Two-way ANOVA, Tukey's and Bonferroni's tests for multiple comparisons.

Acknowledgments

We thank Luis Roberto Mundel and Edilberto Postól for assistance at the animal facility. We also thank Andreia Kuramoto Takara for technical assistance.

References

1. Rassi A, Marin-Neto JA. Chagas disease. Lancet. 2010;375(9723):1388-402. doi: 10.1016/s0140-6736(10)60061-x. PubMed PMID: WOS:000277057800029.

2. Dutra WO, Menezes CAS, Villani FNA, da Costa GC, da Silveira ABM, Reis DD, et al. Cellular and genetic mechanisms involved in the generation of protective and pathogenic immune responses in human Chagas disease. Memorias Do Instituto Oswaldo Cruz. 2009;104:208-18. doi: 10.1590/s0074-02762009000900027. PubMed PMID: WOS:000269123500026.

3. Chevillard C, Nunes JPS, Frade AF, Almeida RR, Pandey RP, Nascimento MS, et al. Disease Tolerance and Pathogen Resistance Genes May Underlie Trypanosoma cruzi Persistence and Differential Progression to Chagas Disease Cardiomyopathy. Frontiers in Immunology. 2018;9. doi: 10.3389/fimmu.2018.02791. PubMed PMID: WOS:000451946600001.

4. Campos MA, Almeida IC, Takeuchi O, Akira S, Valente EP, Procopio DO, et al. Activation of toll-like receptor-2 by glycosylphosphatidylinositol anchors from a protozoan parasite. Journal of Immunology. 2001;167(1):416-23. doi: 10.4049/jimmunol.167.1.416. PubMed PMID: WOS:000170949100056.
5. Ouaissi A, Guilvard E, Delneste Y, Caron G, Magistrelli G, Herbault N, et al. The Trypanosoma cruzi Tc52-released protein induces human dendritic cell maturation, signals via toll-like receptor 2, and confers protection against lethal infection. Journal of Immunology. 2002;168(12):6366-74. doi: 10.4049/jimmunol.168.12.6366. PubMed PMID: WOS:000176145300053.
6. Oliveira AC, Peixoto JR, de Arruda LB, Campos MA, Gazzinelli RT, Golenbock DT, et al. Expression of functional TLR4 confers proinflammatory responsiveness to Trypanosama cruzi glycoinositolphospholipids and higher resistance to infection with T-cruzi. Journal of Immunology. 2004;173(9):5688-96. doi: 10.4049/jimmunol.173.9.5688. PubMed PMID: WOS:000224665900044.
7. Bafica A, Santiago HC, Goldszmid R, Ropert C, Gazzinelli RT, Sher A. Cutting edge: TLR9 and TLR2 signaling together account for MyD88-dependent control of parasitemia in Trypanosoma cruzi infection. Journal of Immunology. 2006;177(6):3515-9. doi: 10.4049/jimmunol.177.6.3515. PubMed PMID: WOS:000240475300002.
8. Campos MA, Closel M, Valente EP, Cardoso JE, Akira S, Alvarez-Leite JI, et al. Impaired production of proinflammatory cytokines and host resistance to acute infection with Trypanosoma cruzi in mice lacking functional myeloid differentiation factor 88. Journal of Immunology. 2004;172(3):1711-8. doi: 10.4049/jimmunol.172.3.1711. PubMed PMID: WOS:000188378700047.
9. Silva GK, Gutierrez FRS, Guedes PMM, Horta CV, Cunha LD, Mineo TWP, et al. Cutting Edge: Nucleotide-Binding Oligomerization Domain 1-Dependent Responses Account for Murine Resistance against Trypanosoma cruzi Infection. Journal of Immunology. 2010;184(3):1148-52. doi: 10.4049/jimmunol.0902254. PubMed PMID: WOS:000273956400005.
10. Goncalves VM, Matteucci KC, Buzzo CL, Miollo BH, Ferrante D, Torrecilhas AC, et al. NLRP3 Controls Trypanosoma cruzi Infection through a Caspase-1-Dependent IL-1R-Independent NO Production. Plos Neglected Tropical Diseases. 2013;7(10). doi: 10.1371/journal.pntd.0002469. PubMed PMID: WOS:000330376500012.
11. Oliveira AC, de Alencar BC, Tzelepis F, Klezewsky W, da Silva RN, Neves FS, et al. Impaired Innate Immunity in Tlr4(-/-) Mice but Preserved CD8(+) T Cell Responses against Trypanosoma cruzi in Tlr4-, Tlr2-, Tlr9- or Myd88-Deficient Mice. Plos Pathogens. 2010;6(4). doi: 10.1371/journal.ppat.1000870. PubMed PMID: WOS:000277722400042.
12. Gao WD, Pereira MA. Interleukin-6 is required for parasite specific response and host resistance to Trypanosoma cruzi. International Journal for Parasitology. 2002;32(2):167-70. doi: 10.1016/s0020-7519(01)00322-8. PubMed PMID: WOS:000173905200006.
13. Aliberti JCS, Cardoso MAG, Martins GA, Gazzinelli RT, Vieira LQ, Silva JS. Interleukin-12 mediates resistance to Trypanosoma cruzi in mice and is produced by murine macrophages in response to live trypomastigotes. Infection and Immunity. 1996;64(6):1961-7. PubMed PMID: WOS:A1996UN18900012.
14. Graefe SEB, Jacobs T, Gaworski I, Klauenberg U, Steeg C, Fleischer B. Interleukin-12 but not interleukin-18 is required for immunity to Trypanosoma cruzi in mice. Microbes and Infection. 2003;5(10):833-9. doi: 10.1016/s1286-4579(03)00176-x. PubMed PMID: WOS:000185085600003.
15. Abrahamsohn IA, Coffman RL. Trypanosoma cruzi: IL-10, TNF, IFN-gamma, and IL-12 regulate innate and acquired immunity to infection. Exp Parasitol. 1996;84(2):231-44. doi: 10.1006/expr.1996.0109. PubMed PMID: 8932773.
16. Chessler ADC, Unnikrishnan M, Bei AK, Daily JP, Burleigh BA. Trypanosoma cruzi Triggers an Early Type I IFN Response In Vivo at the Site of Intradermal Infection. Journal of Immunology.

563 2009;182(4):2288-96. doi: 10.4049/jimmunol.0800621. PubMed PMID:
564 WOS:000263126300058.
565 17. Costa VMA, Torres KCL, Mendonca RZ, Gresser I, Gollob KJ, Abrahamsohn IA. Type I IFNs
566 stimulate nitric oxide production and resistance to Trypanosoma cruzi infection. Journal of
567 Immunology. 2006;177(5):3193-200. doi: 10.4049/jimmunol.177.5.3193. PubMed PMID:
568 WOS:000240002800054.
569 18. Chessler ADC, Caradonna KL, Da'dara A, Burleigh BA. Type I Interferons Increase Host
570 Susceptibility to Trypanosoma cruzi Infection. Infection and Immunity. 2011;79(5):2112-9. doi:
571 10.1128/iai.01176-10. PubMed PMID: WOS:000289672700033.
572 19. Lieke T, Graefe SEB, Klauenberg U, Fleischer B, Jacobs T. NK cells contribute to the
573 control of Trypanosoma cruzi infection by killing free parasites by perforin-independent
574 mechanisms. Infection and Immunity. 2004;72(12):6817-25. doi: 10.1128/iai.72.12.6817-
575 6825.2004. PubMed PMID:WOS:000225453900008.
576 20. Cardillo F, Voltarelli JC, Reed SG, Silva JS. Regulation of Trypanosoma cruzi infection in
577 mice by gamma interferon and interleukin 10: Role of NK cells. Infection and Immunity.
578 1996;64(1):128-34. doi: 10.1128/iai.64.1.128-134.1996. PubMed PMID:
579 WOS:A1996TM71800019.
580 21. Kumar S, Tarleton RL. Antigen-specific Th1 but not Th2 cells provide protection from
581 lethal Trypanosoma cruzi infection in mice. Journal of Immunology. 2001;166(7):4596-603. doi:
582 10.4049/jimmunol.166.7.4596. PubMed PMID: WOS:000170948200040.
583 22. Hoft DF, Schnapp AR, Eickhoff CS, Roodman ST. Involvement of CD4(+) Th1 cells in
584 systemic immunity protective against primary and secondary challenges with Trypanosoma
585 cruzi. Infection and Immunity. 2000;68(1):197-204. doi: 10.1128/iai.68.1.197-204.2000.
586 PubMed PMID: WOS:000084301800029.
587 23. Bryan MA, Guyach SE, Norris KA. Specific Humoral Immunity versus Polyclonal B Cell
588 Activation in Trypanosoma cruzi Infection of Susceptible and Resistant Mice. Plos Neglected
589 Tropical Diseases. 2010;4(7). doi: 10.1371/journal.pntd.0000733. PubMed PMID:
590 WOS:000280412300005.
591 24. Cai CW, Blase JR, Zhang XL, Eickhoff CS, Hoft DF. Th17 Cells Are More Protective Than
592 Th1 Cells Against the Intracellular Parasite Trypanosoma cruzi. Plos Pathogens. 2016;12(10). doi:
593 10.1371/journal.ppat.1005902. PubMed PMID:WOS:000387666900017.
594 25. Tarleton RL. DEPLETION OF CD8+ T-CELLS INCREASES SUSCEPTIBILITY AND REVERSES
595 VACCINE-INDUCED IMMUNITY IN MICE INFECTED WITH TRYPANOSOMA-CRUZI. Journal of
596 Immunology. 1990;144(2):717-24. PubMed PMID: WOS:A1990CH29500045.
597 26. Tarleton RL, Koller BH, Latour A, Postan M. SUSCEPTIBILITY OF BETA-2-
598 MICROGLOBULIN-DEFICIENT MICE TO TRYPANOSOMA-CRUZI INFECTION. Nature.
599 1992;356(6367):338-40. doi: 10.1038/356338a0. PubMed PMID: WOS:A1992HK79400064.
600 27. Nickell SP, Sharma D. Trypanosoma cruzi: roles for perforin-dependent and perforin-
601 independent immune mechanisms in acute resistance. Experimental Parasitology.
602 2000;94(4):207-16. doi: 10.1006/expr.2000.4498. PubMed PMID: WOS:000087566400001.
603 28. Silverio JC, Pereira IR, Cipitelli MD, Vinagre NF, Rodrigues MM, Gazzinelli RT, et al. CD8(+)
604 T-Cells Expressing Interferon Gamma or Perforin Play Antagonistic Roles in Heart Injury in
605 Experimental Trypanosoma Cruzi-Elicited Cardiomyopathy. Plos Pathogens. 2012;8(4). doi:
606 10.1371/journal.ppat.1002645. PubMed PMID:WOS:000303444200037.
607 29. Michailowsky V, Silva NM, Rocha CD, Vieira LQ, Lannes-Vieira J, Gazzinelli RT. Pivotal role
608 of interleukin-12 and interferon-gamma axis in controlling tissue parasitism and inflammation
609 in the heart and central nervous system during Trypanosoma cruzi infection. American Journal
610 of Pathology. 2001;159(5):1723-33. doi: 10.1016/s0002-9440(10)63019-2. PubMed PMID:
611 WOS:000171988000015.
612 30. Laucella SA, Postan M, Martin D, Hubby Fralish B, Albareda MC, Alvarez MG, et al.
613 Frequency of interferon- gamma -producing T cells specific for Trypanosoma cruzi inversely

614 correlates with disease severity in chronic human Chagas disease. J Infect Dis. 2004;189(5):909-
615 18. Epub 20040217. doi: 10.1086/381682. PubMed PMID: 14976609.
616 31. Albareda MC, Laucella SA, Alvarez MG, Armenti AH, Bertochi G, Tarleton RL, et al.
617 Trypanosoma cruzi modulates the profile of memory CD8(+) T cells in chronic Chagas' disease
618 patients. International Immunology. 2006;18(3):465-71. doi: 10.1093/intimm/dxh387. PubMed
619 PMID:WOS:000235771900008.
620 32. Reis MM, Higuchi MD, Benvenuti LA, Aiello VD, Gutierrez PS, Bellotti G, et al. An in situ
621 quantitative immunohistochemical study of cytokines and IL-2R(+) in chronic human chagasic
622 myocarditis: Correlation with the presence of myocardial Trypanosoma cruzi antigens. Clinical
623 Immunology and Immunopathology. 1997;83(2):165-72. doi: 10.1006/clin.1997.4335. PubMed
624 PMID:WOS:A1997WW05600008.
625 33. Koga R, Hamano S, Kuwata H, Atarashi K, Ogawa M, Hisaeda H, et al. TLR-dependent
626 induction of IFN-beta mediates host defense against Trypanosoma cruzi. Journal of Immunology.
627 2006;177(10):7059-66. doi: 10.4049/jimmunol.177.10.7059. PubMed PMID:
628 WOS:000242009700057.
629 34. Chessler ADC, Ferreira LRP, Chang TH, Fitzgerald KA, Burleiph BA. A Novel IFN Regulatory
630 Factor 3-Dependent Pathway Activated by Trypanosomes Triggers IFN-beta in Macrophages and
631 Fibroblasts. Journal of Immunology. 2008;181(11):7917-24. doi:
632 10.4049/jimmunol.181.11.7917. PubMed PMID: WOS:000261220000055.
633 35. Jefferies CA. Regulating IRFs in IFN Driven Disease. Frontiers in Immunology. 2019;10.
634 doi: 10.3389/fimmu.2019.00325. PubMed PMID: WOS:000462781600001.
635 36. Helgason E, Phung QT, Dueber EC. Recent insights into the complexity of Tank-binding
636 kinase 1 signaling networks: The emerging role of cellular localization in the activation and
637 substrate specificity of TBK1. Febs Letters. 2013;587(8):1230-7. doi:
638 10.1016/j.febslet.2013.01.059. PubMed PMID:WOS:000317188700030.
639 37. Hopfner KP, Hornung V. Molecular mechanisms and cellular functions of cGAS-STING
640 signalling. Nature Reviews Molecular Cell Biology. 2020;21(9):501-21. doi: 10.1038/s41580-020-
641 0244-x. PubMed PMID:WOS:000533801300001.
642 38. Ahn J, Barber GN. STING signaling and host defense against microbial infection. Exp Mol
643 Med. 2019;51(12):1-10. Epub 20191211. doi: 10.1038/s12276-019-0333-0. PubMed PMID:
644 31827069; PubMed Central PMCID: PMCPMC6906460.
645 39. Sun YF, Cheng Y. STING or Sting: cGAS-STING-Mediated Immune Response to Protozoan
646 Parasites. Trends in Parasitology. 2020;36(9):773-84. doi: 10.1016/j.pt.2020.07.001. PubMed
647 PMID:WOS:000562473400008.
648 40. Takaoka A, Wang Z, Choi MK, Yanai H, Negishi H, Ban T, et al. DAI (DLM-1/ZBP1) is a
649 cytosolic DNA sensor and an activator of innate immune response. Nature. 2007;448(7152). doi:
650 10.1038/nature06013. PubMed PMID: WOS:000248302700053.
651 41. Yang P, An H, Liu X, Wen M, Zheng Y, Rui Y, et al. The cytosolic nucleic acid sensor
652 LRRFIP1 mediates the production of type I interferon via a beta-catenin-dependent pathway.
653 Nature Immunology. 2010;11(6). doi: 10.1038/ni.1876. PubMed PMID:
654 WOS:000277821300009.
655 42. Zhang ZQ, Yuan B, Bao MS, Lu N, Kim T, Liu YJ. The helicase DDX41 senses intracellular
656 DNA mediated by the adaptor STING in dendritic cells. Nature Immunology. 2011;12(10):959-
657 U62. doi: 10.1038/ni.2091. PubMed PMID: WOS:000295084500011.
658 43. Unterholzner L, Keating SE, Baran M, Horan KA, Jensen SB, Sharma S, et al. IFI16 is an
659 innate immune sensor for intracellular DNA. Nature Immunology. 2010;11(11). doi:
660 10.1038/ni.1932. PubMed PMID: WOS:000283127800009.
661 44. Sun L, Wu J, Du F, Chen X, Chen ZJ. Cyclic GMP-AMP Synthase Is a Cytosolic DNA Sensor
662 That Activates the Type I Interferon Pathway. Science. 2013;339(6121):786-91. doi:
663 10.1126/science.1232458. PubMed PMID:WOS:000314874400039.

664 45. Ahn J, Barber GN. STING signaling and host defense against microbial infection.
665 Experimental and Molecular Medicine. 2019;51. doi: 10.1038/s12276-019-0333-0. PubMed
666 PMID:WOS:000502859600007.
667 46. Tarleton RL. CD8(+) T cells in Trypanosoma cruzi infection. Seminars in
668 Immunopathology. 2015;37(3):233-8. doi: 10.1007/s00281-015-0481-9. PubMed PMID:
669 WOS:000354804700004.
670 47. Rodriguez EVA, Furlan CLA, Vernengo FF, Montes CL, Gruppi A. Understanding CD8(+) T
671 Cell Immunity to Trypanosoma cruzi and How to Improve It. Trends in Parasitology.
672 2019;35(11):899-917. doi: 10.1016/j.pt.2019.08.006. PubMed PMID: WOS:000492674900007.
673 48. Acevedo GR, Girard MC, Gomez KA. The Unsolved Jigsaw Puzzle of the Immune
674 Response in Chagas Disease. Frontiers in Immunology. 2018;9. doi: 10.3389/fimmu.2018.01929.
675 PubMed PMID: WOS:000442628900001.
676 49. Maganto-Garcia E, Punzon C, Terhorst C, Fresno M. Rab5 activation by Toll-like receptor
677 2 is required for Trypanosoma cruzi internalization and replication in macrophages. Traffic.
678 2008;9(8):1299-315. doi: 10.1111/j.1600-0854.2008.00760.x. PubMed PMID:
679 WOS:000257699600007.
680 50. Hardison JL, Wrightsman RA, Carpenter PM, Lane TE, Manning JE. The chemokines
681 CXCL9 and CXCL10 promote a protective immune response but do not contribute to cardiac
682 inflammation following infection with Trypanosoma cruzi. Infection and Immunity.
683 2006;74(1):125-34. doi: 10.1128/iai.74.1.125-134.2006. PubMed PMID:
684 WOS:000234276400013.
685 51. Ferreira CP, Cariste LM, Moraschi BF, Zanetti BF, Han SW, Ribeiro DA, et al. CXCR3
686 chemokine receptor guides Trypanosoma cruzi-specific T-cells triggered by DNA/adenovirus
687 ASP2 vaccine to heart tissue after challenge. Plos Neglected Tropical Diseases. 2019;13(7). doi:
688 10.1371/journal.pntd.0007597. PubMed PMID:WOS:000478662500070.
689 52. Teixeira MM, Gazzinelli RT, Silva JS. Chemokines, inflammation and Trypanosoma cruzi
690 infection. Trends in Parasitology. 2002;18(6):262-5. doi: 10.1016/s1471-4922(02)02283-3.
691 PubMed PMID: WOS:000175784600007.
692 53. Nogueira LG, Santos RHB, Ianni BM, Fiorelli AI, Mairena EC, Benvenuti LA, et al.
693 Myocardial Chemokine Expression and Intensity of Myocarditis in Chagas Cardiomyopathy Are
694 Controlled by Polymorphisms in CXCL9 and CXCL10. Plos Neglected Tropical Diseases.
695 2012;6(10). doi: 10.1371/journal.pntd.0001867. PubMed PMID: WOS:000310527200032.
696 54. Sanoja C, Carbajosa S, Fresno M, Girones N. Analysis of the Dynamics of Infiltrating
697 CD4(+) T Cell Subsets in the Heart during Experimental Trypanosoma cruzi Infection. Plos One.
698 2013;8(6). doi: 10.1371/journal.pone.0065820. PubMed PMID: WOS:000320755400069.
699 55. Albareda MC, Olivera GC, Laucella SA, Alvarez MG, Fernandez ER, Lococo B, et al. Chronic
700 Human Infection with Trypanosoma cruzi Drives CD4(+) T Cells to Immune Senescence. Journal
701 of Immunology. 2009;183(6):4103-8. doi: 10.4049/jimmunol.0900852. PubMed PMID:
702 WOS:000270179700065.
703 56. Thapa M, Welner RS, Pelayo R, Carr DJJ. CXCL9 and CXCL10 expression are critical for
704 control of genital herpes simplex virus type 2 infection through mobilization of HSV-specific CTL
705 and NK cells to the nervous system. Journal of Immunology. 2008;180(2):1098-106. doi:
706 10.4049/jimmunol.180.2.1098. PubMed PMID: WOS:000252290000047.
707 57. dos Santos PVA, Roffe E, Santiago HC, Torres RA, Marino A, Paiva CN, et al. Prevalence
708 of CD8(+)alpha beta T cells in Trypanosoma cruzi-elicited myocarditis is associated with
709 acquisition of CD62L(Low)LFA-1(High)VLA-4(High) activation phenotype and expression of IFN-
710 gamma-inducible adhesion and chemoattractant molecules. Microbes and Infection.
711 2001;3(12):971-84. doi: 10.1016/s1286-4579(01)01461-7. PubMed PMID:
712 WOS:000171578400002.
713 58. Reis DD, Jones EM, Tostes S, Lopes ER, Gazzinelli G, Colley DG, et al. CHARACTERIZATION
714 OF INFLAMMATORY INFILTRATES IN CHRONIC CHAGASIC MYOCARDIAL LESIONS - PRESENCE OF
715 TUMOR NECROSIS FACTOR-ALPHA+ CELLS AND DOMINANCE OF GRANZYME A+, CD8+

716 LYMPHOCYTES. American Journal of Tropical Medicine and Hygiene. 1993;48(5):637-44. doi:
717 10.4269/ajtmh.1993.48.637. PubMed PMID: WOS:A1993LJ65300006.
718 59. Martin DL, Murali-Krishna K, Tarleton RL. Generation of Trypanosoma cruzi-Specific
719 CD8(+) T-Cell Immunity Is Unaffected by the Absence of Type I Interferon Signaling. Infection
720 and Immunity. 2010;78(7):3154-9. doi: 10.1128/iai.00275-10. PubMed PMID:
721 WOS:000278830200029.
722 60. Wilson DC, Matthews S, Yap GS. IL-12 signaling drives CD8(+) T cell IFN-gamma
723 production and differentiation of KLRG1(+) effector subpopulations during Toxoplasma gondii
724 infection. Journal of Immunology. 2008;180(9):5935-45. doi: 10.4049/jimmunol.180.9.5935.
725 PubMed PMID: WOS:000257507000025.
726 61. Henry CJ, Ornelles DA, Mitchell LM, Brzoza-Lewis KL, Hiltbold EM. IL-12 Produced by
727 Dendritic Cells Augments CD8(+) T Cell Activation through the Production of the Chemokines
728 CCL1 and CCL17. Journal of Immunology. 2008;181(12):8576-84. doi:
729 10.4049/jimmunol.181.12.8576. PubMed PMID: WOS:000261583000047.
730 62. Li BF, Jones LL, Geiger TL. IL-6 Promotes T Cell Proliferation and Expansion under
731 Inflammatory Conditions in Association with Low-Level ROR gamma t Expression. Journal of
732 Immunology. 2018;201(10):2934-46. doi: 10.4049/jimmunol.1800016. PubMed PMID:
733 WOS:000449433800009.
734 63. Sanmarco LM, Visconti LM, Eberhardt N, Ramello MC, Ponce NE, Spitale NB, et al. IL-6
735 Improves the Nitric Oxide-Induced Cytotoxic CD8+T Cell Dysfunction in Human Chagas Disease.
736 Frontiers in Immunology. 2016;7. doi: 10.3389/fimmu.2016.00626. PubMed PMID:
737 WOS:000390373300001.
738 64. Kolumam GA, Thomas S, Thompson LJ, Sprent J, Murali-Krishna K. Type I interferons act
739 directly on CD8 T cells to allow clonal expansion and memory formation in response to viral
740 infection. Journal of Experimental Medicine. 2005;202(5):637-50. doi: 10.1084/jem.20050821.
741 PubMed PMID: WOS:000231962700008.
742 65. BRENER Z. Therapeutic activity and criterion of cure on mice experimentally infected
743 with Trypanosoma cruzi. Rev Inst Med Trop Sao Paulo. 1962;4:389-96. PubMed PMID:
744 14015230.
745 66. Piron M, Fisa R, Casamitjana N, López-Chejade P, Puig L, Vergés M, et al. Development
746 of a real-time PCR assay for Trypanosoma cruzi detection in blood samples. Acta Trop.
747 2007;103(3):195-200. Epub 20070623. doi: 10.1016/j.actatropica.2007.05.019. PubMed PMID:
748 17662227.

749

750 Figure captions

751 Fig 1. STING signaling is required for cytokine production in response to *T.*

752 ***cruzi* infection. (A)** Experimental procedure of in vitro *T. cruzi* infection. **(B)** IRF-

753 dependent luciferase activity of uninfected and infected-RAW ISG and RAW ISG

754 STING-KO cells. **(C-E)** Real-time PCR analysis of IFN-β, IL-6 and IL-12 mRNA

755 expression in uninfected and infected-RAW ISG and RAW ISG STING-KO cells.

756 HPRT1 was used as housekeeping gene. **(F-H)** Luminex analysis of IFN-β, IL-6

and IL-12 cytokines in the supernatant of infected-RAW ISG and RAW ISG STING-KO cells. IFN-β, IL-6 and IL-12 values from supernatant of uninfected cells were subtracted. NS = no statistical significance. Two-way ANOVA and Tukey's multiple comparison test **(B-E)**. Mann-Whitney test **(F-H)**. Data are shown as mean ± S.D. **(B-H)**. Experimental figure was created with BioRender.com.

Fig 2. *Trypanosoma cruzi* infection is necessary to activate STING-dependent signaling. (A) Experimental procedure with heat-killed *T. cruzi*. **(B)** IRF-dependent luciferase activity of unexposed and heat-killed *T. cruzi* exposed-RAW ISG and RAW ISG STING-KO cells. **(C-E)** Real-time PCR analysis of IFN-β, IL-6 and IL-12 mRNA expression in unexposed and heat-killed *T. cruzi* exposed-RAW ISG and RAW ISG STING-KO cells. HPRT1 was used as housekeeping gene. NS = no statistical significance. Two-way ANOVA and Tukey's multiple comparison test **(B-E)**. Data are shown as mean ± S.D. **(B-E)**. Experimental figure was created with BioRender.com.

Fig 3. *Trypanosoma cruzi* DNA activates STING-dependent signaling. (A) Experimental procedure of *T. cruzi* DNA transfection. **(B)** IRF-dependent luciferase activity of non-transfected (NT) and *T. cruzi* DNA-transfected RAW ISG and RAW ISG STING-KO cells. **(C-E)** Real-time PCR analysis of IFN-β, IL-6 and IL-12 mRNA expression in non-transfected (NT) and *T. cruzi* DNA-transfected RAW ISG and RAW ISG STING-KO cells. HPRT1 was used as housekeeping gene. NS = no statistical significance. Two-way ANOVA and Tukey's multiple

comparison test **(B-E)**. Data are shown as mean ± S.D. **(B-E)**. Experimental figure was created with BioRender.com.

Fig 4. STING signaling increases resistance to *T. cruzi* infection. (A) Experimental procedure of intraperitoneal in vivo *T. cruzi* infection. **(B)** Parasitemia of STING-KO and C57BL6-infected mice. **(C)** Real-time PCR analysis of *T. cruzi* DNA in the hearts of STING-KO and C57BL6 mice 4, 7 and 13 days after infection. **(D-E)** Histological analysis of the hearts of STING-KO and C57BL6 mice 13 days after infection. NS = no statistical significance. Two-way ANOVA and Bonferroni's multiple comparison test **(B-C)**. Two-way ANOVA and Tukey's multiple comparison test **(E)**. Data are shown as mean ± S.D. (**B, D)**. Data are shown as mean ± S.E.M. **(C)**. Experimental figure was created with BioRender.com.

Fig 5. STING deficiency disrupts immune responses in the heart of T. cruzi-infected mice. (A-F) Real-time PCR analysis of IFN-β, IL-6, IL-12, CXCL9, IFN-γ and PRF1 mRNA expression in the hearts of STING-KO and C57BL6 mice 4, 7 and 13 days after infection. **(G-L)** Correlation analysis of IFN-β, IL-6, IL-12, CXCL9, IFN-γ and PRF1 mRNA expression with *T. cruzi* DNA in the hearts of STING-KO (blue circles) and C57BL6 (red circles) mice 13 days after infection. NS = no statistical significance. Two-way ANOVA and Bonferroni's multiple comparison test **(A-F)**. Pearson's correlation **(G-L)**. Data are shown as mean ± S.E.M. **(A-F)**.

Fig 6. STING deficiency impairs innate and adaptive immune responses in *T. cruzi*-infected mice. (A-C) Real-time PCR analysis of IFN-β, IL-6 and IL-12 mRNA expression in the spleens of STING-KO and C57BL6 mice 4, 7 and 13 days after infection. **(D)** Intracellular flow cytometry analysis of IFN-γ and perforin production by CD8+ T cells. **(E-F)** Number (#) of IFN-γ, perforin and IFN-γ/perforin producing-CD8+ T cells in total splenocytes of uninfected mice, non-stimulated (N.S) or stimulated with TSKB20 peptide 13 days after infection. **(H-J)** Number (#) of IFN-γ, perforin and IFN-γ/perforin producing-CD8+ T cells in total splenocytes of *T. cruzi*-infected mice, non-stimulated (N.S) or stimulated with TSKB20 peptide 13 days after infection. NS = no statistical significance. Two-way ANOVA and Bonferroni's multiple comparison test **(A-C)**. Two-way ANOVA and Tukey's multiple comparison test **(E-J)**. Data are shown as mean ± S.E.M. **(A-C)**. Data are shown as mean ± S.D. **(E-J)**.

S1 Fig. STING deficiency has variable impact on TNF-α response to *T. cruzi*. **(A)** Real-time PCR analysis of TNF-α mRNA expression in uninfected and infected-RAW ISG and RAW ISG STING-KO cells. **(B)** Real-time PCR analysis of TNF-α mRNA expression in unexposed and heat-killed *T. cruzi*-exposed RAW ISG and RAW ISG STING-KO cells. **(C)** Real-time PCR analysis of TNF-α mRNA expression in non-transfected (NT) and *T. cruzi* DNA-transfected RAW ISG and RAW ISG STING-KO cells. **(D-E)** Real-time PCR analysis of TNF-α mRNA expression in the heart and spleen of STING-KO and C57BL6 mice 4, 7 and 13 days after infection. Hprt1 was used as housekeeping gene. NS = no statistical significance. Two-way ANOVA and Tukey's multiple comparison test **(A-C)**. Two-

way ANOVA and Bonferroni's multiple comparison test **(D-E)**. Data are shown as mean ± S.D. **(A-C)**. Data are shown as mean ± S.E.M. **(D-E)**.

S2 Fig. STING deficiency has no impact on nitric oxide production against *T. cruzi*. (A) Nitrite detection in the supernatant of uninfected and infected-RAW ISG and RAW ISG STING-KO cells 48h after infection. **(B)** Nitrite detection in the supernatant of splenocytes from STING-KO and C57BL6 mice at days 4, 7 and 13 after infection, incubated for 48h. NS = no statistical significance. Two-way ANOVA and Tukey's multiple comparison test **(A)**. Two-way ANOVA and Bonferroni's multiple comparison test **(B)**. Data are shown as mean ± S.D. **(A)**. Data are shown as mean ± S.E.M. **(B)**.

S3 Fig. RAW ISG STING-KO cells are responsive to poly IC but not to c-di-GMP transfection. (A) IRF-dependent luciferase activity of non-transfected (NT) and transfected RAW ISG and RAW ISG STING-KO cells. **(B-D)** Real-time PCR analysis of IFN-β, IL-6 and IL-12 mRNA expression in non-transfected (NT) and transfected RAW ISG and RAW ISG STING-KO cells. HPRT1 was used as housekeeping gene. NS = no statistical significance. Two-way ANOVA and Tukey's multiple comparison test **(A-D)**. Data are shown as mean ± S.D. **(A-D)**.

S4 Fig. CXCL9, IFN-γ and perforin gene expression positively correlates in the hearts of infected animals. (A-C) Pearson's correlation analysis of CXCL9,

IFN-γ and PRF1 mRNA expression in the hearts of STING-KO (blue circles) and C57BL6 (red circles) mice 13 days after infection.

Figure 1

Click here to access/download;Figure;Fig 1.pptx

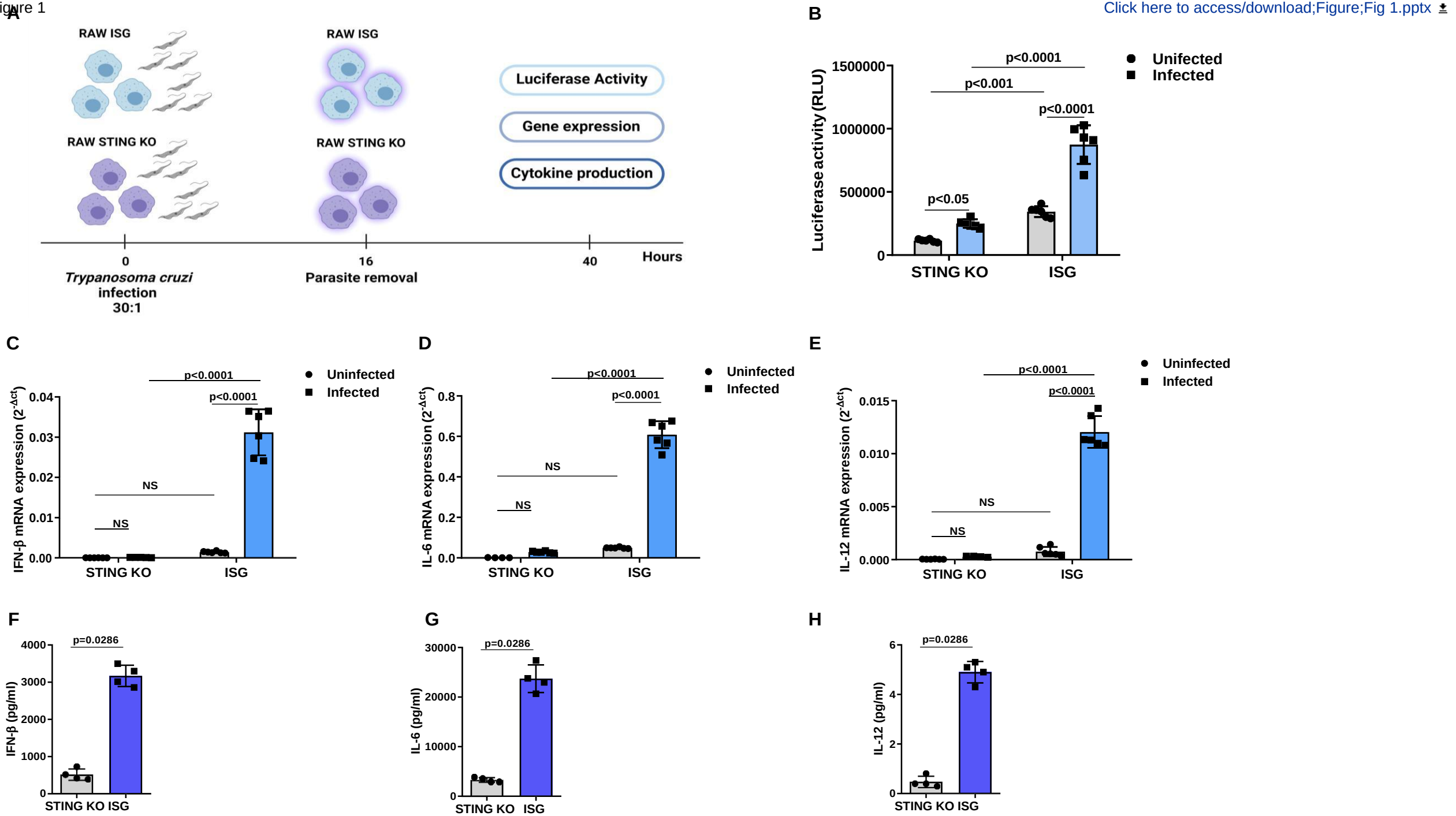

Figure 2

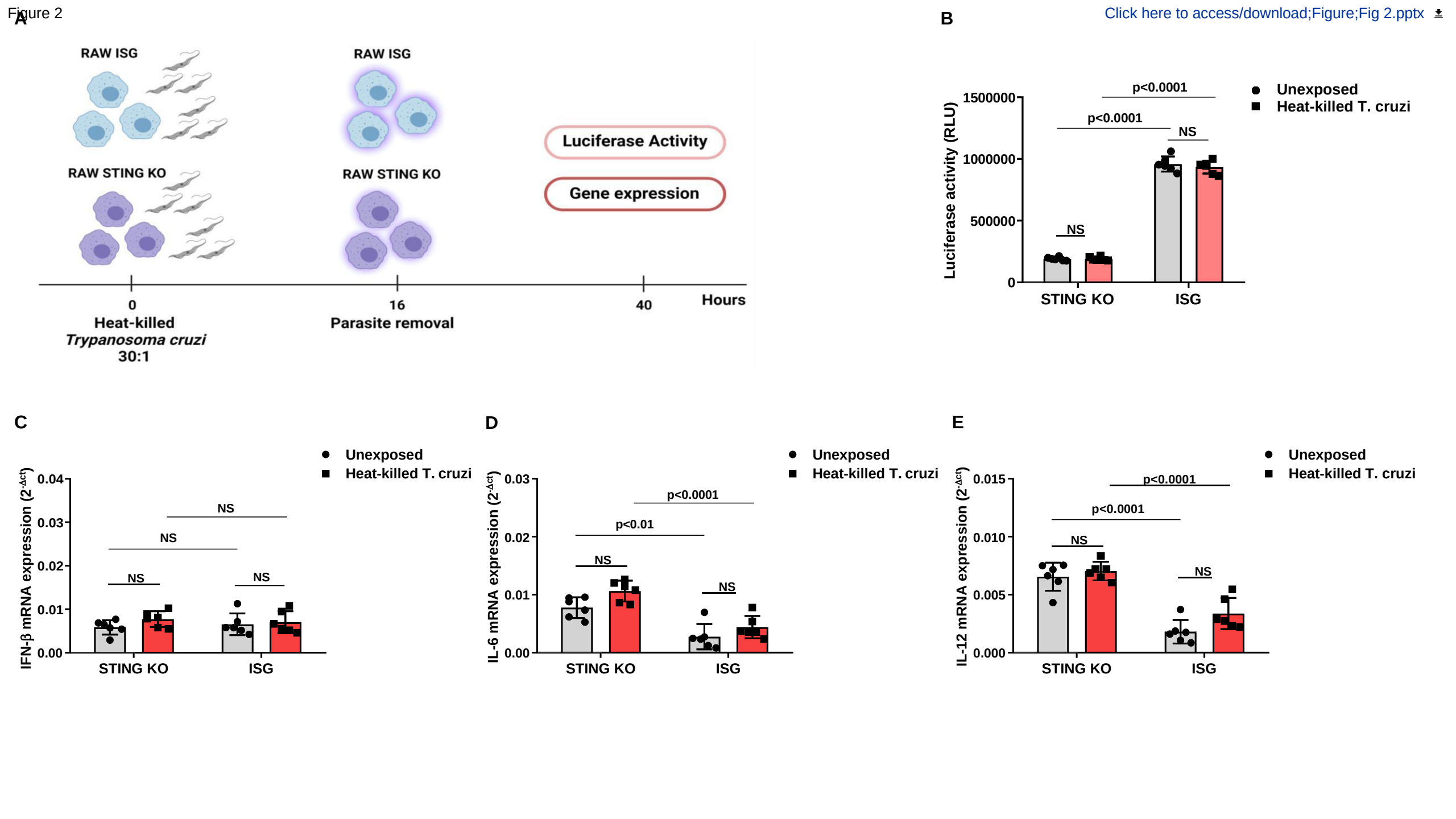

Figure 3

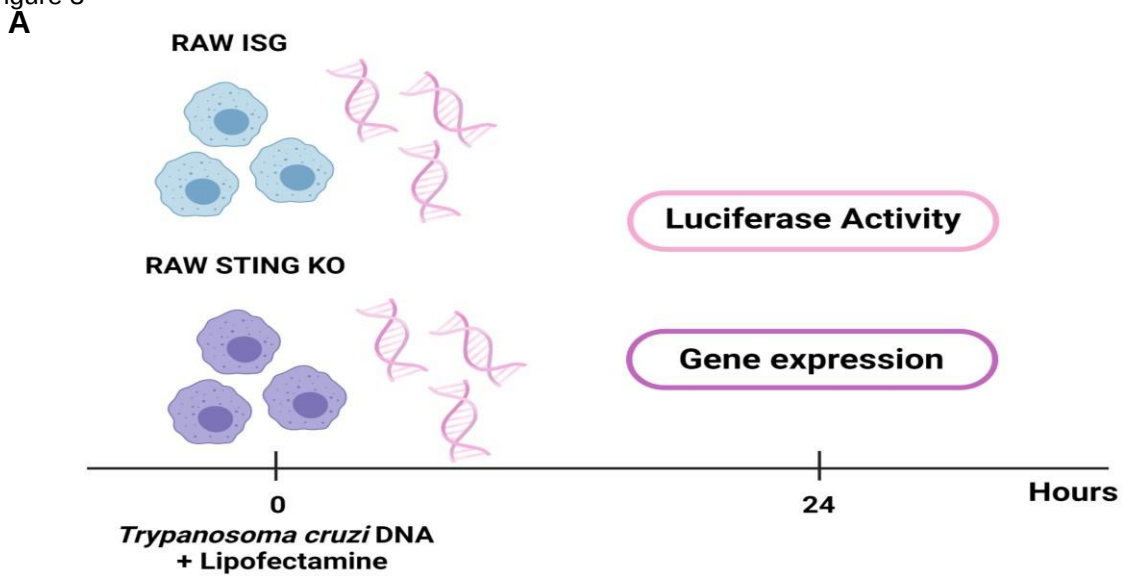

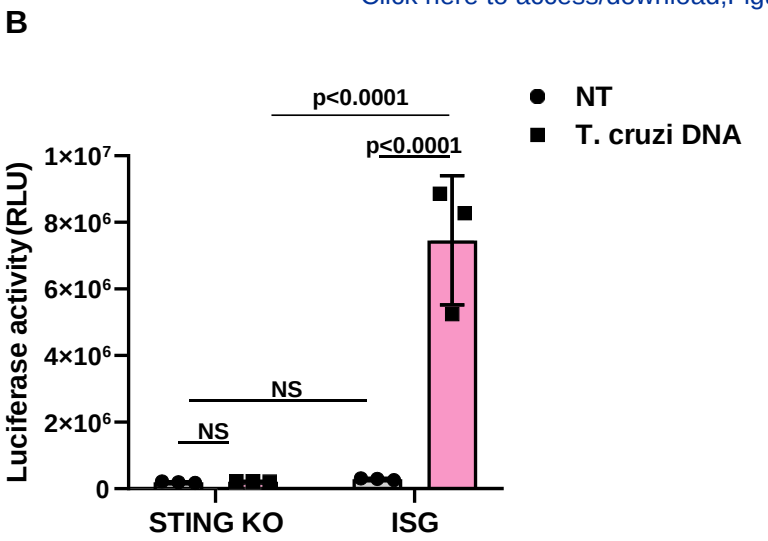

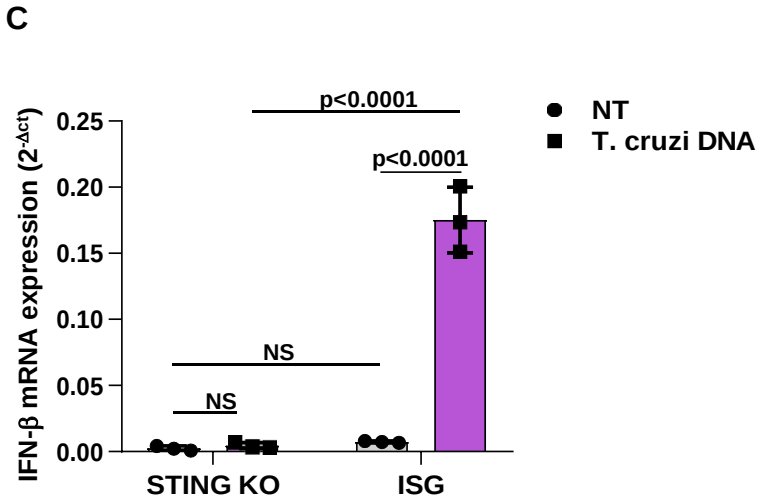

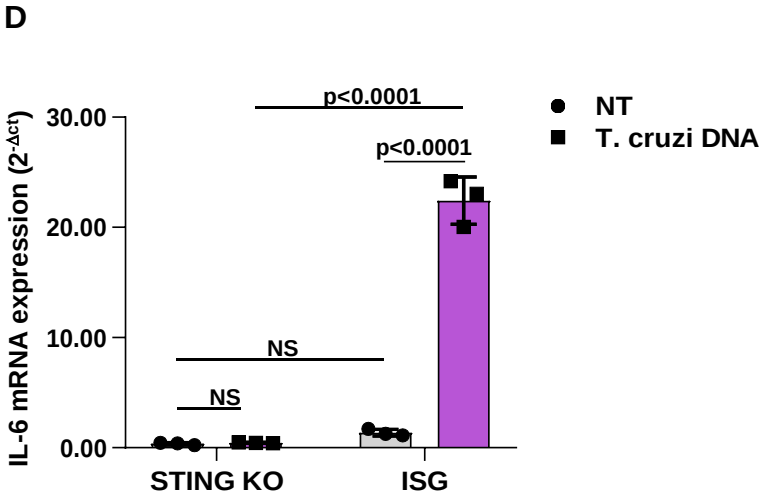

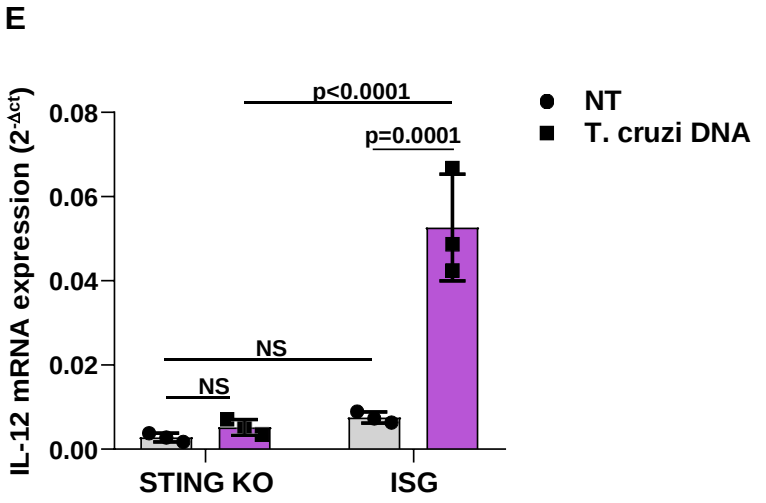

Figure 4

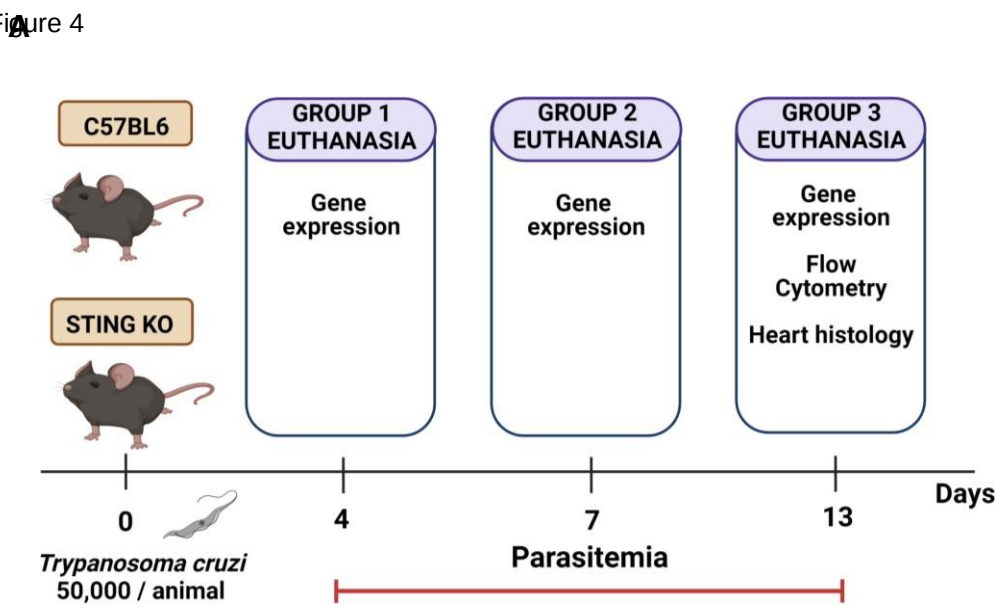

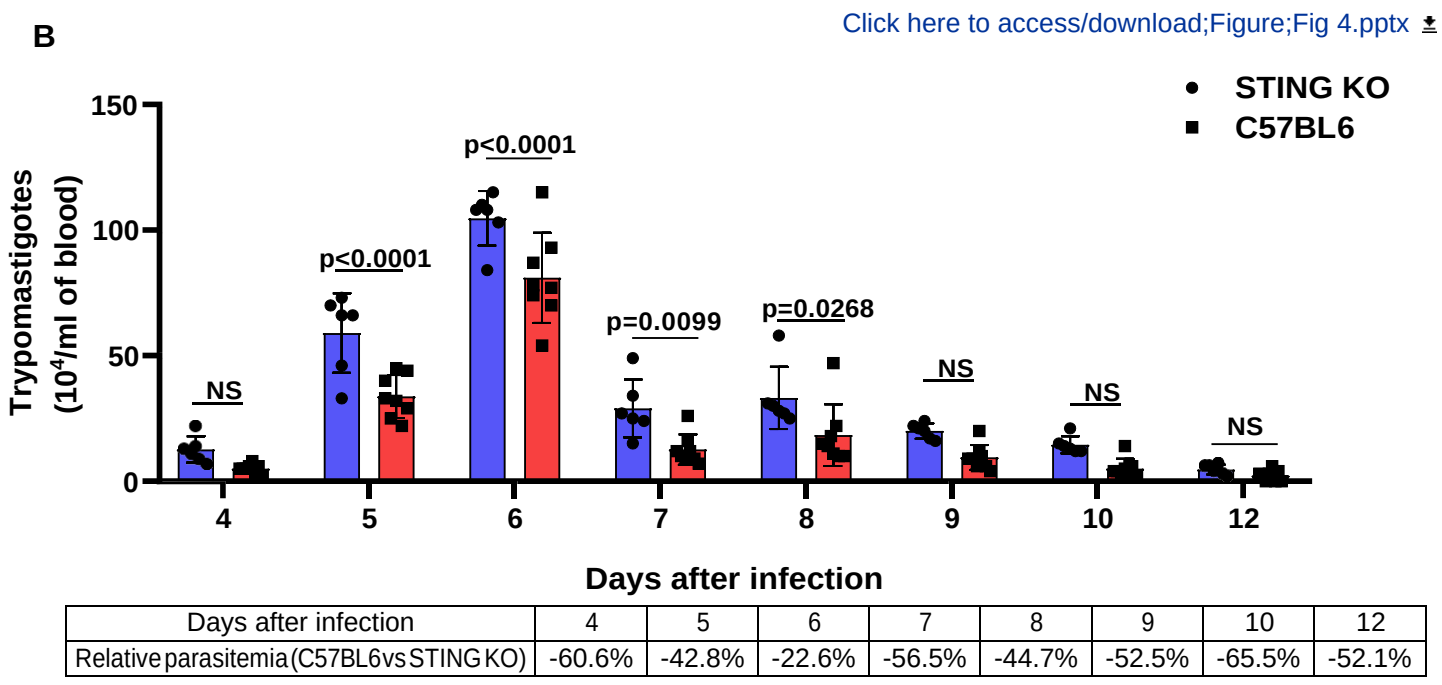

Days after infection	4	5	6	7	8	9	10	12
Relative parasitemia (C57BL6 vs STING KO)	-60.6%	-42.8%	-22.6%	-56.5%	-44.7%	-52.5%	-65.5%	-52.1%

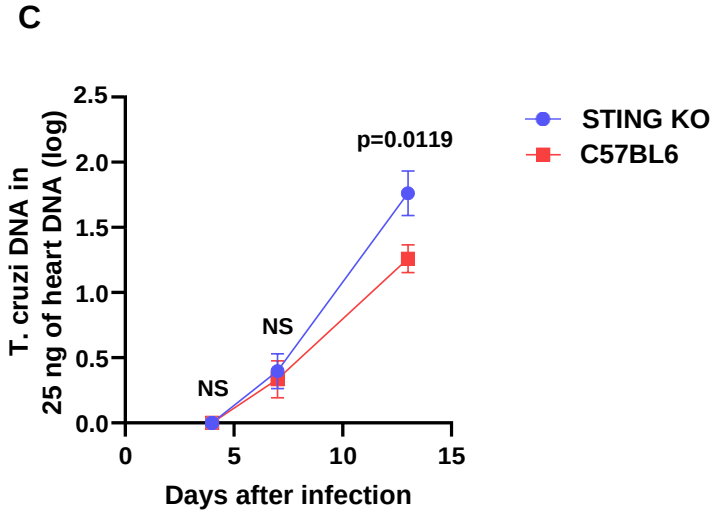

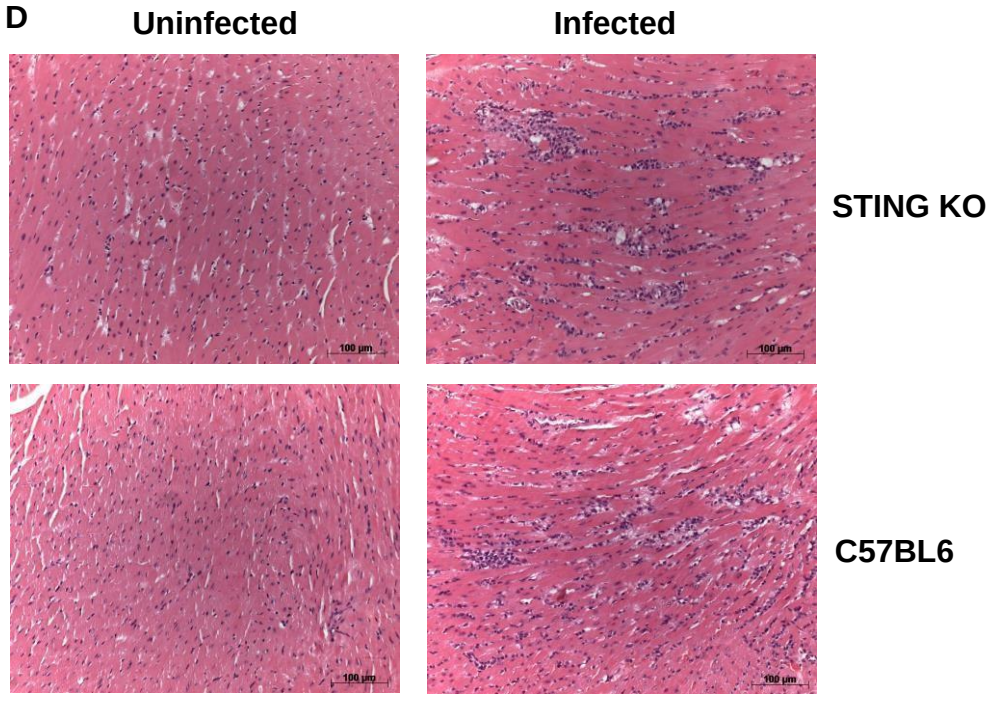

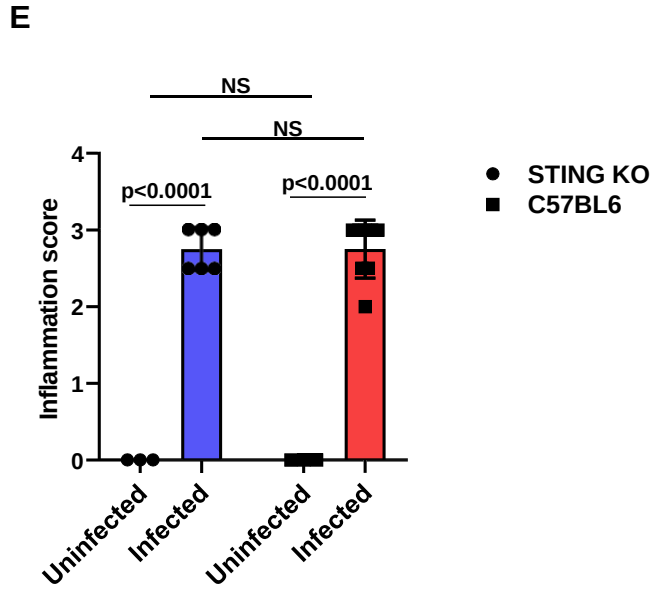

Figure 5

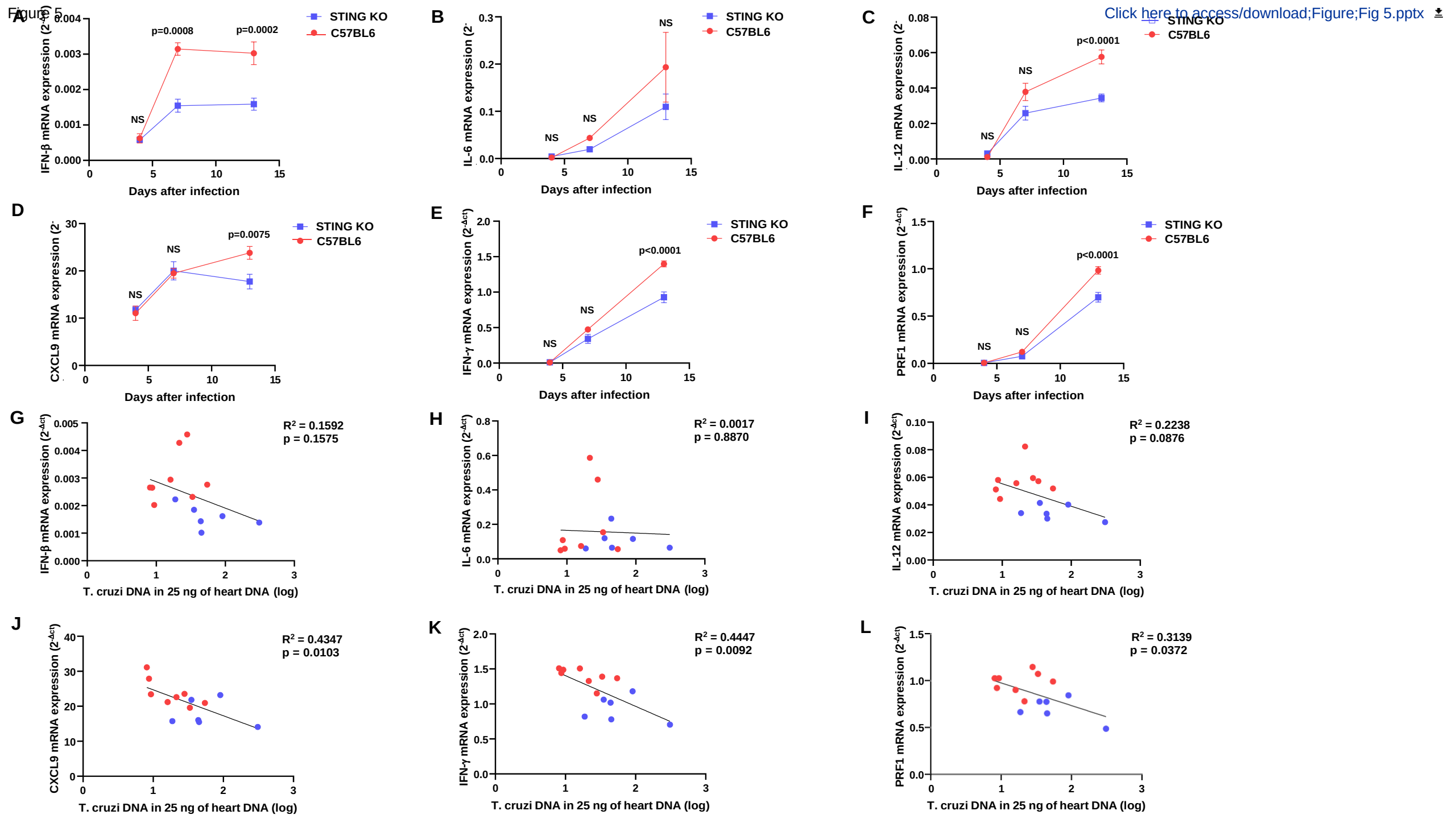

Figure 6

Click here to access/download;Figure;Fig 6.pptx

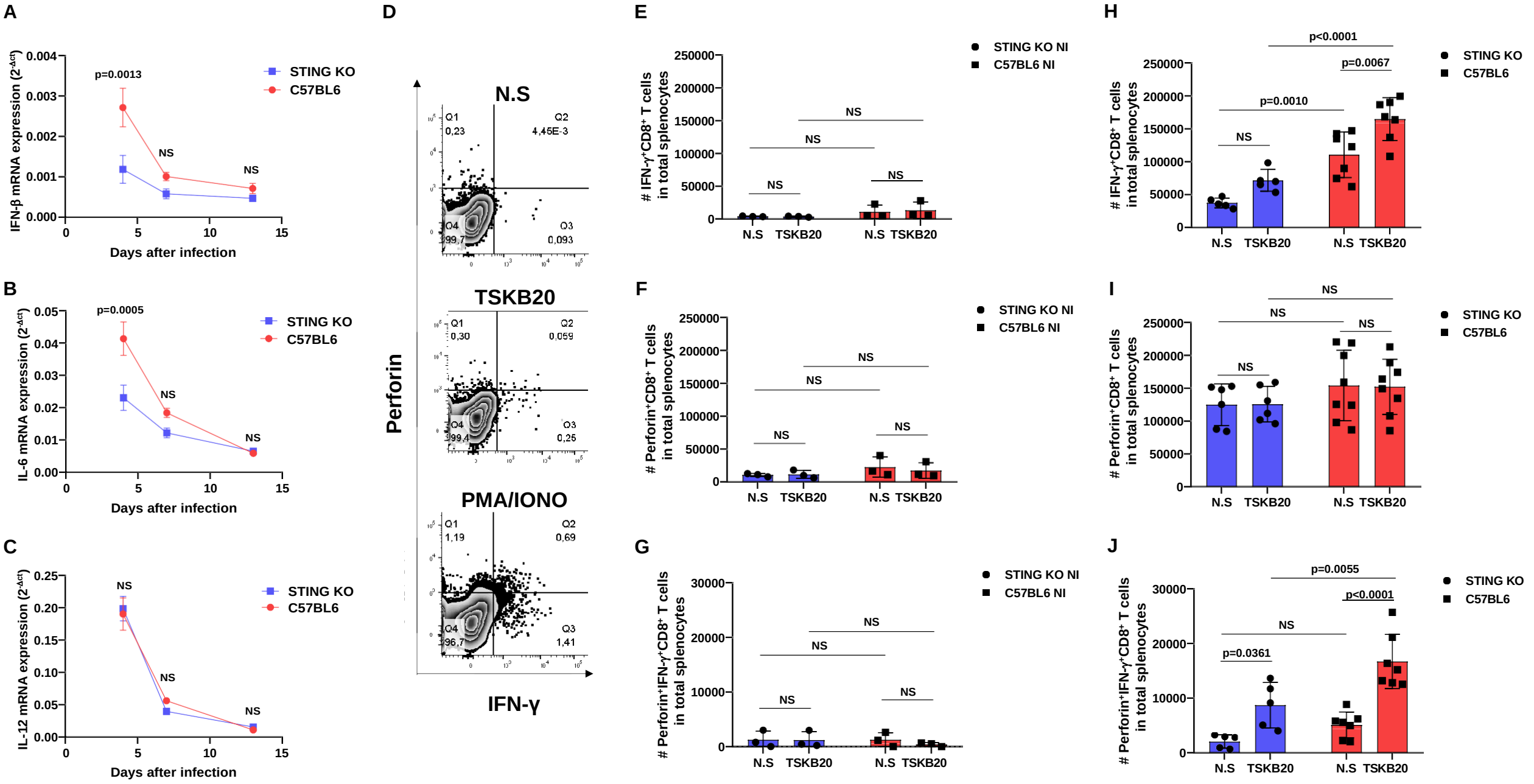

10.4. ANEXO D – PUBLICAÇÃO DURANTE O PERÍODO DO MESTRADO

ORIGINAL RESEARCH
published: 29 January 2019
doi: 10.3389/fimmu.2019.00067

frontiers in Immunology

Butyrate Attenuates Lung Inflammation by Negatively Modulating Th9 Cells

Raquel de Souza Vieira[1], *Angela Castoldi*[1], *Paulo José Basso*[1], *Meire Ioshie Hiyane*[1], *Niels Olsen Saraiva Câmara*[1,2,3†] *and Rafael Ribeiro Almeida*[1,4*†]

[1] *Laboratory of Transplantation Immunobiology, Department of Immunology, Institute of Biomedical Sciences, University of São Paulo, São Paulo, Brazil,* [2] *Nephrology Division, Department of Medicine, Federal University of São Paulo, São Paulo, Brazil,* [3] *Renal Pathophysiology Laboratory, Department of Clinical Medicine, University of São Paulo, São Paulo, Brazil,* [4] *Laboratory of Immunology, Heart Institute (InCor) School of Medicine, University of São Paulo, São Paulo, Brazil*

Th9 cells orchestrate allergic lung inflammation by promoting recruitment and activation of eosinophils and mast cells, and by stimulating epithelial mucus production, which is known to be mainly dependent on IL-9. These cells share developmental pathways with induced regulatory T cells that may determine the generation of one over the other subset. In fact, the FOXP3 transcription factor has been shown to bind *il9* locus and repress IL-9 production. The microbiota-derived short-chain fatty acids (SCFAs) butyrate and propionate have been described as FOXP3 inducers and are known to have anti-inflammatory properties. While SCFAs attenuate lung inflammation by inducing regulatory T cells and suppressing Th2 responses, their effects on Th9 cells have not been addressed yet. Therefore, we hypothesized that SCFAs would have a protective role in lung inflammation by negatively modulating differentiation and function of Th9 cells. Our results demonstrated that butyrate is more effective than propionate in promoting FOXP3 expression and IL-9 repression. In addition, propionate was found to negatively impact *in vitro* differentiation of IL-13-expressing T cells. Butyrate treatment attenuated lung inflammation and mucus production in OVA-challenged mice, which presented lower frequency of lung-infiltrated Th9 cells and eosinophils. Both Th9 cell adoptive transfer and IL-9 treatment restored lung inflammation in butyrate-treated OVA-challenged mice, indicating that the anti-inflammatory effects of butyrate may rely on suppressing Th9-mediated immune responses.

Keywords: butyrate, Th9 cells, tregs, eosinophils, lung inflammation

OPEN ACCESS

Edited by:
Loretta Tuosto,
Sapienza University of Rome, Italy

Reviewed by:
Xian Chang Li,
Houston Methodist Hospital, United States
Youcun Qian,
Shanghai Institutes for Biological Sciences (CAS), China

**Correspondence:*
Rafael Ribeiro Almeida
rafaelbio13@usp.br

†These authors share co-senior authorship

Specialty section:
This article was submitted to T Cell Biology, a section of the journal Frontiers in Immunology

Received: 05 July 2018
Accepted: 11 January 2019
Published: 29 January 2019

Citation:
Vieira RS, Castoldi A, Basso PJ, Hiyane MI, Câmara NOS and Almeida RR (2019) Butyrate Attenuates Lung Inflammation by Negatively Modulating Th9 Cells. Front. Immunol. 10:67. doi: 10.3389/fimmu.2019.00067

INTRODUCTION

Helper T-cell differentiation takes place in secondary lymphoid organs, where the cytokine environment plays a key role in determining the fate of naïve T cells toward many CD4+ T-Cellsubsets. These subsets include effector T helper 1 (Th1), Th2, Th9, and Th17 cells that secrete signature cytokines, and regulatory Foxp3 T (Treg) cells that help hold immune responses in check (1). Interleukin-4 (IL-4) is known to induce the differentiation of Th2 cells, characterized by expressing the transcription factors STAT6 and GATA-3, and by producing the cytokines IL-4, IL-5, and IL-13 (1). These cells are mainly involved in the pathogenesis of allergic diseases, promoting activation of eosinophils and mast cells, mucus production, and triggering antibody class switching to IgE in B cells, which can also be modulated by other T-cell subsets (2).

IL-9-producing T cells, which share developmental pathways with both Th2 and Treg cells, are differentiated in response to IL-4, but only when transforming growth factor-β (TGF-β) is present (3). These cells are characterized by expressing the transcription factors PU.1, STAT6, and IRF4, although other molecules are required for IL-9 production, such as BATF and FOXO1 (4–8). STAT6 is particularly important in cellular polarization as it contributes to repressing TGF-β-mediated expression of FOXP3, known to be an IL-9 suppressor (5). Th9 cells are the main cellular source of IL-9, but also produce other cytokines, such as IL-3, IL-10, and IL-21 (3). While described as important effectors against helminthic infections (9, 10), the role of Th9 cells in many inflammatory diseases, cancer, and allergies has been increasingly studied (11–14).

Th9 cells are found in the draining lymph nodes and respiratory tract, especially during early phases of asthma development (15). The peripheral mononuclear blood cells (PBMC) of atopic infants and adults are featured by a higher frequency of Th9 cells when compared to healthy individuals (15, 16), while single nucleotide polymorphisms (SNPs) in the genes encoding both IL-9 and its receptor (IL9R) have been associated with beneficial outcomes in allergen sensitization (17). Experimental data on the role of Th9 cells in lung inflammation have revealed that it mainly relies on promoting IL-9-dependent eosinophil and mast cell infiltration, mucus production and enhanced release of Th2 cytokines (18). In fact, transgenic expression of IL-9 is sufficient to cause bronchial hyperresponsiveness (19, 20), while antibody-mediated neutralization of this cytokine protects mice from inflammation (8). PU.1, IRF4, and BATF knockout mice present impaired differentiation of Th9 cells and lower inflammation (4, 6, 8). On the other hand, thymic stromal lymphopoietin (TSLP) and nitric oxide-mediated activation of these cells was shown to promote increased IL-9 production and disease exacerbation (21, 22).

Although palliative treatments have reduced the severity of symptoms and death of asthma patients, there is no current therapeutic regimen that can cure the disease. A better understanding of the mechanisms involved in inflammation is likely to provide important cues on how to improve treatment and even cure asthma. In this context, an increasing interest in determining the role of the microbiota and their metabolites during disease development has arisen (23).

Mucosal organs such as gut and lungs harbor a large collection of bacteria and other microorganisms that shape local and distal immune responses (23, 24). Birth mode (vaginal or via cesarean section), diet, use of antibiotics and the surrounding environment represent some of the factors that influence microbiota diversity, which is suggested to play an important role in asthma susceptibility (23). Early life differential colonization may have a determinant role in this process and airway microbial diversity appears to be inversely associated with sensitization to house dust mites in childhood (25, 26).

Experimental data on germ-free (GF) mice have demonstrated that lack of microbiota results in stronger ovalbumin (OVA)-induced type 2 airway inflammation and hypersensitivity, which can be reversed by co-housing GF mice with specific pathogen-free (SPF)-raised animals (27). In line with these observations, it has also been shown that antibiotic-mediated depletion of the microbiota renders mice more susceptible to lung inflammation (28). However, not only the microorganisms but also their metabolites have been indicated as key players in controlling immune responses. In fact, microbiota metabolism of dietary fibers and production of short-chain fatty acids (SCFA), such as propionate and acetate, has been considered a major mechanism by which microorganisms control airway inflammation. Induction of Tregs and dendritic cells with impaired capability of promoting effector Th2 responses were shown to play an important role in attenuating disease (29, 30). Nevertheless, the role of SCFAs on other T-cell subsets that participate in lung inflammation, such as Th9 cells, is yet to be addressed.

Given the well-established role of butyrate and propionate in promoting FOXP3 expression during differentiation of Tregs (31, 32) and that FOXP3 is a potent IL-9 repressor (5, 33), we hypothesized that these SCFAs would have a negative impact on the development and function of Th9 cells. We confirmed previous data by showing that butyrate and propionate promote higher FOXP3 expression in the context of Treg differentiation. We then demonstrated an inverse correlation between IL-9 and FOXP3 expression when CD4+ T cells were exposed *in vitro* to butyrate and propionate early during differentiation into Th9 cells. Butyrate was found to be more efficient than propionate in promoting FOXP3 expression and IL-9 repression. In addition, we demonstrated an opposite effect of butyrate and propionate on Th2 cells. While *in vitro* butyrate treatment was responsible for inducing a small, but significant increase in the frequency of IL-13+ T cells, propionate treatment negatively impacted the same cells. Moreover, we found that butyrate-treated OVA-challenged mice presented lower frequency of lung-infiltrated Th9 cells and attenuated inflammation, represented by lower frequency of lung-infiltrated eosinophils, less inflammatory infiltrates and lower mucus production. Adoptive transfer of OVA-specific Th9 cells and recombinant IL-9 treatment were both sufficient to restore lung inflammation in butyrate-treated mice, indicating that butyrate-mediated effects were likely to be dependent on suppression of Th9 cells.

MATERIALS AND METHODS

Animals and Ethics Statement

Male C57BL/6, FOXP3 GFP, and OT-II mice (6–8 weeks old) were obtained from the animal facility of the Institute of Biomedical Sciences, University of São Paulo. Animals were housed in groups of up to 5 per cage in a light- and temperature-controlled room (12 h light/dark cycles, 21 ± 2°C) with free access to food and water. This study was carried out in accordance with the recommendations of the National Institute of Health, Guide for the Care and Use of Laboratory Animals and the Brazilian National Law (11.794/2008). The protocol was approved by the Institutional Animal Care and Use Committee (CEUA) of the University of São Paulo, under protocol number 2015/006.

OVA-Induced Lung Inflammation

Male C57BL/6 mice were intraperitoneally (IP) injected with 30 μg of ovalbumin (OVA) grade V (Sigma) dissolved in Imject Alum (1.6 mg) (Thermo Fisher), diluted in 200 μl of PBS at days 0 and 7. OVA-sensitized mice were nebulized with an OVA-distillated water solution (3%), using an ultrasonic nebulizer device (Respira Max®) for 15 min at days 14, 15, and 16. Control mice were sensitized as described and nebulized with water only. Mice were euthanized 24 h after the last nebulization (challenge) and lungs were extracted for further analysis.

Butyrate Treatment

Male C57BL/6 mice were IP injected with 250 μl of 1M butyric acid (butyrate) (Sigma) diluted in PBS (pH: 7.2) or PBS only at days 0, 1, 2, 7, 8, and 9 of OVA-sensitization. Mice treated during sensitization also received butyrate (IP) or PBS during the 3 days of OVA-nebulization (challenge).

IL-9 Treatment and T Cell Adoptive Transfer

OVA-sensitized butyrate-treated mice were intraperitoneally injected with 150 ng of recombinant murine IL-9 (R&D Systems) diluted in 200 μl of PBS or PBS only at days 1 and 2 of OVA nebulization. Alternatively, butyrate-treated mice were intraperitoneally injected with 2×10^6 OT-II Th0, Th2, or Th9 cells the day before OVA nebulization. OT-II Th2 and Th9 cells were differentiated *in vitro* as described in T cell differentiation topic.

Lung Digestion and Flow Cytometry

Mice were euthanized and lungs collected, washed in ice-cold PBS, cut in small pieces and incubated in R-10 medium [RPMI-1640 (Thermo Fisher) supplemented with 10% FBS (Thermo Fisher), 2 mM L-glutamine (Thermo Fisher), 1 mM sodium pyruvate (Thermo Fisher), 1% non-essential amino acids (Thermo Fisher), 1% Pen/Strept (Thermo Fisher), 1% vitamin solution (Thermo Fisher), and 5×10^{-5} M 2β-mercaptoetanol (Sigma)] containing 0.5 mg/ml of collagenase IV (Thermo Fisher) and 30 μg/ml of DNAse (Sigma), at 37°C for 45 min and 180 rpm. Digested tissues were passed through 100 μm cell strainers (Sigma) and centrifuged. Pellets were resuspended in 1 ml of ACK buffer (Thermo Fisher) for 2 min, centrifuged and

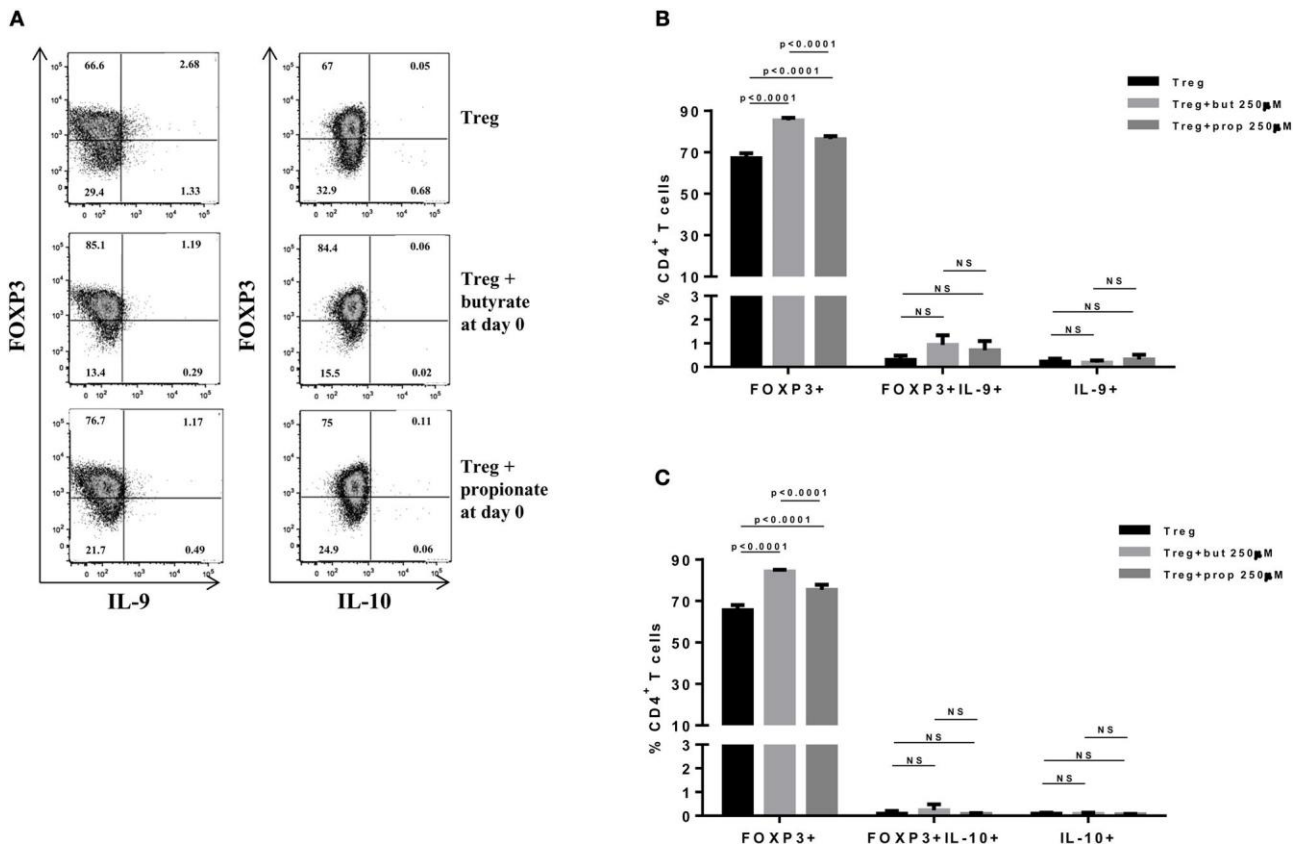

FIGURE 1 | Butyrate and propionate enhances FOXP3 expression in CD4+ T cells differentiated into Tregs. Naïve CD4+ T cells (CD62L+CD44low) were sorted from spleens of FOXP3 GFP mice and cultured in 96-well flat bottom plates with plate bound anti-CD3 (2 μg/ml) and soluble anti-CD28 (0.5 μg/ml) in the presence of Treg (TGF-β 2 ng/ml and IL-2 10 ng/ml) differentiation condition for 4 days. Butyrate and propionate (250 μM) were added in the culture at day 0. At day 4, cells were restimulated with with PMA (50 ng/ml), ionomycin (500 ng/ml), and brefeldin A (5 μg/ml) for 4 h at 37°C and 5% CO_2, and analyzed by flow cytometry (A). The frequencies of FOXP3+ and/or IL-9+ CD4+ T cells (B) and FOXP3+ and/or IL-10+ CD4+ T cells (C) are represented by bar graphs. Data are shown as mean ± S.D. Linear regression, Two-way ANOVA and Tukey's multiple comparison test were used for statistical analysis. NS, not significant.

resuspended in R-10 medium for further analysis. Cells extracted from lungs were stimulated with PMA (Sigma) 50 ng/ml, ionomycin (Sigma) 500 ng/ml, and brefeldin A (Biolegend) 5 µg/ml for 4 h at 37°C and 5% CO_2. T cell surface staining was performed for 30 min at 4°C using the following antibodies diluted in PBS: anti-CD45 PercP (BD Biosciences), anti-CD4 APCCy7 (Biolegend) and anti-CD8 FITC (Biolegend). Cells were then fixed and permeabilized using the Cytofix/Cytoperm kit (BD Biosciences). Intracellular staining was performed for 30 min at 4°C with the following antibodies diluted in Perm/wash buffer (BD Biosciences): anti-CD3 APC (BD Biosciences), anti-IL-9 PE (Biolegend), and anti-IL-13 PECy7 (Biolegend). To evaluate lung-infiltrated Tregs, cells were surfaced stained for 30 min at 4°C using the following antibodies diluted in PBS: anti-CD45 PercP (BD Biosciences), anti-CD3 APC (BD Biosciences), and anti-CD4 APCCy7 (Biolegend). FOXP3 expression was determined using the FOXP3/Transcription Factor Staining Buffer Set (eBioscience) with anti-FOXP3 PE (Biolegend), according to the manufacturer's instruction. To evaluate lung-infiltrated eosinophils, cells were surfaced stained for 30 min at 4°C using the following antibodies diluted in PBS: anti-CD45 PercP (BD Biosciences), anti-CD11b APCCy7 (Biolegend), anti-CD11c BV421 (Biolegend), anti-CD64 PE (Biolegend), anti-Ly6G FITC (BD Biosciences), and anti-Siglec F Alexa 647 (BD Biosciences). All samples were acquired with a FACS Canto II (BD Biosciences) and analyzed using FlowJo software (version 9.0.2, Tree Star).

T Cell Differentiation

Splenocytes from FOXP3 GFP mice were surfaced stained for 30 min at 4°C using the following antibodies diluted in PBS: anti-CD4 PercP (BD Biosciences), anti-CD44 PECy7

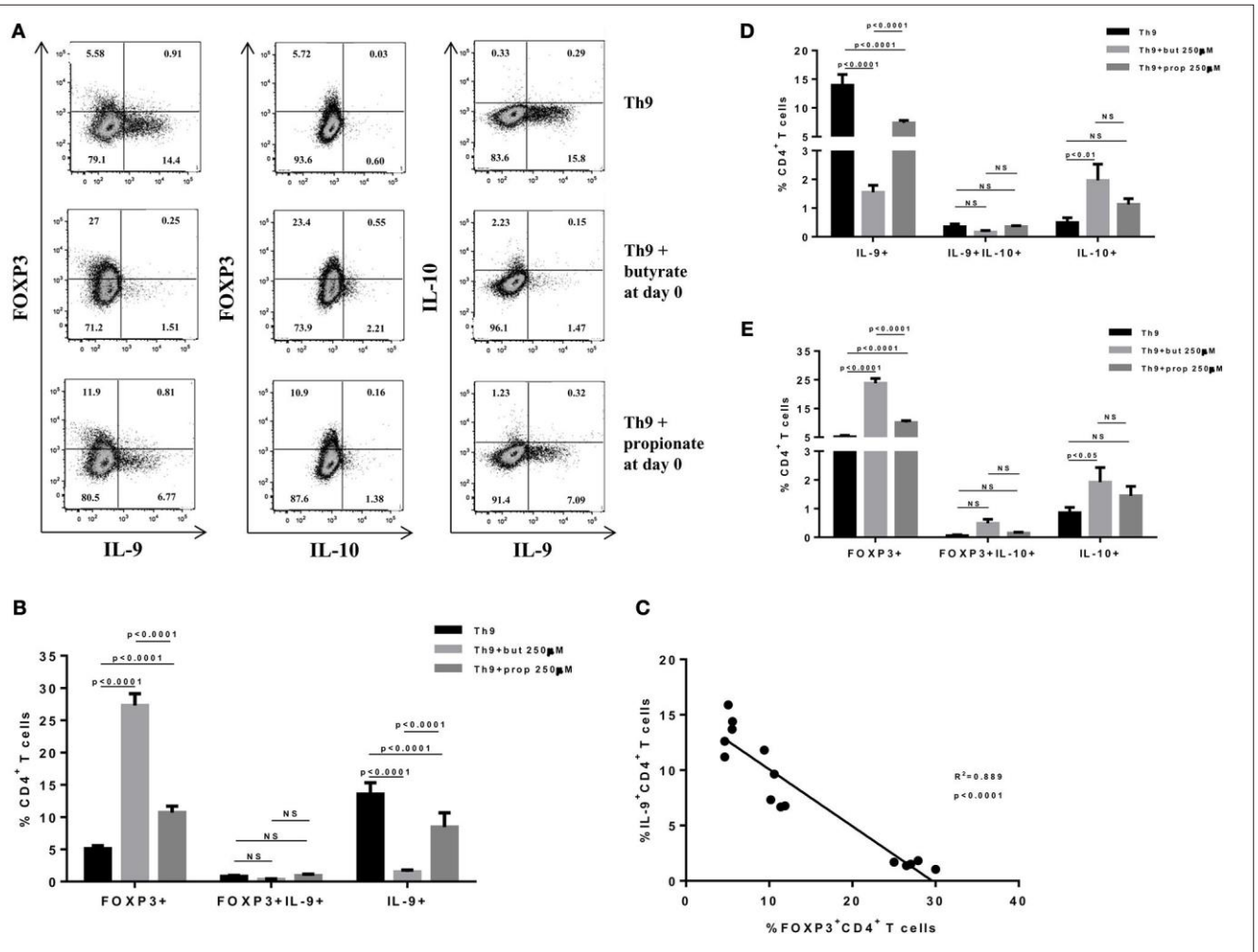

FIGURE 2 | Butyrate enhances FOXP3 expression in CD4+ T cells and impairs the differentiation of Th9 cells. Naïve CD4+ T cells (CD62L+CD44low) were sorted from spleens of FOXP3 GFP mice and cultured in 96-well flat bottom plates with plate bound anti-CD3 (2 µg/ml) and soluble anti-CD28 (0.5 µg/ml) in the presence of Th9 (TGF-β 2 ng/ml, IL-4 10 ng/ml and anti-IFNγ 10 µg/ml) differentiation condition for 4 days. Butyrate and propionate (250 µM) were added in the culture at day 0. At day 4, cells were restimulated with with PMA (50 ng/ml), ionomycin (500 ng/ml), and brefeldin A (5 µg/ml) for 4 h at 37°C and 5% CO_2, and analyzed by flow cytometry (A). The frequencies of FOXP3+ and/or IL-9+ CD4+ T cells are represented by bar graphs (B). A correlation analysis of IL-9 and FOXP3 expression was performed (C). The frequencies of IL-9+ and/or IL-10+ CD4+ T cells (D) and FOXP3+ and/or IL-10+ CD4+ T cells (E) were determined and are represented by bar graphs. Data are shown as mean ± S.D. Two-way ANOVA and Tukey's multiple comparison test were used for statistical analysis. NS, not significant.

(Biolegend) and anti-CD62L APC (BD Biosciences). Naïve CD4+ T cells (CD62L+CD44^{low}) were sorted using a FACS Aria III (BD Biosciences) and cultured in R-10 medium in 96-well flat bottom plates (Sigma) with plate bound anti-CD3 (2 μg/ml) (BD Biosciences) and soluble anti-CD28 (0.5 μg/ml) (BD Biosciences) in the presence of Th9 [TGF-β 2 ng/ml (R&D Systems), IL-4 10 ng/ml (Peprotech) and anti-IFNγ 10 μg/ml (BD Biosciences)], Th2 [IL-4 10 ng/ml (Peprotech), anti-IL-12 10 μg/ml (BD Biosciences) and anti-IFNγ 10 μg/ml (BD Biosciences)] or Treg [TGF-β 2 ng/ml (R&D Systems) and IL-2 10 ng/ml (Peprotech)] differentiation conditions for 4 days. Butyric and propionic acids (Sigma) diluted in PBS (250 μM–pH: 7.2) were added in the culture at day 0. At day 4, cells were restimulated with PMA (50 ng/ml) (Sigma), ionomycin (500 ng/ml) (Sigma), and brefeldin A (5 μg/ml) (Biolegend) for 4 h at 37°C and 5% CO_2. Alternatively, naïve CD4+ T cells were incubated in the presence of Th9 differentiation condition for 4 days. The supernatants were removed and fresh R-10 medium added to the wells. The cells were incubated for additional 4 days in the presence or absence of butyric acid (Sigma) diluted in PBS (250 μM–pH: 7.2). At day 8, cells were restimulated with PMA (50 ng/ml) (Sigma), ionomycin (500 ng/ml) (Sigma), and brefeldin A (5 μg/ml) (Biolegend) for 4 h at 37°C and 5% CO_2. Cells were then fixed and permeabilized using the Cytofix/Cytoperm kit (BD Biosciences). Intracellular staining was performed for 30 min at 4°C with the following antibodies diluted in Perm/wash buffer (BD Biosciences). Th9 and Treg cells: anti-CD3 APCCy7 (BD Biosciences), anti- IL-9 PE (Biolegend), and anti-IL-10 PercPCy5.5 (Biolegend). Th2 cells: anti-CD3 APCCy7 (BD Biosciences), anti-IL-4 PE (Biolegend), anti-IL-5 APC (Biolegend) and anti-IL-13 PECy7 (Biolegend). Samples were acquired with a FACS Canto II (BD Biosciences) and analyzed using FlowJo software (version 9.0.2, Tree Star).

Histology

Extracted lungs were cut and the left inferior lobes were fixed in 2 ml of 4% buffered formalin at 4°C and embedded into

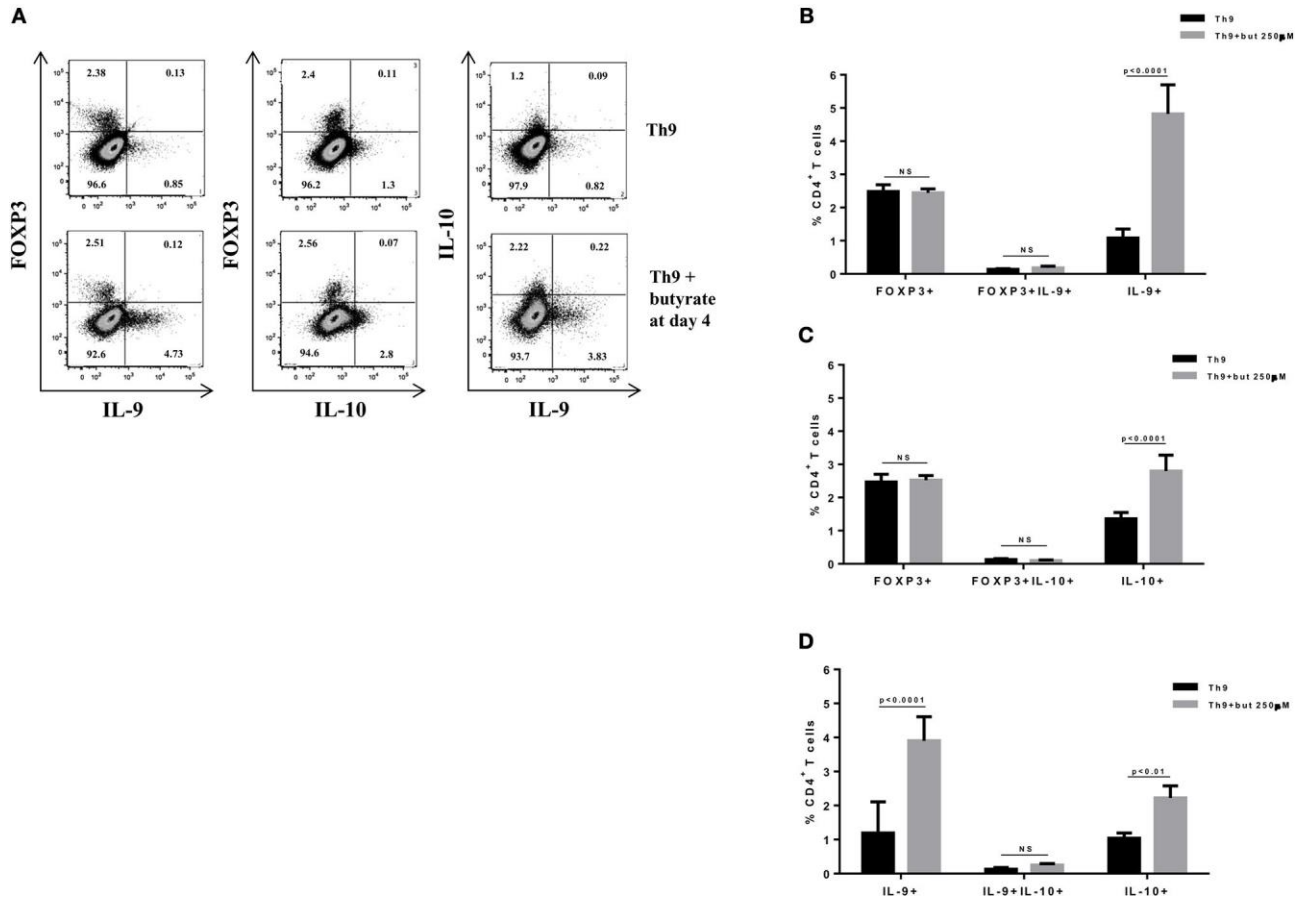

FIGURE 3 | Butyrate sustains cytokine production by differentiated Th9 cells. Naïve CD4+ T cells (CD62L+CD44low) were sorted from spleens of FOXP3 GFP mice and cultured in 96-well flat bottom plates with plate bound anti-CD3 (2 μg/ml) and soluble anti-CD28 (0.5 μg/ml) in the presence of Th9 (TGF-β 2 ng/ml, IL-4 10 ng/ml, and anti-IFNγ 10 μg/ml) differentiation condition for 4 days. At day 4, the medium was replaced by fresh R-10 and butyrate (250 μM) was added in the culture. At day 8, cells were restimulated with with PMA (50 ng/ml), ionomycin (500 ng/ml) and brefeldin A (5 μg/ml) for 4 h at 37°C and 5% CO_2, and analyzed by flow cytometry (A). The frequencies of FOXP3+ and/or IL-9+ CD4+ T cells (B), FOXP3+ and/or IL-10+ CD4+ T cells (C) and IL-9+ and/or IL-10+ CD4+ T cells (D) are represented by bar graphs. Data are shown as mean ± S.D. Two-way ANOVA and Sidak's multiple comparison test were used for statistical analysis. NS, not significant.

paraffin. Prepared sections (5 μm) were stained with either H&E or PAS reagents using standardized protocols and analyzed with an Eclipse Ti-E microscope (Nikon Instruments Inc.).

Statistical Analysis

Statistical analysis was carried out with Graph Pad Prism 6.0 Software. Two-way ANOVA followed by Dunnett's multiple comparison test or One-way ANOVA followed by Tukey's multiple comparison test were used for statistical analysis, depending on data comparisons. $P < 0.05$ was considered significant.

RESULTS

Butyrate Impairs Th9 Cell Differentiation

SCFAs directly modulate the differentiation of CD4+ T cells into Tregs by promoting FOXP3 expression (31), which has been shown to impair IL-9 production (33). Therefore, we first asked whether the SCFAs butyrate and propionate would have any impact on *in vitro* differentiation of Th9 cells. To address this question, naïve CD4+ T cells were sorted from spleens of FOXP3 GFP mice and differentiated into Th9 cells in the presence or absence of butyrate or propionate. Alternatively, naïve CD4+ T cells were differentiated into Tregs and Th2 cells, also in the presence or absence of butyrate or propionate. We confirmed previous data by showing that butyrate and propionate promote FOXP3 expression in the context of Treg differentiation. As expected, butyrate was found to be more efficient in promoting FOXP3 expression than propionate (**Figures 1A–C**). No significant impact on FOXP3+IL-9+ and FOXP3+IL-10+ T cells was observed (**Figures 1A–C**). We then demonstrated that butyrate added to the culture at day 0 significantly shifted the cellular differentiation from IL-9-expressing to FOXP3-expressing T cells, while propionate was

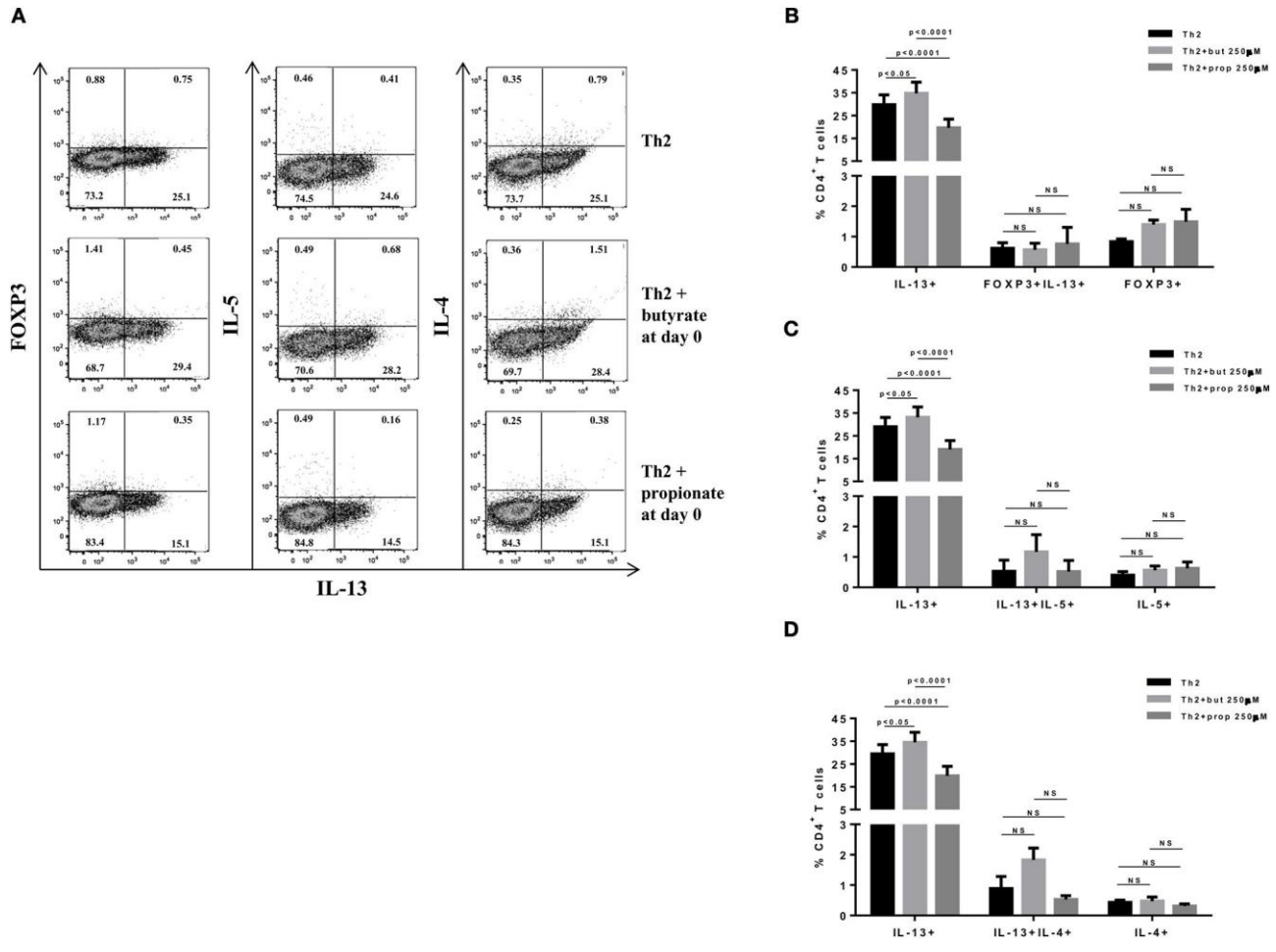

FIGURE 4 | SCFAs have opposite effects on IL-13-expressing T cells. Naïve CD4+ T cells (CD62L+CD44low) were sorted from spleens of FOXP3 GFP mice and cultured in 96-well flat bottom plates with plate bound anti-CD3 (2 μg/ml) and soluble anti-CD28 (0.5 μg/ml) in the presence of Th2 (IL-4 10 ng/ml, anti-IL-12 10 μg/ml, and anti-IFNγ 10 μg/ml) differentiation condition for 4 days. Butyrate and propionate (250 μM) were added in the culture at day 0. At day 4, cells were restimulated with with PMA (50 ng/ml), ionomycin (500 ng/ml), and brefeldin A (5 μg/ml) for 4 h at 37°C and 5% CO_2, and analyzed by flow cytometry (A). The frequencies of FOXP3+ and/or IL-13+ CD4+ T cells (B), IL-13+ and/or IL-5+ CD4+ T cells (C) and IL-13+ and/or IL-4+ CD4+ T cells (D) are represented by bar graphs. Data are shown as mean ± S.D. Two-way ANOVA and Tukey's multiple comparison test were used for statistical analysis. NS, not significant.

less effective in promoting the same shift (**Figures 2A,B**). We found an inverse correlation between IL-9 and FOXP3 expression when all groups were analyzed together (**Figure 2C**). We also evaluated the impact of butyrate and propionate on IL-10 expression and observed that butyrate treatment resulted in a significantly higher frequency of IL-10-expressing T cells, while IL-10+FOXP3+ and IL-10+IL-9+ T cells were not affected (**Figures 2D,E**). To further characterize the impact of butyrate on IL-9, IL-10, and FOXP3, we differentiated Th9 cells for 4 days and incubated them for additional 4 days in the presence or absence of butyrate. We found that butyrate treatment had no effect on FOXP3 expression when cells were already differentiated (**Figures 3A–C**). Most Th9 cells were not expressing IL-9 after 8 days of culture. However, we observed a less intense decrease in the frequency of IL-9-expressing T cells when differentiated Th9 cells were treated with butyrate (**Figures 3A,B**). No differences were found in FOXP3+IL-9+, FOXP3+IL-10+ and IL-9+IL-10+ T cells (**Figures 3B–D**). In addition, we demonstrated an opposite effect of butyrate and propionate on Th2 cells. While butyrate was responsible for inducing a small, but significant increase in the frequency of IL-13+ T cells, propionate treatment negatively impacted the same cells. In contrast to Th9 cells, no significant impact on FOXP3 expression was observed in the context of Th2 differentiation (**Figures 4A,B**). We also evaluated the impact of butyrate and propionate on the frequency of IL-4 and IL-5-expressing T cells and found no significant differences upon treatment (**Figures 4C,D**). Together, our results demonstrate that

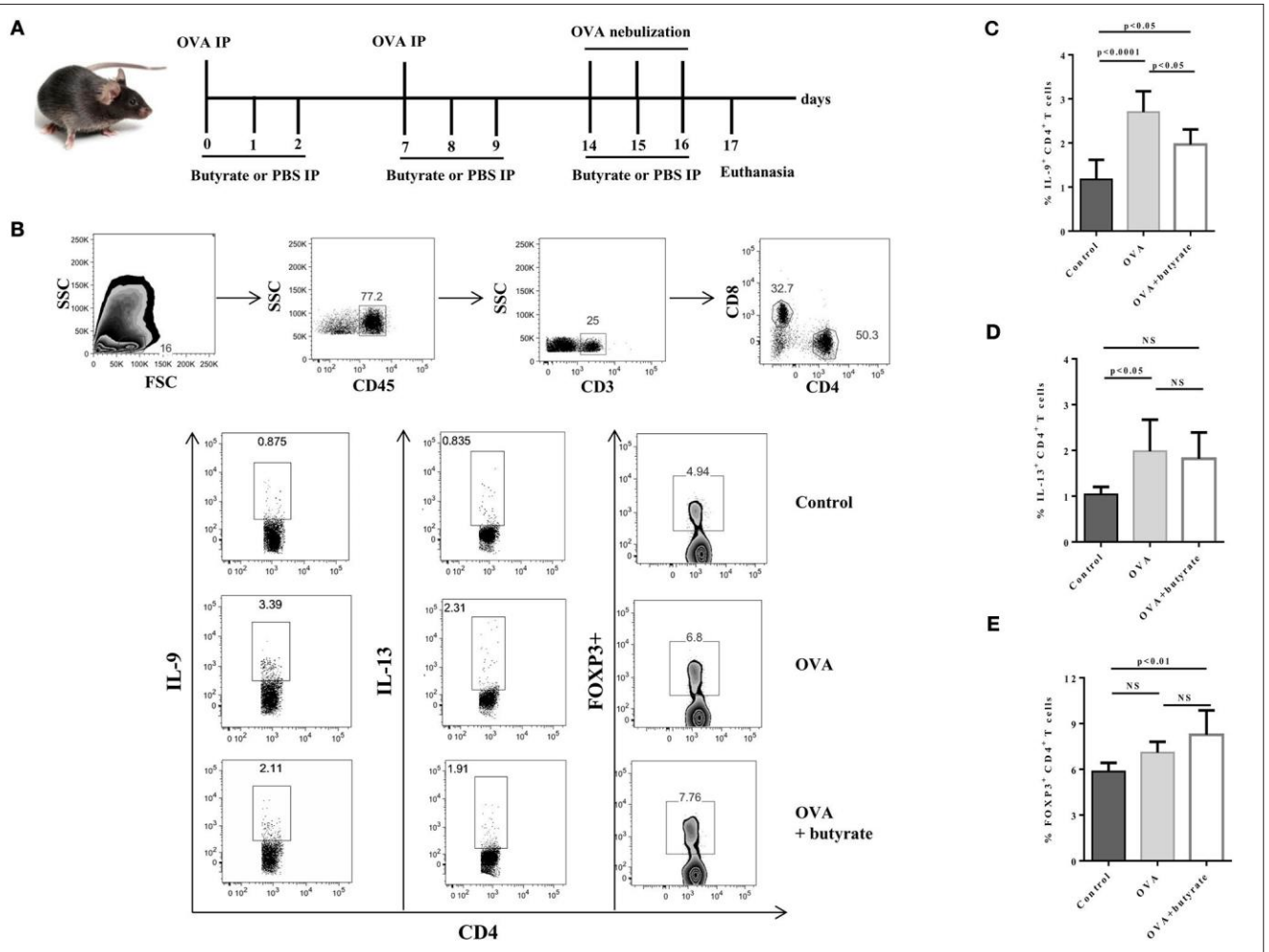

FIGURE 5 | Butyrate treatment negatively impact Th9 cells in the lungs of OVA-challenged mice. Male C57BL/6 mice were intraperitoneally (IP) injected with OVA (30 **µ**g) + Al(OH)3 (1.6 mg) at days 0 and 7. Mice also received 250 **µ**l of either PBS or butyrate (1M) (IP) at days 0, 1, 2, 7, 8, and 9. OVA-sensitized mice were nebulized with an OVA solution (3%) for 15 min at days 14, 15, and 16. The group that received butyrate during sensitization was also treated during challenge. A control group was sensitized and challenged without OVA. Euthanasia was performed 24 h after the last challenge (A). Lungs were digested, cells stimulated with PMA (50 ng/ml), ionomycin (500 ng/ml) and brefeldin A (5 **µ**g/ml) for 4 h at 37°C and 5% CO_2, and stained with monoclonal antibodies to determine the frequencies of IL-9+, IL-13+, and FOXP3+ CD4+ T cells by flow cytometry (B). Bar graphs show the frequencies of IL-9+ (C), IL-13+ (D) and FOXP3+ (E) CD4+ T cells in the different groups. Data are shown as mean ± SD. One-way ANOVA followed by Tukey's multiple comparison test were used for statistical analysis. *n* = 5–7 mice per group. NS, not significant.

butyrate and propionate differently modulate the differentiation of Th9, Th2, and Tregs.

Butyrate Treatment Negatively Impacts Th9 Cells and Attenuates Lung Inflammation

Given the *in vitro* effect of butyrate on Th9 cells, we next sought to determine whether it would also have an *in vivo* impact on these cells. To address this question, we induced OVA-mediated lung inflammation in C57BL/6 mice treated or not with butyrate (**Figure 5A**) and evaluated the frequencies of lung-infiltrated Th9, Th2, and Treg cells by flow cytometry (**Figure 5B**). We found that butyrate-treated animals presented a significantly lower frequency of lung-infiltrated Th9 cells (**Figure 5C**) while no difference was observed for IL-13-expressing Th2 cells (**Figure 5D**). Butyrate-treated OVA-challenged mice had significantly higher lung-infiltrated Treg cells when compared to control, but no statistical significance was found when compared to OVA-challenged mice (**Figure 5E**). Considering the pre-established role of IL-9 in promoting the recruitment of eosinophils to the lungs and supporting inflammation (34), we further analyzed animal lungs for the presence of eosinophils (CD45+CD64-Ly6G-CD11b+Siglec-F+CD11c-) (**Figure 6A**) and found a significantly higher frequency of these cells infiltrated in the lungs of OVA-challenged mice when compared to both control and butyrate-treated OVA-challenged mice (**Figure 6B**). Higher inflammation and mucus production were also observed in OVA-challenged mice when compared to the other groups (**Figure 6C**). Therefore, our results indicate that butyrate may protect mice from

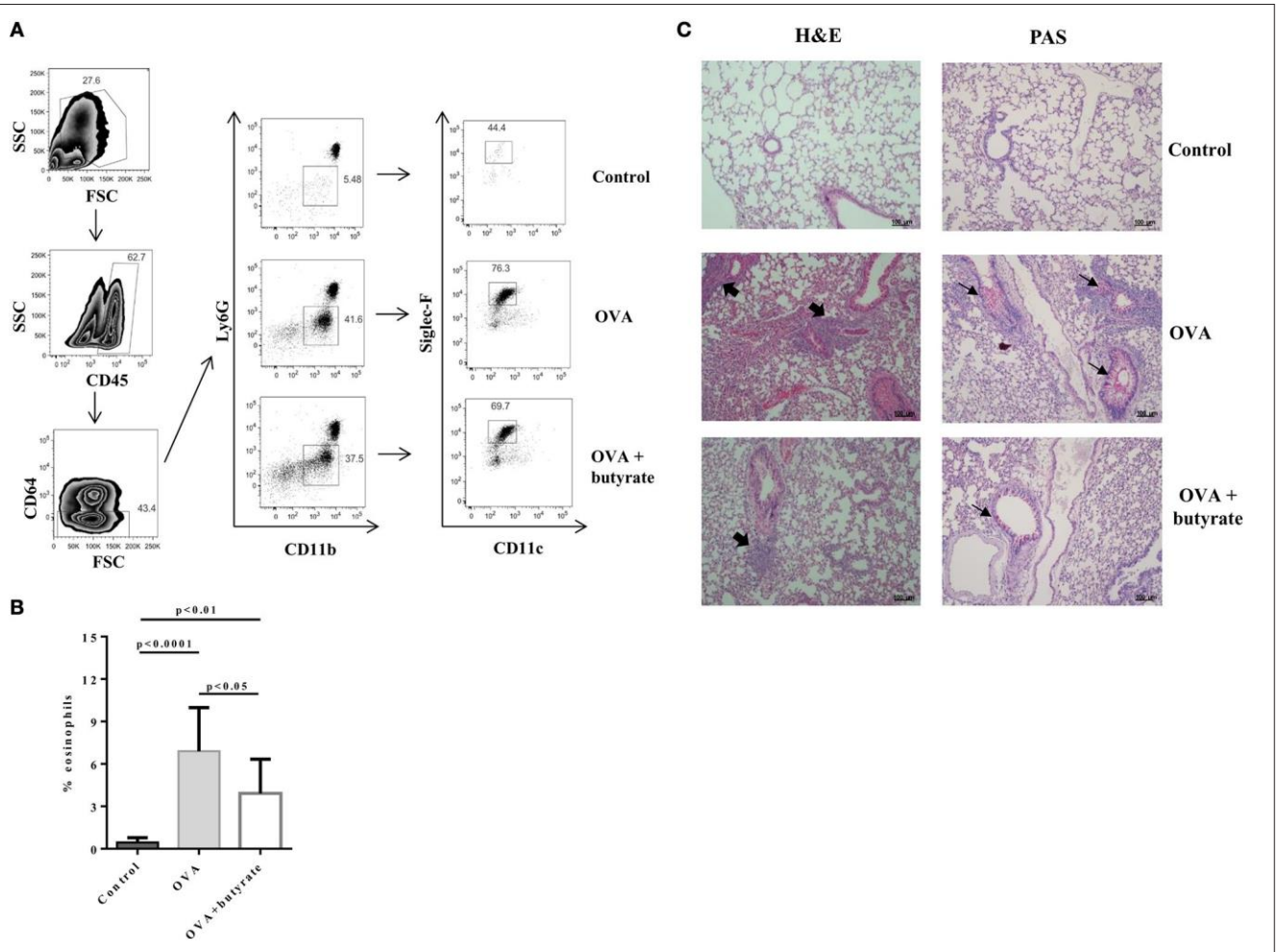

FIGURE 6 | Butyrate treatment protects OVA-challenged mice from lung inflammation. Male C57BL/6 mice were intraperitoneally (IP) injected with OVA (30 μg) + Al(OH)3 (1.6 mg) at days 0 and 7. Mice also received 250 μl of either PBS or butyrate (1 M) (IP) at days 0, 1, 2, 7, 8, and 9. OVA-sensitized mice were nebulized with an OVA solution (3%) for 15 min at days 14, 15, and 16. The group that received butyrate during sensitization was also treated during challenge. A control group was sensitized and challenged without OVA. Euthanasia was performed 24 h after the last challenge. Lungs were digested and cells stained with monoclonal antibodies to determine the frequency of eosinophils (CD45+CD64-Ly6G-CD11b+Siglec-F+CD11c-) by flow cytometry (A). Bar graph shows the frequency of eosinophils in the different groups (B). Lung tissues were also stained with hematoxylin/eosin (H&E) and periodic acid–Schiff (PAS), scale bars: 100 μm. Thick and thin arrows indicate inflammatory infiltrates and mucus production, respectively (C). Data are shown as mean ± SD. One-way ANOVA followed by Tukey's multiple comparison test were used for statistical analysis. *n* = 5–7 mice per group.

lung inflammation by impairing the differentiation of Th9 cells.

Adoptive Transfer of Th9 Cells Reverses Butyrate Effects on Lung Inflammation

To confirm that butyrate treatment protected mice from lung inflammation by negatively modulating the differentiation of Th9 cells, we performed OVA-challenge experiments as previously described, in which butyrate-treated mice also received an adoptive transfer of either naïve OT-II Th0 cells or *in vitro*-differentiated OT-II Th2 or Th9 cells one day before initiating OVA-challenge (**Figure 7A**). We observed that adoptive transfer of Th9 cells restored the frequency of lung-infiltrated eosinophils in butyrate-treated OVA-challenged mice to the same level of mice not treated with butyrate (**Figure 7B**). Th2 adoptive transfer resulted in a higher frequency of lung-infiltrated eosinophils, although it was not statistically significant (**Figure 7B**). We also demonstrated that the frequency of lung-infiltrated Th9 cells was restored in animals that received these cells (**Figure 7C**). Th2 adoptive transfer resulted in a small increase in the frequency of these cells into the lungs of butyrate-treated OVA-challenged mice (**Figure 7D**). Lung inflammation and mucus production were also higher in animals that received adoptive transfer of Th9 cells, and in a lesser extent in those that received Th2 cells, when compared to butyrate-treated Th0-injected mice (**Figure 7E**). Taken together, these results reinforce our hypothesis that butyrate treatment attenuates lung inflammation by negatively modulating Th9 cells.

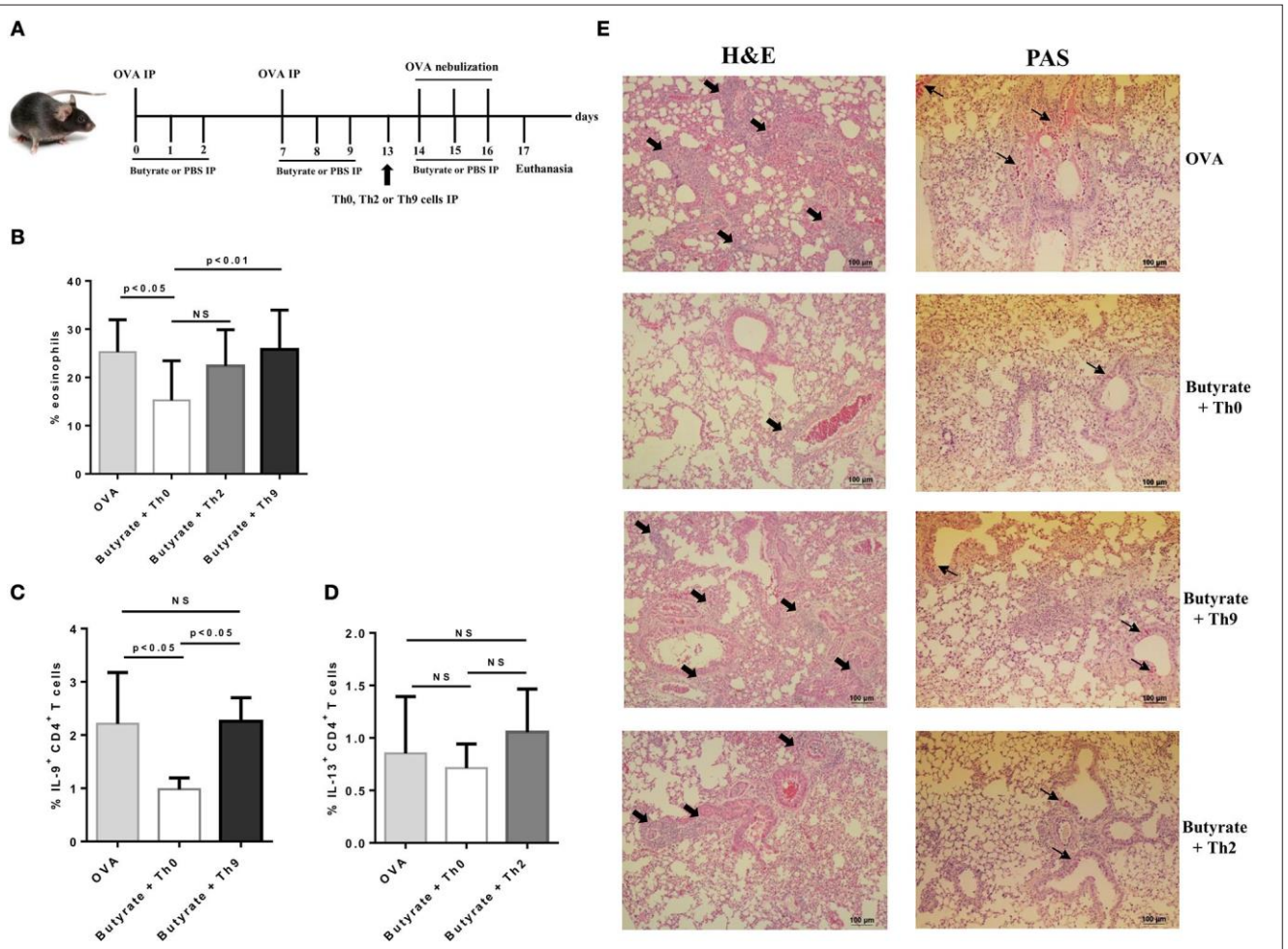

FIGURE 7 | Adoptive transfer of Th9 cells restores lung inflammation in butyrate-treated OVA-challenged mice. Male C57BL/6 mice were intraperitoneally (IP) injected with OVA (30 μg) + Al(OH)3 (1.6 mg) at days 0 and 7. Mice also received 250 μl of either PBS or butyrate (1 M) (IP) at days 0, 1, 2, 7, 8, and 9. OVA-sensitized mice were nebulized with an OVA solution (3%) for 15 min at days 14, 15, and 16. The groups that received butyrate during sensitization were treated during challenge. Butyrate-treated mice also received an adoptive transfer (IP) of OT-II Th0, Th2, or Th9 cells 24 h before challenge initiation. Euthanasia was performed 24 h after the last challenge (A). Lungs were digested and cells stained with monoclonal antibodies to determine the frequency of eosinophils as shown by the bar graph (B). Alternatively, cells were stimulated with PMA (50 ng/ml), ionomycin (500 ng/ml), and brefeldin A (5 μg/ml) for 4 h at 37°C and 5% CO_2, and stained with monoclonal antibodies to determine the frequency of IL-9+CD4+ and IL-13+CD4+ T cells as shown by the bar graphs (C,D), respectively. Lung tissues were also stained with hematoxylin/eosin (H&E) and periodic acid–Schiff (PAS), scale bars: 100 μm. Thick and thin arrows indicate inflammatory infiltrates and mucus production, respectively (E). Data are shown as mean ± SD. One-way ANOVA followed by Tukey's multiple comparison test were used for statistical analysis. $n = 5–7$ mice per group. NS, not significant.

IL-9 Treatment Counteracts Butyrate Effects on Lung Inflammation

To address the question whether butyrate treatment was attenuating lung inflammation by decreasing IL-9 effects, we performed OVA-challenge experiments as previously described, but including a new group of butyrate-treated mice that also received recombinant IL-9 (**Figure 8A**). We demonstrated that intraperitoneal treatment with IL-9 during OVA-challenge was sufficient to restore the frequency of lung-infiltrated eosinophils in butyrate-treated mice to a similar level of OVA-challenged mice (**Figure 8B**). We also observed that IL-9 treatment promoted higher inflammation and mucus production in butyrate-treated mice when compared to animals not treated with IL-9 (**Figure 8C**). We then looked at the frequencies of lung-infiltrated Th9, Th2, and Treg cells and found that IL-9 treatment had no effect on these cells (**Figures 9A–C**, respectively). Thus, these results indicate that butyrate may exert an anti-inflammatory impact on OVA-challenged mice by reducing IL-9 effects.

DISCUSSION

In this study, we demonstrate that butyrate is more effective than propionate in promoting FOXP3 expression and IL-9 repression. In addition, we show that propionate negatively impact *in vitro* differentiation of IL-13-expressing T cells. Butyrate treatment attenuated lung inflammation and mucus production in OVA-challenged mice, which presented lower frequency of lung-infiltrated Th9 cells and eosinophils. Both Th9 cell adoptive transfer and IL-9 treatment restored lung inflammation in

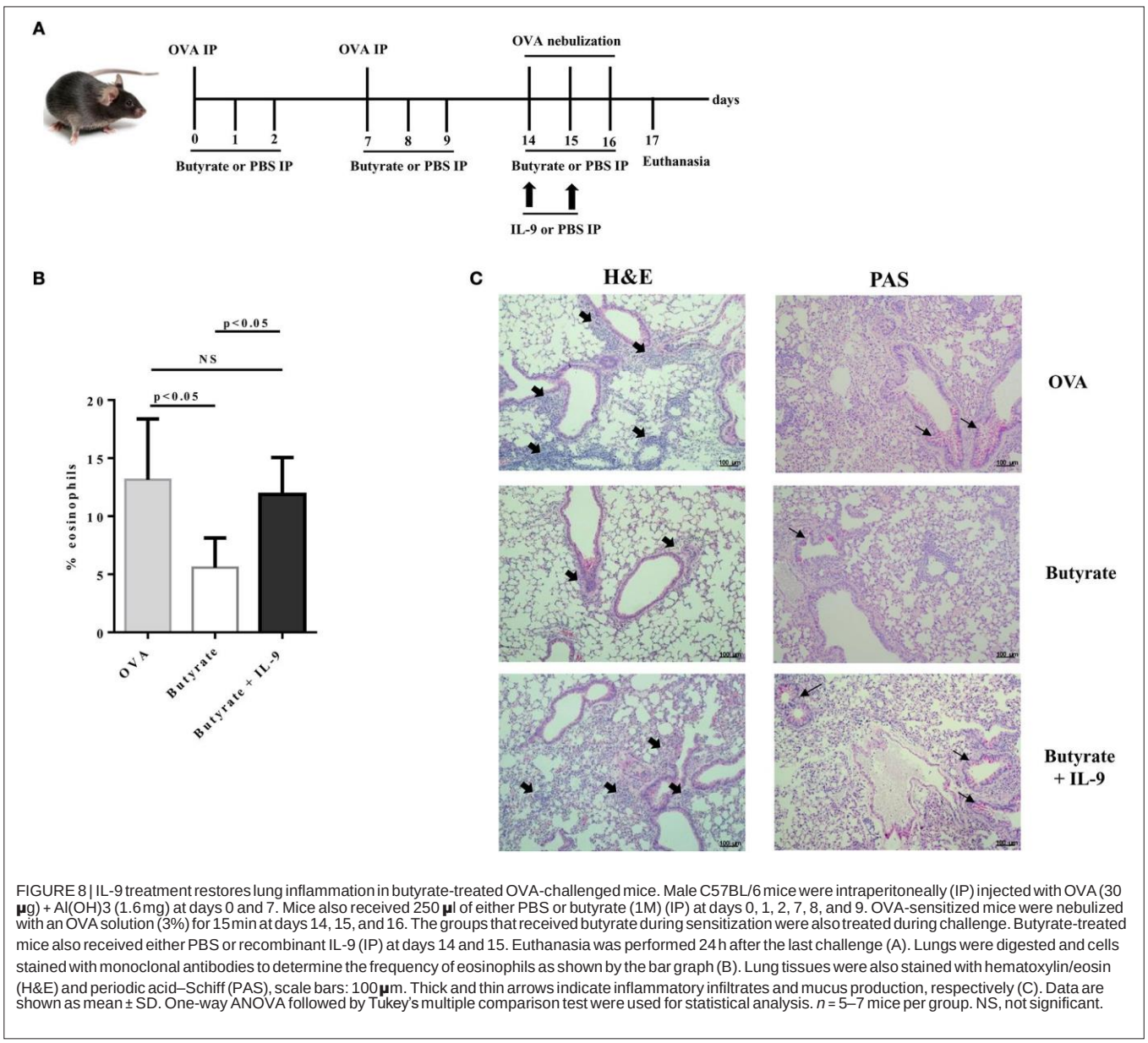

FIGURE 8 | IL-9 treatment restores lung inflammation in butyrate-treated OVA-challenged mice. Male C57BL/6 mice were intraperitoneally (IP) injected with OVA (30 **µ**g) + Al(OH)3 (1.6 mg) at days 0 and 7. Mice also received 250 **µ**l of either PBS or butyrate (1M) (IP) at days 0, 1, 2, 7, 8, and 9. OVA-sensitized mice were nebulized with an OVA solution (3%) for 15 min at days 14, 15, and 16. The groups that received butyrate during sensitization were also treated during challenge. Butyrate-treated mice also received either PBS or recombinant IL-9 (IP) at days 14 and 15. Euthanasia was performed 24 h after the last challenge (A). Lungs were digested and cells stained with monoclonal antibodies to determine the frequency of eosinophils as shown by the bar graph (B). Lung tissues were also stained with hematoxylin/eosin (H&E) and periodic acid–Schiff (PAS), scale bars: 100 **µ**m. Thick and thin arrows indicate inflammatory infiltrates and mucus production, respectively (C). Data are shown as mean ± SD. One-way ANOVA followed by Tukey's multiple comparison test were used for statistical analysis. *n* = 5–7 mice per group. NS, not significant.

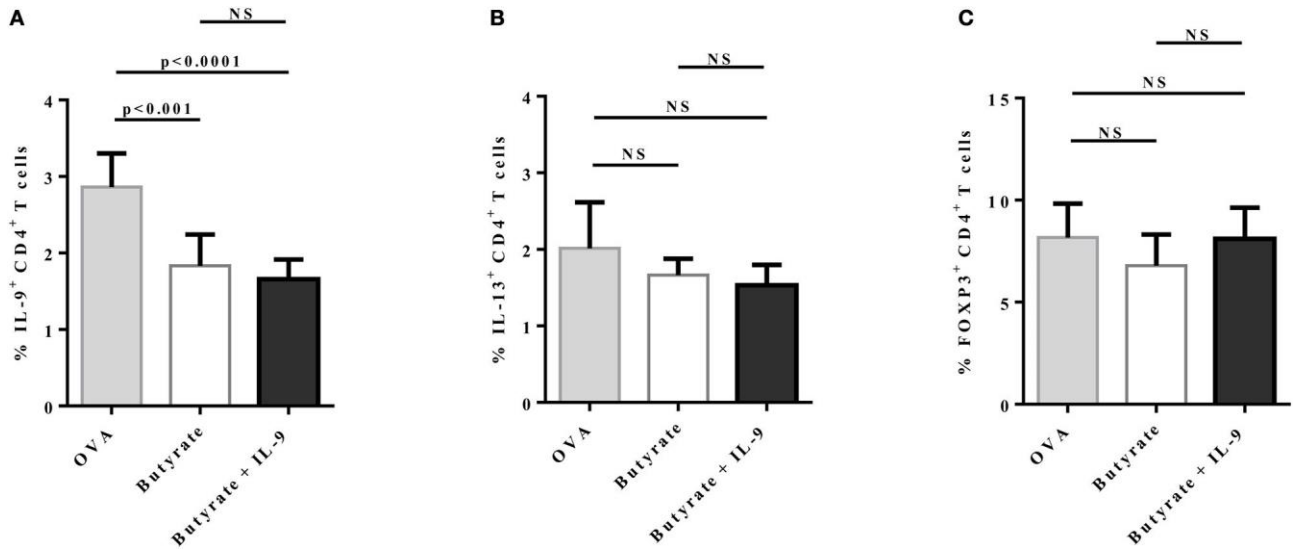

FIGURE 9 | IL-9 treatment has no impact on IL-9+, IL-13+, and FOXP3+ CD4+ T cells in the lungs of butyrate-treated OVA-challenged mice. Male C57BL/6 mice were intraperitoneally (IP) injected with OVA (30 μg) + Al(OH)3 (1.6 mg) at days 0 and 7. Mice also received 250 μl of either PBS or butyrate (1 M) (IP) at days 0, 1, 2, 7, 8, and 9. OVA-sensitized mice were nebulized with an OVA solution (3%) for 15 min at days 14, 15, and 16. The groups that received butyrate during sensitization were also treated during challenge. Butyrate-treated mice also received either PBS or recombinant IL-9 (IP) at days 14 and 15. Euthanasia was performed 24 h after the last challenge. Lungs were digested, cells stimulated with PMA (50 ng/ml), ionomycin (500 ng/ml), and brefeldin A (5 μg/ml) for 4 h at 37°C and 5% CO_2, and stained with monoclonal antibodies to determine the frequencies of IL-9+ (A), IL-13+ (B), and FOXP3+ (C) CD4+ T cells in the different groups. Data are shown as mean ± SD. One-way ANOVA followed by Tukey's multiple comparison test were used for statistical analysis. *n* = 5–7 mice per group. NS, not significant.

butyrate-treated OVA-challenged mice, indicating that the anti-inflammatory effects of butyrate may rely on suppressing Th9-mediated immune responses.

Given the increasing evidence that microbiota-derived metabolites contribute to modulating inflammatory diseases such as asthma, colitis and arthritis (29, 30, 35–37), we sought to evaluate whether the SCFAs butyrate and propionate would have an impact on the differentiation of Th9 cells, key players in inflammation (3). We demonstrated that butyrate added to the culture at day 0 significantly shifted the cellular differentiation from IL-9-expressing to FOXP3-expressing T cells, while propionate was less effective in promoting the same shift. A strong inverse correlation between IL-9 and FOXP3 expression was found when all groups were analyzed together. Additional analysis showed that butyrate treatment led to higher frequency of IL-10-expressing T cells that were not expressing either FOXP3 or IL-9. Although we cannot assume that the cells generated by the exposition to butyrate or propionate under Th9 differentiation were converted to induced regulatory T cells (iTregs), we were still able to demonstrate the negative impact of these SCFAs on Th9 cells.

To further characterize the impacts of butyrate on Th9 cells, we treated differentiated cells and found no impact on FOXP3 expression. We found that most Th9 cells were not expressing IL-9 after 8 days of culture, when compared to cells stimulated with PMA after 4 days of differentiation. Surprisingly, we observed a less intense decrease in the frequency of IL-9-expressing T cells when differentiated Th9 cells were treated with butyrate, suggesting that this SCFA may have opposite effects on naïve CD4+ T cells and differentiated Th9 cells. A higher frequency of IL-10-expressing T cells was also found when differentiated Th9 cells were exposed to butyrate. A recent study demonstrated that butyrate promotes IL-10 expression by differentiated Th1 cells through interaction with the GPR43 receptor (38), supporting our findings. Although we also observed higher frequency of IL-9-expressing T cells when Th9 cells were treated with butyrate, no impact on IFN-γ-expressing T cells was demonstrated in the previous report, suggesting that the effector cytokines produced by Th9 and Th1 cells are differentially affected by butyrate.

The effects of butyrate and other SCFAs on FOXP3 expression in CD4+ T cells differentiated into iTregs have been previously demonstrated (31, 32), as we have also shown here. It is known that Th9 cells and iTregs share key transcription factors and common induction pathways that may determine the generation of one over the other subset. While GITR engagement was shown to subvert iTregs differentiation by favoring Th9 cells, FOXP3-mediated repression of the *Il9* locus contributed to blocking the differentiation of Th9 cells (33). Therefore, we believe that the negative impact of butyrate on Th9 cells are likely to be dependent on FOXP3-mediated repression of IL-9 early during differentiation, as we have not found the same effect when exposing differentiated cells to butyrate. This SCFA could also be acting through epigenetic remodeling of the *Il9* locus (39) or by breaking down signal pathways involved in IL-9 expression. Studies with FOXP3-deficient cells could be performed to further confirm the role of FOXP3 in mediating butyrate-induced IL-9 repression.

To further investigate the effects of butyrate on Th9 cells, we established an OVA-induced lung inflammation model and demonstrated that butyrate treatment resulted in lower frequency

of lung-infiltrated Th9 cells, while no impact on Th2 cells was observed. Higher frequency of lung-infiltrated FOXP3+ T cells was found in butyrate-treated OVA-challenged mice when compared to control animals, but no significant differences were found when compared to OVA-challenged mice. Acetate-mediated protection against house dust mite extract (HDM)-induced lung inflammation has been previously reported, indicating that SCFAs may act through induction of iTregs to inhibit inflammation. However, a 3 week-treatment period was necessary for the observed results (30). In our experiments, animals were treated for a much shorter period, which could explain the lack of significant difference in terms of lung-infiltrated FOXP3+ T cells between OVA-challenged groups. As regulatory T cells naturally migrate to inflamed tissues to suppress inflammation (40), it is possible that butyrate-mediated induction of iTregs was masked in OVA-challenged mice due to the increased influx of these cells into the lungs, independently of their origin. On the other hand, iTregs generated in the gut upon intraperitoneal butyrate treatment may have not appropriately responded to the lung OVA challenge, resulting in less lung infiltration than expected. The *in vivo* instability of iTregs (41) could also be an explanation for not having a significant increase in lung infiltration upon butyrate treatment. These cells may have lost FOXP3 expression during the sensitization period. Therefore, it is unlikely that induction of iTregs played a major role in our study, although our *in vitro* experiments suggest an inverse correlation of FOXP3 and IL-9 expression upon treatment with SCFAs.

Lung-infiltrated eosinophils were used as a parameter to evaluate Th9-mediated immune responses in our model, given the well-established role of IL-9 in promoting eotaxin/CCL11 expression and influx of these cells into different body tissues, including lungs (34, 42, 43). We found that butyrate-treated OVA-challenged mice presented lower frequency of lung-infiltrated eosinophils, attenuated inflammatory infiltrates and mucus production, indicating that Th9-mediated immune responses were suppressed. In line with our observations, a previous study has demonstrated that dietary fiber and the SCFA propionate protected mice from lung inflammation and asthma symptoms. However, the effects of propionate relied on promoting dendritic cells with impaired capability of inducing effector Th2 cells in an HDM-mediated model. Significant differences in the immunological parameters of propionate-treated mice were observed 5–6 days after the last challenge (29). In our study, we have found a more acute effect of butyrate, with significant differences 24 h after the last challenge, suggesting that these SCFAs may have different impacts on the immune system in the context of lung inflammation.

Although we have demonstrated that *in vitro* butyrate treatment induced a small, but significant increase in the frequency of IL-13-expressing T cells, no *in vivo* effects on these cells were observed, indicating that Th9-mediated immune responses were likely to be the most affected in our model. As we have not found a significant *in vitro* impact of butyrate on the frequency of IL-4 and IL-5-expressing T cells, these cytokines were not evaluated in our *in vivo* experiments. However, to further characterize the effects of SCFAs on Th2 cells, we also treated naïve CD4+ T cells with propionate and demonstrated that it partially impaired the differentiation of IL-13-expressig T cells while not affecting IL-4 and IL-5. We understand that more studies are still necessary to unveil the mechanisms involved in this phenomenon, but conceive that our results complement the previous report on the impact of propionate on Th2 cells.

To confirm that butyrate was attenuating lung inflammation by suppressing Th9 cells, we performed either adoptive transfer of OVA-specific OT-II Th9 cells or recombinant IL-9 treatment and found that both strategies were sufficient to restore lung inflammation in butyrate-treated OVA-challenged mice. Adoptive transfer of OT-II Th2 cells also increased lung inflammation, but to a lesser extent than that observed with Th9 transfer. Although it has been shown that IL-9 may promote IL-13-mediated lung inflammation and mucus production (20), we found no difference in the frequency of lung-infiltrated IL-13-expressing Th2 cells in IL-9-treated mice, suggesting that other cells may have mediated the inflammatory process. In fact, type II innate lymphoid cells (ILC2) are known to produce IL-13 and to play a role in experimental and clinical asthma pathology (44, 45). A synergistically effect of ILC2 and Th9 cells in lung inflammation has also been described (46, 47), suggesting that ILC2 may have a role in our model. On the other hand, our results could be partially explained by the fact that IL-9 exerts a direct effect on lung epithelial cells and promotes mucus production (48). We cannot rule out the possibility that butyrate directly impacted ILC2 and even other cell populations, as recently reported (49). However, our data strongly suggest that Th9/IL-9 played a major role in our model. Further studies are still necessary to mechanistically confirm our hypothesis.

Our findings bring new insights on the mechanisms by which microbiota-derived metabolites regulate diseases, suggesting that butyrate attenuates lung inflammation most likely through a negative modulation of Th9 cell-mediated immune responses. Therefore, butyrate should be clinically considered in the treatment of inflammatory diseases in which suppression of Th9 cells is necessary.

AUTHOR CONTRIBUTIONS

RA and RV conceived and designed the experiments. RV, AC, and PB performed and analyzed experiments. RA and RV prepared figures and wrote the manuscript. RA and NC performed final review of the manuscript. NC provided structure and reagents. All authors read and approved the final article.

FUNDING

This research was supported by Fundação de Amparo à Pesquisa do Estado de São Paulo (FAPESP 2017/02564-7), Conselho Nacional de Desenvolvimento Científico e Tecnológico (CNPq) and Coordenação de Aperfeiçoamento de Pessoal de Nível Superior (CAPES). RA, RV, AC, and PB are recipients of FAPESP scholarships: 2015/13817-0, 2016/03532-1, 2017/00721-0 and 2015/26682-6, respectively.

ACKNOWLEDGMENTS

We would like to thank the animal facility of the Biomedical Science Institute for proving all animals used in this study, and Paulo Albe for experimental support. We also thank Centro de Facilidades de Apoio à Pesquisa (CEFAP-USP) for flow cytometry support.

REFERENCES

1. DuPage M, Bluestone JA. Harnessing the plasticity of CD4(+) T cells to treat immune-mediated disease. *Nat Rev Immunol.* (2016) 16:149–63. doi: 10.1038/nri.2015.18
2. Lloyd CM, Hessel EM. Functions of T cells in asthma: more than just T(H)2 cells. *Nat Rev Immunol*. (2010) 10:838–48. doi: 10.1038/nri2870
3. Kaplan MH, Hufford MM, Olson MR. The development and *in vivo* function of T helper 9 cells. *Nat Rev Immunol*. (2015) 15:295–307. doi: 10.1038/nri3824
4. Chang HC, Sehra S, Goswami R, Yao W, Yu Q, Stritesky GL, et al. The transcription factor PU.1 is required for the development of IL-9-producing T cells and allergic inflammation. *Nat Immunol.* (2010) 11:527–34. doi: 10.1038/ni.1867
5. Goswami R, Jabeen R, Yagi R, Duy P, Zhu J, Goenka S, et al. STAT6-dependent regulation of Th9 development. *J Immunol.* (2012) 188:968–75. doi: 10.4049/jimmunol.1102840
6. Jabeen R, Goswami R, Awe O, Kulkarni A, Nguyen ET, Attenasio A, et al. Th9 cell development requires a BATF-regulated transcriptional network. *J Clin Invest.* (2013) 123:4641–53. doi: 10.1172/JCI 69489
7. Malik S, Sadhu S, Elesela S, Pandey RP, Chawla AS, Sharma D, et al. Transcription factor Foxo1 is essential for IL-9 induction in T helper cells. *Nat Commun.* (2017) 8:815. doi: 10.1038/s41467-017-00674-6
8. Staudt V, Bothur E, Klein M, Lingnau K, Reuter S, Grebe N, et al. Interferon-regulatory factor 4 is essential for the developmental program of T helper 9 cells. *Immunity* (2010) 33:192–202. doi: 10.1016/j.immuni.2010.07.014
9. Licona-Limon P, Henao-Mejia J, Temann AU, Gagliani N, Licona-Limon I, Ishigame H, et al. Th9 cells drive host immunity against gastrointestinal worm infection. *Immunity* (2013) 39:744–57. doi: 10.1016/j.immuni.2013.07.020
10. Turner JE, Morrison PJ, Wilhelm C, Wilson M, Ahlfors H, Renauld JC, et al. IL-9-mediated survival of type 2 innate lymphoid cells promotes damage control in helminth-induced lung inflammation. *J Exp Med*. (2013) 210:2951–65. doi: 10.1084/jem.20130071
11. Lu Y, Hong S, Li H, Park J, Hong B, Wang L, et al. Th9 cells promote antitumor immune responses *in vivo*. *J Clin Invest.* (2012) 122:4160–71. doi: 10.1172/JCI65459
12. Purwar R, Schlapbach C, Xiao S, Kang HS, Elyaman W, Jiang X, et al. Robust tumor immunity to melanoma mediated by interleukin-9-producing T cells. *Nat Med*. (2012) 18:1248–53. doi: 10.1038/nm.2856
13. Gerlach K, Hwang YY, Nikolaev A, Atreya R, Dornhoff H, Steiner S, et al. T(H)9 cells that express the transcription factor PU.1 drive T cell-mediated colitis via IL-9 receptor signaling in intestinal epithelial cells. *Nat Immunol*. (2014) 15:676–86. doi: 10.1038/ni.2920
14. Ciccia F, Guggino G, Rizzo A, Manzo A, Vitolo B, La Manna MP, et al. Potential involvement of IL-9 and Th9 cells in the pathogenesis of rheumatoid arthritis. *Rheumatology* (2015) 54:2264–72. doi: 10.1093/rheumatology/kev252
15. Jones CP, Gregory LG, Causton B, Campbell GA, Lloyd CM. Activin A and TGF-beta promote T(H)9 cell-mediated pulmonary allergic pathology. *J Allergy Clin Immunol.* (2012) 129:1000–10.e3. doi: 10.1016/j.jaci.2011.12.965
16. Jia L, Wang Y, Li JP, Li S, Zhang YN, Shen J, et al. Detection of IL-9 producing T cells in the PBMCs of allergic asthmatic patients. *BMC Immunol.* (2017) 18:38. doi: 10.1186/s12865-017-0220-1
17. Namkung JH, Lee JE, Kim E, Park GT, Yang HS, Jang HY, et al. An association between IL-9 and IL-9 receptor gene polymorphisms and atopic dermatitis in a Korean population. *J Dermatol Sci.* (2011) 62:16–21. doi: 10.1016/j.jdermsci.2011.01.007
18. Koch S, Sopel N, Finotto S. Th9 and other IL-9-producing cells in allergic asthma. *Semin Immunopathol.* (2017) 39:55–68. doi: 10.1007/s00281-016-0601-1
19. Temann UA, Geba GP, Rankin JA, Flavell RA. Expression of interleukin 9 in the lungs of transgenic mice causes airway inflammation, mast cell hyperplasia, and bronchial hyperresponsiveness. *J Exp Med.* (1998) 188:1307–20. doi: 10.1084/jem.188.7.1307
20. Temann UA, Ray P, Flavell RA. Pulmonary overexpression of IL-9 induces Th2 cytokine expression, leading to immune pathology. *J Clin Invest*. (2002) 109:29–39. doi: 10.1172/JCI0213696
21. Niedbala W, Besnard AG, Nascimento DC, Donate PB, Sonego F, Yip E, et al. Nitric oxide enhances Th9 cell differentiation and airway inflammation. *Nat Commun.* (2014) 5:4575. doi: 10.1038/ncomms5575
22. Yao WG, Zhang YL, Jabeen R, Nguyen ET, Wilkes DS, Tepper RS, et al. Interleukin-9 is required for allergic airway inflammation mediated by the cytokine TSLP. *Immunity* (2013) 38:360–72. doi: 10.1016/j.immuni.2013.01.007
23. Sokolowska M, Frei R, Lunjani N, Akdis CA, O'Mahony L. Microbiome and asthma. *Asthma Res Pract*. (2018) 4:1. doi: 10.1186/s40733-017-0037-y
24. Ignacio A, Morales CI, Saraiva Camara NO, Almeida RR. Innate sensing of the gut microbiota: modulation of inflammatory and autoimmune diseases. *Front Immunol.* (2016) 7:54. doi: 10.3389/fimmu.2016.00054
25. Abrahamsson TR, Jakobsson HE, Andersson AF, Bjorksten B, Engstrand L, Jenmalm MC. Low gut microbiota diversity in early infancy precedes asthma at school age. *Clin Exp Allergy* (2014) 44:842–50. doi: 10.1111/cea.12253
26. Arrieta MC, Stiemsma LT, Dimitriu PA, Thorson L, Russell S, Yurist-Doutsch S, et al. Early infancy microbial and metabolic alterations affect risk of childhood asthma. *Sci Transl Med.* (2015) 7:307ra152. doi: 10.1126/scitranslmed.aab2271
27. Herbst T, Sichelstiel A, Schar C, Yadava K, Burki K, Cahenzli J, et al. Dysregulation of allergic airway inflammation in the absence of microbial colonization. *Am J Respir Crit Care Med.* (2011) 184:198–205. doi: 10.1164/rccm.201010-1574OC
28. Sudo N, Yu XN, Aiba Y, Oyama N, Sonoda J, Koga Y, et al. An oral introduction of intestinal bacteria prevents the development of a long-term Th2-skewed immunological memory induced by neonatal antibiotic treatment in mice. *Clin Exp Allergy* (2002) 32:1112–6. doi: 10.1046/j.1365-2222.2002.01430.x
29. Trompette A, Gollwitzer ES, Yadava K, Sichelstiel AK, Sprenger N, Ngom-Bru C, et al. Gut microbiota metabolism of dietary fiber influences allergic airway disease and hematopoiesis. *Nat Med*. (2014) 20:159–66. doi: 10.1038/nm.3444
30. Thorburn N, McKenzie CI, Shen S, Stanley D, Macia L, Mason LJ, et al. Evidence that asthma is a developmental origin disease influenced by maternal diet and bacterial metabolites. *Nat Commun*. (2015) 6:7320. doi: 10.1038/ncomms8320
31. Arpaia N, Campbell C, Fan X, Dikiy S, van der Veeken J, deRoos P, et al. Metabolites produced by commensal bacteria promote peripheral regulatory T-cell generation. *Nature* (2013) 504:451–5. doi: 10.1038/nature12726
32. Furusawa Y, Obata Y, Fukuda S, Endo TA, Nakato G, Takahashi D, et al. Commensal microbe-derived butyrate induces the differentiation of colonic regulatory T cells. *Nature* (2013) 504:446–50. doi: 10.1038/nature12721
33. Xiao X, Shi X, Fan Y, Zhang X, Wu M, Lan P, et al. GITR subverts Foxp3(+) Tregs to boost Th9 immunity through regulation of histone acetylation. *Nat Commun.* (2015) 6:8266. doi: 10.1038/ncomms9266
34. Dong Q, Louahed J, Vink A, Sullivan CD, Messler CJ, Zhou YH, et al. IL-9 induces chemokine expression in lung epithelial cells and baseline airway eosinophilia in transgenic mice. *Eur J Immunol.* (1999) 29:2130–9. doi: 10.1002/(SICI)1521-4141(199907)29:07<2130::AID-IMMU2130>3.0.CO;2-S

35. Halnes I, Baines KJ, Berthon BS, MacDonald-Wicks LK, Gibson PG, Wood LG. Soluble fibre meal challenge reduces airway inflammation and expression of GPR43 and GPR41 in asthma. *Nutrients* (2017) 9:317–27. doi: 10.3390/nu9010057
36. Maslowski M, Vieira AT, Ng A, Kranich J, Sierro F, Yu D, et al. Regulation of inflammatory responses by gut microbiota and chemoattractant receptor GPR43. *Nature* (2009) 461:1282–6. doi: 10.1038/nature 08530
37. Singh N, Gurav A, Sivaprakasam S, Brady E, Padia R, Shi H, et al. Activation of Gpr109a, receptor for niacin and the commensal metabolite butyrate, suppresses colonic inflammation and carcinogenesis. *Immunity* (2014) 40:128–39. doi: 10.1016/j.immuni.2013.12.007
38. Sun MM, Wu W, Chen L, Yang WJ, Huang XS, Ma CY, et al. Microbiota-derived short-chain fatty acids promote Th1 cell IL-10 production to maintain intestinal homeostasis. *Nat Commun.* (2018) 9:3555. doi: 10.1038/s41467-018-05901-2
39. Canani RB, Di Costanzo M, Leone L. The epigenetic effects of butyrate: potential therapeutic implications for clinical practice. *Clin Epigenetics* (2012) 4:4. doi: 10.1186/1868-7083-4-4
40. Campbell DJ. Control of regulatory T cell migration, function, and homeostasis. *J Immunol.* (2015) 195:2507–13. doi: 10.4049/jimmunol.1500801
41. Kanamori M, Nakatsukasa H, Okada M, Lu QJ, Yoshimura A. Induced regulatory T cells: their development, stability, and applications. *Trends Immunol.* (2016) 37:803–11. doi: 10.1016/j.it.2016. 08.012
42. Louahed J, Zhou YH, Maloy WL, Rani PU, Weiss C, Tomer Y, et al. Interleukin 9 promotes influx and local maturation of eosinophils. *Blood* (2001) 97:1035–42. doi: 10.1182/blood.V97. 4.1035
43. Gounni S, Hamid Q, Rahman SM, Hoeck J, Yang J, Shan LY. IL-9-mediated induction of eotaxin1/CCL11 in human airway smooth muscle cells. *J Immunol.* (2004) 173:2771–9. doi: 10.4049/jimmunol.173.4.2771
44. Jia Y, Fang X, Zhu XH, Bai CX, Zhu L, Jin ML, et al. IL-13(+) Type 2 innate lymphoid cells correlate with asthma control status and treatment response. *Am J Respir Cell Mol Biol.* (2016) 55:675–83. doi: 10.1165/rcmb.2016-0099OC
45. Wolterink R, KleinJan A, van Nimwegen M, Bergen I, de Bruijn M, Levani Y, et al. Pulmonary innate lymphoid cells are major producers of IL-5 and IL-13 in murine models of allergic asthma. *Eur J Immunol.* (2012) 42:1106–16. doi: 10.1002/eji.201142018
46. Moretti S, Renga G, Oikonomou V, Galosi C, Pariano M, Iannitti R, et al. A mast cell-ILC2-Th9 pathway promotes lung inflammation in cystic fibrosis. *Nat Commun.* (2017) 8:14017. doi: 10.1038/ncomms14017
47. Ying XY, Su ZL, Bie QL, Zhang P, Yang HJ, Wu YM, et al. Synergistically increased ILC2 and Th9 cells in lung tissue jointly promote the pathological process of asthma in mice. *Mol Med Rep.* (2016) 13:5230–40. doi: 10.3892/mmr.2016.5174
48. Louahed J, Toda M, Jen J, Hamid Q, Renauld JC, Levitt RC, et al. Interleukin-9 upregulates mucus expression in the airways. *Am J Respir Cell Mol Biol.* (2000) 22:649–56. doi: 10.1165/ajrcmb.22.6.3927
49. Thio CL, Chi PY, Lai AC, Chang YJ. Regulation of type 2 innate lymphoid cell–dependent airway hyperreactivity by butyrate. *J Allergy Clin Immunol.* (2018) 142:1867–83.e12 doi: 10.1016/j.jaci.2018.02.032

Conflict of Interest Statement: The authors declare that the research was conducted in the absence of any commercial or financial relationships that could be construed as a potential conflict of interest.